The clinical application of a novel instrumented wheelchair pushrim

Thesis submitted to University College London for the degree of
Doctorate of Philosophy

Andrew Symonds

Centre for Rehabilitation and Assistive Technology Engineering,
Institute of Orthopaedics and Musculoskeletal Science

February 2017

I, Andrew Symonds, confirm that the work presented in this thesis is my own. Where information has been derived from other sources, I confirm that this has been indicated in the thesis.

Abstract

Sustained manual wheelchair propulsion is related to shoulder injury, which is associated with increasing age and time as a wheelchair user. Consequently, the biomechanics of manual wheelchair propulsion have been widely examined, both to quantify the demand of a task and also to guide optimisation of technique. Such analysis has incorporated assessment of push rim kinetics using instrumented wheelchair wheels. The major limitation of the instrumented wheels currently available is that they add significant weight to the wheelchair, increasing the demand on the user and altering propulsion biomechanics. This thesis presents the design and potential clinical application of a novel lightweight instrumented wheelchair wheel, the 'Sensewheel'. In this thesis, the Sensewheel is used to investigate the influence of ageing on propulsion biomechanics and to quantify shoulder joint demand during various types of over ground propulsion. Propulsion demand is quantified with the use of surface electromyography and a musculoskeletal model of the trunk and upper limbs, animated with data collected from the Sensewheel. The Sensewheel is also used to identify pushing technique differences during over ground propulsion, and also to provide real time feedback as a training intervention to improve technique.

This thesis consists of a series of short clinical studies exploring the use of the Sensewheel. The design and measurement capabilities of the Sensewheel are introduced, alongside discussion of current limitations and future development requirements. The first experimental study investigates age related differences in propulsion biomechanics and muscle activity levels during wheelchair propulsion on a treadmill. The results of the study are not conclusive in supporting the theory that older wheelchair users are at greater risk of injury due to greater relative muscle demand. The second experimental study examines shoulder joint demand during level, 2.5% cross slope, 6.5% and 12% incline over ground propulsion. The results demonstrate significantly greater levels of shoulder joint demand during incline propulsion, with glenohumeral (GH) joint contact force rising above 2000N and muscle activity levels rising to 92% of maximum during the 12%

incline task. The results also demonstrate a strong positive correlation between force applied at the wheelchair push rim and resultant GH joint contact force.

The <u>third</u> experimental study compares the propulsion technique of novices and experts during the same over ground propulsion tasks. The results demonstrate that the experts are able to use the force they apply to the push rim more effectively to reduce the repetition of the task, but that during more challenging tasks this may increase shoulder joint demand.

A systematic review of the literature identifies that push rate and push arc can be successfully optimised using real time feedback. The <u>fourth</u> experimental study describes how the Sensewheel is used to provide real time data to inform real time verbal feedback to novice non wheelchair users, with the goal of optimising push arc. The intervention is successful in increasing push arc, reducing the number of pushes required whilst maintaining shoulder joint load within the range of normal daily activity.

In summary, the thesis introduces the various potential clinical applications of a novel lightweight instrumented wheelchair wheel. In this thesis, the Sensewheel is used to assess the extent of the shoulder demand experienced during manual wheelchair propulsion, and to identify the importance of optimising pushing effectiveness. It is also used to successfully provide an intervention to improve propulsion technique.

Acknowledgements

I would like to thank my supervisors Dr Stephen Taylor and Dr Catherine Holloway for their support throughout the project. I am grateful to have had the opportunity to work with the 'Sensewheel', which is introduced in Chapter 4 of this thesis. The Sensewheel was conceptualised by Dr Holloway and Mr Peter Smitham and designed and manufactured by Dr Taylor. With the assistance of Dr Taylor I have summarised the design and function of the Sensewheel in Chapter 4, including the stages that I have been involved in, including load cell calibration, building the load cells on to the wheels and developing the data processing strategy.

I would like to thank the UCL PAMELA staff for their advice and practical assistance in setting up the laboratory and helping to run the experiments. I would also like to thank Giulia Barbareschi, for collaborating to produce the systematic reviews presented in this thesis. I would also like to thank Dr Erica Cook for her statistical advice which has been applied during each of the experimental chapters reported.

Thanks to my parents and brother for your ongoing support, and to Jane, Lucie and Ben, thank you for allowing me the freedom to take this project on, I could not have completed it without you.

Preface

The research presented throughout the current thesis has been peer reviewed through the following publications and communications:

Publications

Chapter 3:

SYMONDS, A., Barbareschi, G., Taylor, S. & Holloway, C. 2017 A Systematic Review: the influence of real time feedback on wheelchair propulsion biomechanics. *Disability and Rehabilitation: Assistive Technology*, ISSN: 1748-3107.

Chapter 6:

VELHO, R., HOLLOWAY, C., **SYMONDS, A**. & BALMER, B. 2016. The effect of transport accessibility on the social inclusion of wheelchair users: a mixed method analysis. *Social Inclusion*, ISSN: 2183-2803.

Chapter 7:

SYMONDS, A., HOLLOWAY, C., SUZUKI, T., SMITHAM, P., GALL, A. & TAYLOR, S. 2016. Identifying key experience-related differences in over-ground manual wheelchair propulsion biomechanics. *Journal of Rehabilitation and Assistive Technologies Engineering.* DOI: 10.1177/2055668316678362.

Chapter 8:

SYMONDS, A., TAYLOR, S.J.G. & HOLLOWAY, C. 2016. Sensewheel: an adjunct to wheelchair skills training. *Healthcare Technology Letters.* ISSN: 2053-3713

Conference communications

Chapter 5:

SYMONDS, A., TAYLOR, S., SMITHAM, P. & HOLLOWAY, C. Age related differences in shoulder joint biomechanics during manual wheelchair propulsion (*Poster*). 53rd Annual Scientific Meeting of The International Spinal Cord Injury Society, Maastricht, 2014.

Chapter 6:

HOLLOWAY, C. S., **SYMONDS, A**., SUZUKI, T., GALL, A., SMITHAM, P. & TAYLOR, S. 2015. Linking wheelchair kinetics to glenohumeral joint demand during everyday accessibility activities. *Conference proceedings: Annual International Conference of the IEEE Engineering in Medicine and Biology Society. IEEE Engineering in Medicine and Biology Society. Annual Conference,* 2015, 2478-81.

SYMONDS, A., TAYLOR, S., SMITHAM, P., SUZUKI, T., GALL, A. & HOLLOWAY, C. Development and implementation of a method using OpenSim to calculate Glenohumeral joint contact force during manual wheelchair propulsion accessibility tasks (*Poster*). XXV Congress of the International Society of Biomechanics, Glasgow, 2015. Short listed for the David Winter Young Investigator Award.

Table of contents

XII

Table of figures

Table of tables

List of Abbreviations

Throughout this thesis, the following abbreviations were used to represent frequently used terms. All abbreviations were defined the first time they appeared in the text.

AC	Acromioclavicular
AD	Anterior Deltoid
AMD	Anterior/Middle Deltoid
BB	Biceps Brachii
EMG	Electromyography
FEF	Fraction of effective force
GH	Glenohumeral
GUI	Graphical user interface
IMU	Inertial measurement unit
IS	Infraspinatus
LD	Latissimus Dorsi
MD	Middle Deltoid
MEF	Mechanical effective force
MRI	Magnetic resonance imaging
MVIC	Maximum voluntary isometric contraction
OA	Osteoarthritis
PAMELA	Pedestrian accessibility and movement environment laboratory
PC	Personal computer
PD	Posterior Deltoid
PM	Pectoralis Major
RMS	Root mean square
SCI	Spinal Cord Injury
SENIAM	Surface electromyography for the non-invasive assessment of muscles
SS	Supraspinatus
SSc	Subscapularis
TB	Triceps Brachii
TM	Teres Minor

TTL	Transistor-transistor logic
UCL	University College London
UHF	Ultra-high frequency
WST	Wheelchair skills test

Chapter 1 Introduction

1.1 Overview

It is estimated that there are almost one million wheelchair users in the United Kingdom (Papworth Trust, 2013). Sustained manual wheelchair use leads to upper extremity injury, including shoulder injury (Dalyan et al., 1999). Injury to the rotator cuff muscles is the most commonly reported shoulder problem in manual wheelchair users (Akbar et al., 2010) and is associated with increasing age and time as a wheelchair user (Akbar et al., 2011). Rotator cuff injury can lead to secondary degenerative complications at the shoulder joint, including Osteoarthritis (OA) (Boninger et al., 2003, Mercer et al., 2006). Manual wheelchair users rely on upper limb function for their independence, so shoulder pain and injury can have a significantly negative impact on subjective quality of life and physical activity scores (Gutierrez et al., 2007). Thus, it is vital to measure upper limb demand and risk of injury during manual wheelchair propulsion to inform how chair design and set up and propulsion technique can be optimised.

1.2 The need for a lightweight instrumented wheelchair wheel

Instrumented wheelchair wheels are commonly used in the biomechanical analysis of manual wheelchair propulsion. Those currently available are limited in that they add a significant amount of weight to the wheelchair wheel. Previous research has demonstrated a strong positive correlation between body weight and peak propulsion force (Boninger et al., 1999). This indicates that the instrumented wheels currently available may increase the force required from the wheelchair user and reduce the accuracy of biomechanical analysis. There exists a need for an instrumented wheelchair wheel that does not add additional weight to a standard wheelchair wheel.

1.3 Upper limb demand during manual wheelchair propulsion

The prevalence of rotator cuff degeneration is greater in manual wheelchair users (Akbar et al., 2010) and is associated with increasing age and time as

a wheelchair user (Akbar et al., 2011). In addition, models of tendon degeneration suggest that injury is caused by repetitive overloading of the tendon (Nho et al., 2008). Therefore task repetition and force application during wheelchair propulsion need to be quantified and minimised. Upper limb demand during manual wheelchair propulsion has been widely measured and reported in the biomechanics literature. The advent of instrumented wheelchair wheels has enabled the measurement of the temporal and kinetic parameters of wheelchair propulsion (Cowan et al., 2008). Trunk and upper limb kinematics can be measured using motion capture systems (de Groot et al., 2003) and inertial measurement systems (Hooke et al., 2009, Starrs et al., 2012) and surface Electromyography (EMG) has been used to record muscle activity level during wheelchair propulsion (Mulroy et al., 1996). In addition kinetic and kinematic data collected during manual wheelchair propulsion have been applied to musculoskeletal models to estimate glenohumeral (GH) joint contact forces (Veeger et al., 2002, Morrow et al., 2010b). Relating to the fact that rotator cuff injury is associated with ageing and increased loading, there exists little evidence to examine the demand that manual wheelchair propulsion places on ageing muscles. Additionally, the majority of research quantifying shoulder demand focuses on ergometer based propulsion, whereas assessment of over ground propulsion would be more informative in quantifying injury risk during daily propulsion activity.

1.4   Improving the effectiveness of manual wheelchair propulsion

Manual wheelchair propulsion technique can be optimised by improving the physical capacity of the user, provision of a lightweight wheelchair, adjustment of the wheelchair and also technique training. Wheelchair adjustments include positioning of the seat (van der Woude et al., 2009, Boninger et al., 2000), the relative position of the rear axle with respect to the seat (Mulroy et al., 2005, Gutierrez et al., 2005) and camber (Mason et al., 2012b) and diameter of the wheels (Mason et al., 2012a). Wheelchair skills training has also demonstrated beneficial effects (MacPhee et al., 2004). Real time feedback, using data recorded with instrumented wheelchair

wheels has been shown to assist wheelchair skills training (Rice et al., 2013, Richter et al., 2011). These interventions have been provided visually, during ergometer wheelchair propulsion. Further research is required, both to identify the key propulsion parameters to focus on during over ground propulsion and also to assess the optimal delivery of these parameters as real time feedback.

1.5 Aims and objectives of the thesis

The principal aims of the thesis were:

1) To introduce the design and potential clinical application of a novel lightweight instrumented wheelchair wheel, the 'Sensewheel'.
2) To explore risk of shoulder injury related to ageing and loading during over ground manual wheelchair propulsion.
3) To investigate the optimisation of propulsion technique during over ground manual wheelchair propulsion.

In order to achieve this, five main objectives were formulated:

1) To introduce the design and measurement capability of the Sensewheel, by using it to complete a number of experimental 'proof of concept' studies (Chapters 4, 5, 6, 7 and 8).
2) To investigate age related differences in propulsion technique and muscle activity levels and relate these factors to risk of shoulder injury (Chapter 5).
3) To measure shoulder joint demand during over ground manual wheelchair propulsion and investigate the relationship between forces applied to the wheelchair push rim and shoulder joint demand (Chapter 6).
4) To examine key experience related differences in manual wheelchair propulsion biomechanics to inform optimal technique (Chapter 7).
5) To investigate the application of real time verbal feedback to optimise propulsion technique during over ground manual wheelchair propulsion (Chapter 8).

3

1.6   Organisation of the thesis

This thesis is structured into a background chapter (Chapter 2) followed by a chapter reporting a systematic review (Chapter 3), a chapter introducing the Sensewheel (Chapter 4), four experimental chapters (Chapters 5 – 9) and a chapter for general discussion and conclusion (Chapter 9). The background chapter incorporates a review of the literature, with focus on shoulder injury caused by manual wheelchair propulsion, how the biomechanics of wheelchair propulsion can be measured and how manual wheelchair propulsion can be optimised to minimise injury risk. This chapter includes an introduction of the currently available instrumented wheelchair wheels, to enable comparison with the Sensewheel. Chapter 3 reports a systematic review of the literature, investigating the influence of real time feedback on wheelchair propulsion biomechanics. Chapter 4 introduces the design and measurement capabilities of the Sensewheel, in addition to identification of its current limitations and requirement for future development.   The Sensewheel is used in each of the subsequent experimental chapters.

The first experimental chapter (Chapter 5) examines age related differences in wheelchair propulsion biomechanics and muscle activity levels of non wheelchair users during propulsion on an ergometer. Chapter 6 measures shoulder joint demand experienced by manual wheelchair users during over ground propulsion, including level, cross slope and incline tasks. This chapter also investigates the relationship between force applied to the wheelchair push rim and shoulder joint demand. Chapter 7 investigates the differences in propulsion technique demonstrated by novices and expert manual wheelchair users, to identify key propulsion parameters associated with effective technique. Chapter 8 reports the results of an intervention aimed at improving technique during over ground manual wheelchair propulsion via provision of real time verbal feedback. Chapter 9 combines and summarises the findings of the experimental chapters, identifies limitations and suggests future research possibilities in view of the results presented and concludes the thesis.

Chapter 2 Background

2.1 Overview

This chapter begins by identifying a clinical problem within an ageing population, that there exists a high incidence of shoulder pain among manual wheelchair users. To provide a background to this clinical problem, shoulder joint anatomy and normal biomechanics are introduced. The mechanisms by which the shoulder joint is injured are then presented, and the direct evidence linking wheelchair propulsion and injury is discussed. Methods of biomechanical analysis to quantify upper limb demand during manual wheelchair propulsion are reported, and techniques for optimising propulsion are considered. Finally, conclusions are made, highlighting areas in which further investigation is required.

2.2 Upper extremity pain in manual wheelchair users

Upper extremity pain is common among manual wheelchair users, with the shoulder, elbow and wrist joints potentially affected (Dalyan et al., 1999). Shoulder pain is most common, with a reported incidence ranging from 42% (Dalyan et al., 1999) to 66% (Fullerton et al., 2003). Rotator cuff injury is the most commonly identified shoulder injury (Akbar et al., 2010). In a study comparing the Magnetic Resonance Imaging (MRI) scans of 100 paraplegic participants (Spinal Cord Injury level T2-L3) versus 100 aged matched controls, the prevalence of rotator cuff tear was significantly greater in the paraplegic group (63% vs. 15%) (Akbar et al., 2010). The majority of the tears were to the supraspinatus muscle (SS), but tears to the infraspinatus (IS) and subscapularis (SSc) tendons were also identified. The results of the study also demonstrated a greater prevalence of GH joint OA in the paraplegic group (19% vs. 1%) and a greater prevalence of acromioclavicular (AC) joint OA in the paraplegic group (42% vs. 26%). Other reported MRI findings in manual wheelchair users include subacromial spur formation and coracoacromial ligament thickening (Boninger et al., 2003, Mercer et al., 2006). Manual wheelchair propulsion is thought to cause shoulder injury due to repetitive loading of the shoulder joint (Boninger et al., 2005a) and

shoulder injury is positively associated with increasing age and length of time as a manual wheelchair user (Akbar et al., 2011). Manual wheelchair users rely on their upper limbs for independent and functional mobility including transfers, so shoulder pain and injury can have a significantly negative impact. A study investigating 80 manual wheelchair users reported a significant inverse relationship between reported pain intensity and subjective quality of life and physical activity scores (Gutierrez et al., 2007).

2.3 Disability in the UK; an ageing population

It is estimated that 19% of the UK population live with a disability, of which approximately 8% use a manual wheelchair for mobility, which equates to approximately one million people (Papworth Trust, 2013). The UK population is ageing, both in terms of the median age and also the proportion of older people in the population. It is predicted that by the year 2035, 23% of the UK population will be aged 65 and over (Office for National Statistics, 2012). It is therefore evident that the number of wheelchair users will also increase.

People can become wheelchair dependent due to a sudden onset of disability caused by Spinal Cord Injury (SCI), cerebrovascular accident or lower limb amputation, or due to gradual onset of progressive disability caused by OA and progressive neuromuscular diseases (Requejo et al., 2015). Under such circumstances, wheelchair provision can improve functional independence (Hoenig et al., 2003); however insufficiency in terms of optimisation of the user and the wheelchair can lead to upper extremity dysfunction which can lead to reduced mobility and quality of life (Requejo et al., 2015). A review presenting 'evidence-based strategies for preserving mobility of elderly and ageing manual wheelchair users' advises prescribing wheelchair users with a customisable wheelchair to allow optimal positioning, and also optimising propulsion technique to minimise the repetition and forces required to complete a task (Requejo et al., 2015).

To understand how the demands placed on the shoulder should be quantified, and also how wheelchair propulsion technique can be optimised

to minimise injury risk, it is important to understand how the 'healthy' shoulder functions, and how manual wheelchair propulsion can cause dysfunction and injury.

2.4   Shoulder joint anatomy and biomechanics

In this section, the normal anatomy and biomechanics of the shoulder joint will be introduced, with particular focus on the stabilising effect of the rotator cuff complex.   An understanding of this mechanism is vital, as rotator cuff injury is the most commonly reported injury following sustained manual wheelchair use (Akbar et al., 2011, Akbar et al., 2010).   The biomechanical effect of rotator cuff deficiency will be presented and the mechanism via which rotator cuff degeneration and injury occur will be discussed, with consideration to the potential contribution of manual wheelchair propulsion. The secondary effect of the altered biomechanics caused by such an injury will also be introduced.

2.4.1   Joints of the shoulder girdle

The shoulder girdle is comprised of the GH joint, the AC joint, sternoclavicular joint and scapulothoracic articulation (Terry and Chopp, 2000).   The GH joint is highly mobile due to the relatively large size of the humeral head with respect to the glenoid fossa, with only 25% to 30% of the humeral head in contact with the glenoid at any time (Terry and Chopp, 2000).   The benefit of this anatomy is that the GH joint enables combined movement throughout 3 planes.   A combination of both passive and active restraints are required to maintain GH joint stability (Terry and Chopp, 2000).

2.4.2   GH joint stability: passive restraints

The passive restraints include the glenoid labrum, the joint capsule and joint ligaments. The glenoid labrum is a fibrous structure attached to the glenoid acting to enhance stability by deepening the concavity in which the humeral head articulates (Howell and Galinat, 1989). In the superior inferior direction, the labrum contributes 50% of the depth of the socket and in the anterior

7

posterior direction, the labrum contributes up to 60% of the depth of the socket (Howell and Galinat, 1989). The glenoid fossa and glenoid labrum are shown in figure 2-1. The shoulder joint capsule is a continuous layer of fibrous tissue that surrounds the GH joint that tightens to assist in stabilising the joint in extremes of movement (Terry and Chopp, 2000). The stabilising ligaments at the GH joint include the coracohumeral ligament and the superior, middle and inferior GH ligaments (Terry and Chopp, 2000). The main role of the coracohumeral ligament is to constrain movement in adduction, the superior GH ligament prevents inferior and posterior translation, the middle GH ligament limits anterior and inferior translation and the inferior GH ligament stabilises against anterior translation (Terry and Chopp, 2000). The shoulder joint capsule is shown in figure 2-2.
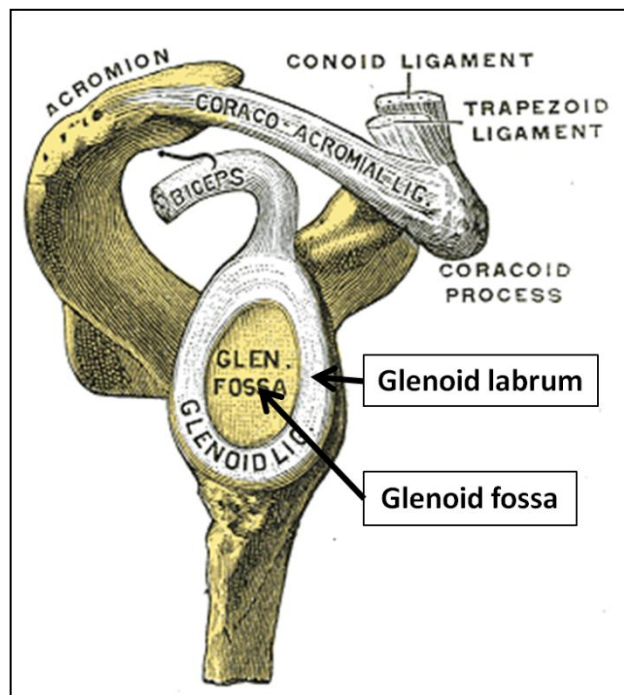
Figure 2-1: GH joint passive restraints – glenoid fossa and glenoid labrum (Gray's Anatomy of the Human Body (1918)).
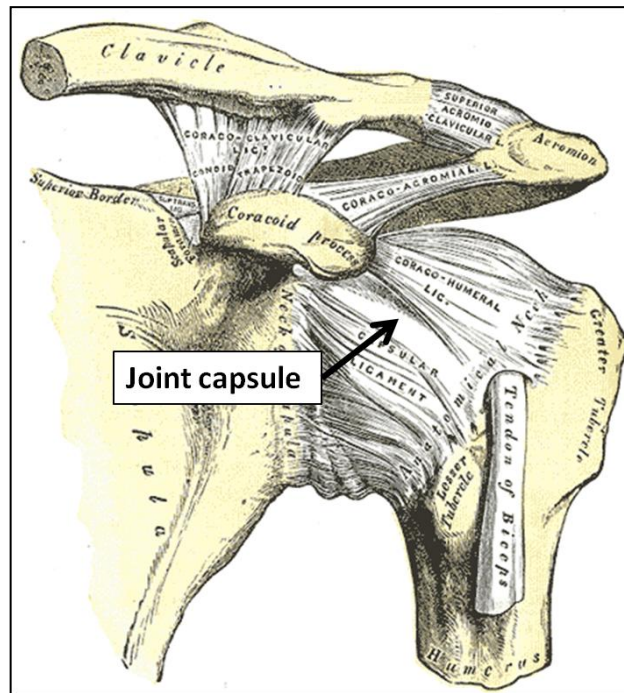
Figure 2-2: GH joint passive restraints: capsule and ligaments (Gray's Anatomy of the Human Body, (1918)).

2.4.3 GH joint stability: active restraints

The main dynamic constraint to aid GH joint stability is the rotator cuff complex, a group of muscles including the SS, IS, SSc and teres minor (TM) muscles. The rotator cuff muscles are shown in figures 2-3 and 2-4. The rotator cuff muscles provide dynamic stabilisation of the GH joint via concavity compression, in opposition to contraction of the prime movers of the shoulder joint, including the deltoid, pectoralis major (PM) and latissimus dorsi (LD) muscles (Terry and Chopp, 2000). An example of such a 'force couple', is the mechanism by which the rotator cuff complex maintains the humeral head in a centred position with respect to the glenoid in opposition to the cephalad movement of the humeral head as a result of deltoid muscle contraction (Bunker, 2002). If the rotator cuff muscle complex becomes dysfunctional, this mechanism of stabilisation is lost. Previous studies have demonstrated that disruption of the force couple, as occurs in rotator cuff tears, leads to increased translations and subluxations of the humeral head and also alterations in the direction and magnitude of joint reaction forces at the GH joint (Karas et al., 2011, Parsons et al., 2002, Thompson et al.,

1996). With this loss of the required stabilising function, increased anterior and superior migration of the humeral head can lead to secondary problems including hypertrophy of the coracoacromial ligament and formation of bone spurs on the under surface of the acromium (Bunker, 2002). In severe cases, the biomechanical changes caused by rotator cuff tears can result in rotator cuff tear arthropathy (De Wilde et al., 2004).
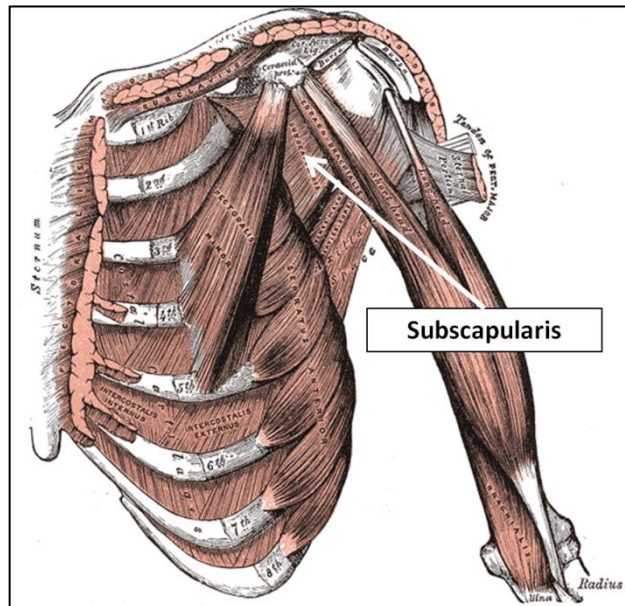
Figure 2-3: Anterior view of the shoulder girdle musculature (Gray's Anatomy of the Human Body, (1918)).
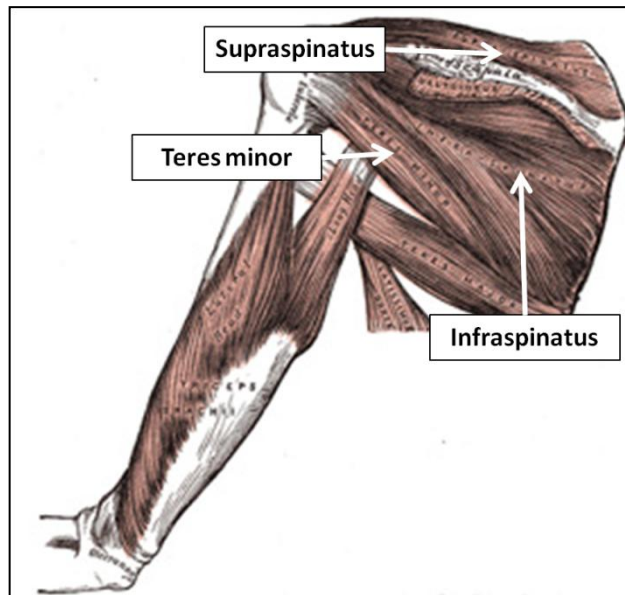
Figure 2-4: Posterior view of the shoulder musculature (Gray's Anatomy of the Human Body, (1918)).

2.5   Aetiology of rotator cuff degeneration and injury

The next section will introduce how the insight into the aetiology of rotator cuff degeneration has developed. Historically, it was proposed that rotator cuff degeneration and injury were caused by extrinsic mechanical compression of the SS tendon by the under surface of the acromion in the subacromial space (Bunker, 2002). It is now thought that this so called 'impingement' is actually a symptom of rotator cuff degeneration, rather than the cause. Bunker (2002) suggests that 'degeneration and/or overload of the collagen fibres of the tendon is the initiating factor in a pathological cascade, which ends in rotator cuff tear.' The author also suggests that if the rotator cuff becomes dysfunctional, the stabilising mechanism of the rotator cuff is lost and secondary extrinsic mechanical compression between the SS and acromion lead to the secondary changes observed.

2.5.1   Rotator cuff tendon degeneration

Previous literature has demonstrated a positive relationship between increasing age and increasing prevalence of rotator cuff tear (Tempelhof et al., 1999). Cadaveric studies have also demonstrated a significant increase

in muscle degeneration and related muscle tears of the rotator cuff during the seventh decade of life (Ozaki et al., 1988). Degenerative histological changes include loss of cellularity, loss of vascularity, loss of fibro cartilage mass (Kannus and Jozsa, 1991) and thinning and disorientation of the collagen fibres (Hashimoto et al., 2003).

2.5.2 Micro trauma theory

A positive association has also been demonstrated between mechanical overuse and rotator cuff tear (Nho et al., 2008). It is theorised that repeated loading of the tendon leads to injuries within the tendon that are not given time to heal, eventually leading to muscle tears (Nho et al., 2008). This theory is supported by animal models. Soslowsky et al., (2000b) overloaded the shoulders of a group of rats by enforcing a treadmill training regime. The results demonstrated histological findings consistent with degenerative change, including change in cell shape and decrease in organisation of collagen fibres when compared to the control group.

In summary, it is evident that the rotator cuff muscles play a vital role in optimising shoulder joint biomechanics. Rotator cuff injury is associated with increasing age and repetitive loading, and such injuries can lead to secondary complications. These findings are in accordance with the data presented specific to manual wheelchair users, that rotator cuff injury is most common (Akbar et al., 2010) and that such injuries are associated with increasing age and time as a wheelchair user (Akbar et al., 2011). The findings highlight the importance of quantifying the load placed on the shoulder complex and rotator cuff muscle during manual wheelchair propulsion, and how these loads are associated with injury.

2.6 Measurement of a direct link between manual wheelchair propulsion and injury

The previous sections have highlighted the high incidence of upper limb injury in manual wheelchair users and the impact such injuries can have on quality of life and functional capacity. The reported mechanisms behind the

most commonly reported pathologies have also been presented. This section will focus on investigating the evidence to support a direct link between manual wheelchair propulsion biomechanics and injury.

A systematic review of the literature was completed to identify literature investigating the link between manual wheelchair propulsion and shoulder injury. The electronic databases PubMed, Web of Science, Science Direct, Cochrane Library and IEEE Xplore were searched, including their full archive history to May 2015, using the following search terms:

Shoulder injury AND biomechanics AND manual wheelchair propulsion

The titles and abstracts of all studies identified were reviewed and if matching the review inclusion criteria full text articles were obtained and reviewed. The reference lists of all selected full text articles were also reviewed. The inclusion criteria for the review were as follows:

- Clinical or controlled trial
- Investigated manual wheelchair users
- Included quantitative measures of manual wheelchair propulsion biomechanics (propulsion kinetics, joint kinematics, EMG, joint kinetics)
- Reported links between biomechanical outcome measures and shoulder injury, including clinical assessment and medical imaging

The literature review process is summarised in the figure below.

```
Records identified, Web of Science: 86, PubMed: 19,
Science Direct: 19, Cochrane library: 0, IEEE Xplore: 7
```

```
38 duplicate          90 articles excluded on
articles excluded     review of abstract
```

```
Full text articles assessed for eligibility (n = 3)
```

```
1 article identified from reference list
on full text review
```

```
Studies included in qualitative
synthesis (n = 4)
```
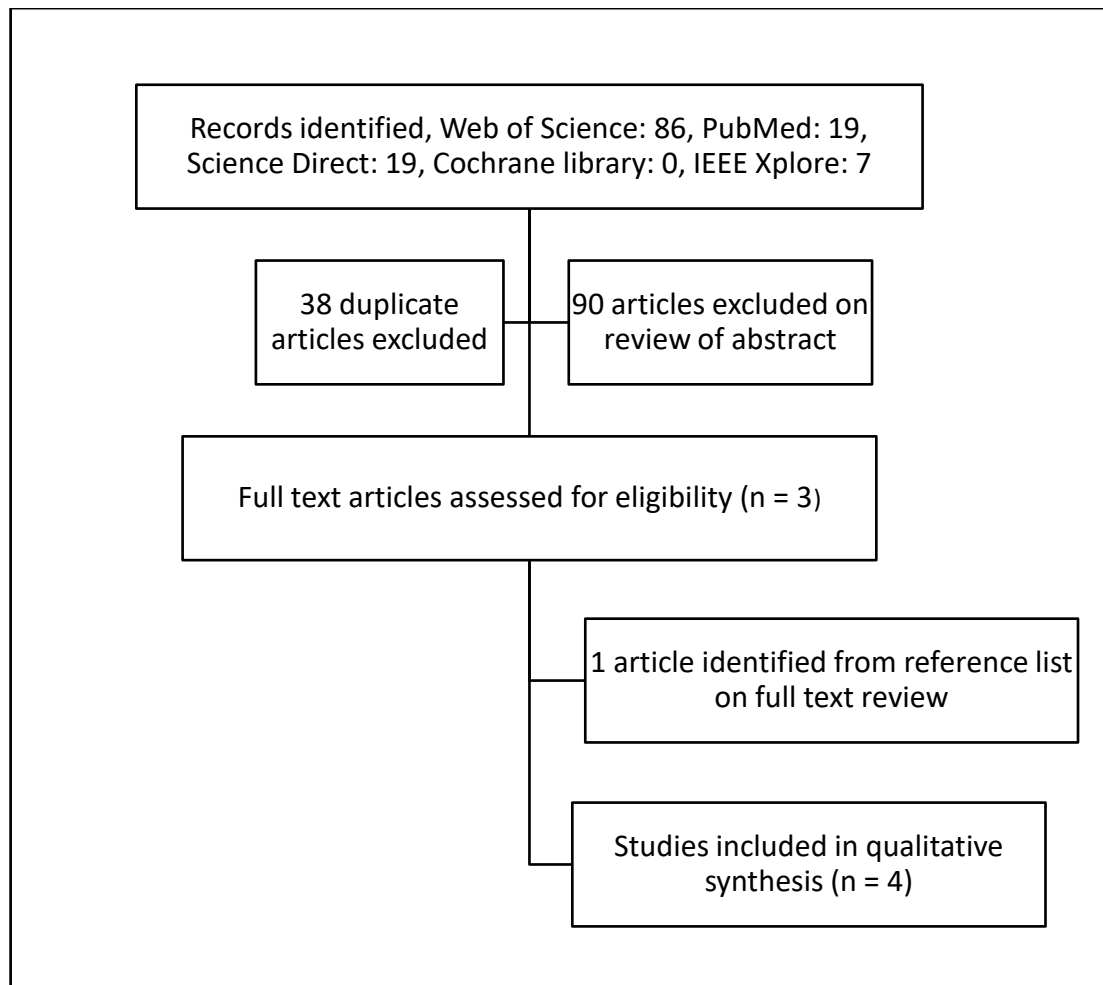
Figure 2-5: Flowchart of literature review process investigating the direct link between manual wheelchair propulsion and shoulder injury.

On review of the literature, 4 studies were identified that investigated whether biomechanical parameters were associated with measures of shoulder joint injury (Boninger et al., 2003, Collinger et al., 2010, Gil-Agudo et al., 2014, Mercer et al., 2006).

Boninger et al., (2003) completed a longitudinal case series, performing a baseline assessment of dynamometer propulsion at 0.9 and $1.8\text{m}^{\cdot}\text{s}^{-1}$ and bilateral shoulder MRI scans at both baseline and at a second visit after 2 years. The MRI scans were used to assess for rotator cuff tears, AC joint degeneration, subacromial spur formation and coracoacromial ligament thickening. Participants were retrospectively divided into 2 groups, those demonstrating an increase in MRI abnormalities over the 2 year follow-up

period, and those who did not. The results demonstrated a positive association between weight normalised radial propulsion force (directed from the push rim to the wheel hub) and an increase in MRI findings. This study does not detail the specifics of the MRI abnormalities detected, so it is not possible to determine if, as theorised rotator cuff degeneration preceded the secondary degenerative changes. In addition, as the study did not control for potential confounding variables such as volume and variety of pushing completed in the follow up period, it is not possible to determine whether greater radial force was the main cause of injury.

Mercer el al., (2006) also analysed shoulder injury using MRI. 33 participants completed a similar test protocol to Boninger et al., (2003), propelling their own wheelchairs on a dynamometer at 0.9 and 1.8m$\cdot$s^{-1}. The authors applied experimental data from an instrumented wheel to an inverse dynamic model to calculate joint forces and moments. The review of MRI scans included assessment for rotator cuff tears, AC joint degeneration; subacromial osseus spur formation and coracoacromial ligament thickening. The authors excluded rotator cuff tear from the analysis as only 1 case was reported, and did not include any measure of rotator cuff degeneration. The results demonstrated that higher posterior force was linked to coracoacromial ligament oedema and higher lateral forces to coracoacromial ligament thickening. During this study, the experimental data and MRI images were collected at a single visit, so it is not possible to deduce whether the observed biomechanical changes were a potential cause of the observed injuries, or a secondary effect of them.

Collinger et al., (2010) used grayscale-based quantitative ultrasound scanning to assess for immediate soft tissue changes following wheelchair propulsion. The authors highlight that ultrasound can be used to identify markers of soft tissue change that are associated with risk of long term injury. The study examined 22 manual wheelchair users, who were required to complete a 15 minute over ground propulsion task (3 x 4 minute trials with a 90 second rest). Ultrasound imaging of the SS and long head of biceps tendon were completed before and immediately after the propulsion task and

at 5 minute intervals until 30 minutes after the propulsion task had finished. Although increased resultant force at the push rim was associated with tendon changes in the long head of biceps, this was not the case for the SS tendon. The authors question their method of transverse imaging of the SS tendon, which was chosen as it offers the most consistent view for analysis. It is suggested that future studies, the SS tendon should be imaged longitudinally to provide the best view of collagen fibre organisation.

Gil-Agudo et al., (2014) also used ultrasound imaging to diagnose shoulder pathology following wheelchair propulsion. In this study, 14 participants performed both high and low intensity manual wheelchair propulsion on a wheelchair treadmill. Push rim and motion analysis data were applied to an inverse dynamic model to calculate net shoulder joint forces and moments. The ultrasound scans were analysed differently to those collected by Collinger et al., (2010), focusing on anatomical measurements, for example tendon thickness and also estimates of tendon elasticity. The results demonstrated no significant differences in ultrasound parameters after wheelchair propulsion. The authors conclude that using grayscale-based quantitative ultrasound (Collinger et al., 2010) to identify markers of microscopic damage would be beneficial, ahead of the more global measures used.

In summary, the studies using MRI to quantify shoulder injury suggested an association between peak forces applied to the push rim and peak joint forces and shoulder injury. The study by Mercer et al., (2006) was not a longitudinal study, so cause or effect cannot be determined. The study by Boninger et al., (2003) was longitudinal, but potential confounding variables in the follow-up period were not considered, so the presented association between biomechanics and injury should be interpreted with caution. The studies using ultrasound to quantify tendon changes used better methods as they assessed for tendon changes immediately following cessation of wheelchair propulsion. However, these studies were unable to associate wheelchair propulsion biomechanics with SS tendon changes. It is possible that the wheelchair propulsion tasks were not hard enough in intensity and

duration to cause significant changes. It is also possible that the ultrasound technique used by Gil-Agudo et al., (2014) was not sensitive to any changes that may have occurred. Moving forward, grayscale-based ultrasound imaging appears to be the modality of choice as it was able to detect microscopic changes in the long head of biceps tendon. Alternative approaches to imaging the SS have been suggested (Collinger et al., 2010). Additionally, although logistically challenging, longitudinal studies commencing when participants first start using a manual wheelchair, combining biomechanical assessment and repeat imaging would be optimal.

2.7 Biomechanical analysis of manual wheelchair propulsion: quantifying upper limb demand

It is clear that there is limited evidence available to directly link the demands of manual wheelchair propulsion and shoulder joint pathology. What is known is that the prevalence of rotator cuff degeneration is greater in manual wheelchair users compared to aged matched controls (Akbar et al., 2010) and that within a population of manual wheelchair users, rotator cuff degeneration is associated with increasing age and time as a wheelchair user (Akbar et al., 2011). In addition, models of tendon degeneration support the theory that tendon micro trauma is caused by repetitive overloading of the tendon (Nho et al., 2008). It is therefore assumed that to minimise risk of injury, both repetition and peak force application should be minimised during manual wheelchair propulsion (Boninger et al., 2005a, Sawatzky et al., 2015). With this assumption in mind, there is a large body of biomechanical evidence available that has been used to both quantify upper limb demand during various propulsion tasks and also provide a measure of outcome to quantify the success of interventions. The biomechanical analysis methods used include measurement of force applied to the push rim using instrumented wheelchair wheels, measurement of joint kinematics using motion capture and inertial measurement systems and also measurement of muscle activity levels and activation patterns using EMG. This experimental data has then been used to drive musculoskeletal models, in order to provide an estimate of both joint moments and joint contact forces.

The next section will introduce the biomechanical methods used to quantify upper limb demand.

2.7.1 Push rim kinetics: instrumented wheelchair wheels

The development of instrumented wheelchair wheels has enabled analysis of the forces applied by the user to the wheelchair push rim. Such data has been used to measure the demand of various tasks, quantify propulsion technique and generate data to animate musculoskeletal models. The SmartWheel is commercially available and is capable of measuring three dimensional force and torque applied to the wheelchair push rim and weighs 4.08kg (Cowan et al., 2008). The OptiPush instrumented wheelchair wheel also measures three dimensional force and torque, transmitting data via Bluetooth and weighs 5.7kg (Richter et al., 2011). The weight of the currently available instrumented wheelchair wheels is a major limitation, as the total weight addition to the chair ranges from 8kg to 12kg, having a significant impact on the forces required to push the chair (Boninger et al., 1999). To improve the validity of the biomechanical analysis of manual wheelchair propulsion, a lightweight instrumented wheelchair wheel would be beneficial. Selected characteristics of the SmartWheel and OptiPush instrumented wheelchair wheels are presented in table 2.1.

Table 2.1: Selected characteristics of the SmartWheel and OptiPush instrumented wheelchair wheels.

	SmartWheel	OptiPush
Weight	4.08kg	5.7kg
Available wheel sizes	22, 24, 25 and 26 inches	20 to 26 inches
Sampling frequency	240Hz	200Hz
Communication type	2.4 GHz Wi-Fi	Bluetooth
Battery type	9V alkaline	7.4V 2600mAh Li-ion
Battery life	3+ hours	3+ hours
Cost	~ £13000	Not specified

2.7.1.1 Instrumented wheelchair wheels: the propulsion cycle

Data recorded using instrumented wheelchair wheels can be used to analyse both the kinetic and temporal aspects of wheelchair propulsion. For the purpose of analysis, the wheelchair propulsion stroke cycle is divided into the contact phase (initial contact, propulsion and release) and the recovery phase (Kwarciak et al., 2009) (Figures 2-6 and 2-7).
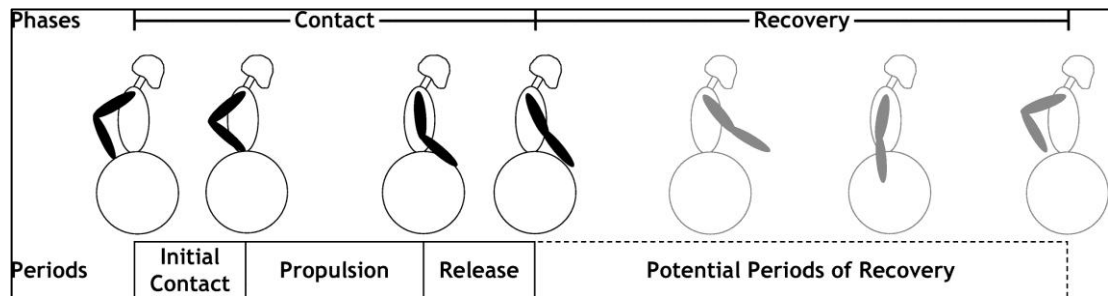
Figure 2-6: The manual wheelchair propulsion stroke cycle (Kwarciak et al., 2009).

Kwarciak et al., (2009) defines the different phases of the propulsion cycle as follows:

- Initial contact: hand contact without propulsive moment, the interval between the onset of force application and the onset of propulsive moment.
- Propulsion period: the interval between the onset and cessation of propulsive moment.
- Release period: hand contact without propulsive moment, the interval between the cessation of propulsive moment and total force on the push rim.
- Recovery phase: the interval when no force is applied.
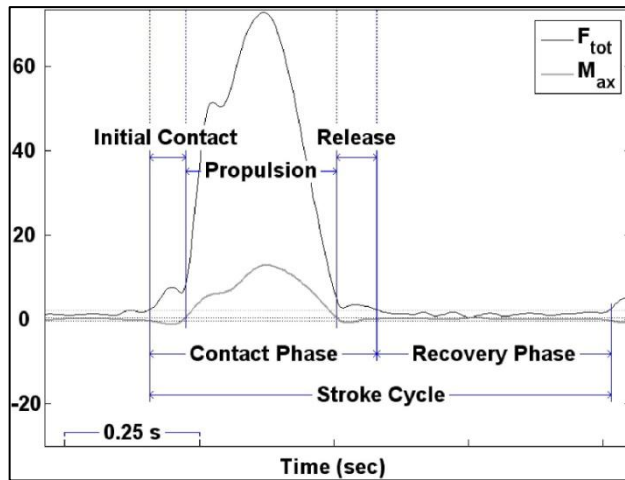
Figure 2-7: The different phases of the manual wheelchair propulsion cycle (Kwarciak et al., 2009) (Y-axis shows force/moment).

The push phase is either determined by measurement of wheel moment above 0 Nm (de Groot et al., 2002) or measurement of a positive resultant force (Sabick et al., 2004). Cowan et al., (2008) reported that greatest peak force occurs during the second push of the 'start-up' process and that 'steady state' propulsion is achieved after the third push.

2.7.1.2 Instrumented wheelchair wheels: commonly reported parameters

Cowan et al., (2008) identified four key parameters to be measured during the analysis of wheelchair propulsion, including velocity, average peak resultant force, push frequency and push arc (Table 2.2). These suggestions are based on the guidelines for preservation of upper limb function following SCI (Boninger et al., 2005a). Fraction of effective force (FEF) is also commonly reported (Desroches et al., 2008a), and is calculated by measuring the ratio of total force applied horizontally to the push rim (Arnet et al., 2012). In terms of measurement of the capacity of the wheelchair user, peak and mean power, and work per cycle have been reported (Mason et al., 2012c).

Table 2.2: Key manual wheelchair propulsion measurement parameters (Cowan et al., 2009).

Parameter	Description
Average velocity ($m \cdot s^{-1}$)	Average velocity during the measured push strokes
Average peak resultant propulsion force (N)	The resultant force is the vector sum of the force applied to the push rim by combining tangential force (F_x), radial force (F_y) and axial force (F_z)
Push rate (s^{-1})	The frequency of push rim contact, in contacts per second
Push arc (°)	The distance travelled by the hand on the push rim from the point of contact to the point of release, measured in degrees

2.7.2 Measurement of trunk and upper limb kinematics during manual wheelchair propulsion

Trunk and upper limb kinematics during manual wheelchair propulsion have been widely examined using motion analysis systems. The wheelchair propulsion stroke is a repetitive motion. At the start of the push phase, the GH joint is positioned in extension, abduction and internal rotation (Collinger et al., 2008). During the push phase, the GH joint moves into flexion, adduction and external rotation. By the end of the push phase, the GH joint is in a position of flexion and relatively less abduction and internal rotation compared to the start of the push phase (Boninger et al., 1998). During the recovery phase, the GH joint moves into extension, abduction and internal rotation (Mulroy et al., 1996). The measurement of trunk and upper limb kinematics has been used for different purposes including assessment of potentially injury causing postures (Boninger et al., 2005a, Morrow et al., 2011), analysing propulsion technique (de Groot et al., 2003) and to generate experimental input for musculoskeletal models to estimate joint moments and contact forces (Morrow et al., 2010a, Morrow et al., 2010c). The majority of studies utilise laboratory based motion capture systems to analyse

wheelchair propulsion kinematics during treadmill or ergometer propulsion (Gagnon et al., 2015).   Laboratory based optoelectric motion analysis systems are considered the 'gold standard', but are limited as they are restricted to the laboratory, expensive to purchase and require expert technicians to support their use (Reininga et al., 2011). Such systems can be used to measure kinematics during over ground propulsion (Morrow et al., 2010a), but their limited range of analysis dictate that is it not possible to analyse 'real life' pushing experience. Inertial measurement units (MIMU's) attached to the body of the wheelchair user offer the potential to record the kinematics of wheelchair propulsion in more complex environments away from the laboratory setting.

2.7.2.1 The use of inertial measurement units in biomechanical analysis

MIMU's are sensors that integrate data from gyroscopes, accelerometers and magnetometers and can be used to track human kinematics (Kobrick et al., 2012). Through the application of sensor fusion algorithms, the orientation of the unit (and hence that of the body part to which it is attached) is known with respect to a global coordinate system (Ferrari et al., 2010).   The use of MIMU's in biomechanical analysis is increasing. The use of MIMU's in gait analysis has been proposed, a previous study having compared the accuracy of MIMU's versus an optoelectronic system (Vicon measurement system, Oxford Metrics Group, UK) during over ground walking in 4 healthy participants (Ferrari et al., 2010).   The results demonstrated median differences in joint angle up to 1.5˚, with a range up to 5˚ difference. The potential use of MIMU's in the measurement of pathological gait pattern has also been examined.   Reininga et al., (2011) examined the accuracy of MIMU's versus the Optotrak motion analysis system (Optotrak, Northern Digital Inc, Waterloo, Canada); in 3 participants with end stage Osteoarthritis of the hip during over ground walking. The results demonstrated small mean differences (<1.0˚) between the MIMU's and the optical system. Body worn MIMU's have also been promoted as a potential clinical assessment tool for detecting balance and gait deficit in multiple sclerosis patients (Spain et al., 2012).

2.7.2.2 The use of inertial measurement units: upper limb kinematics and manual wheelchair propulsion

The use of MIMU's for the kinematic analysis of the trunk and upper limb has also been examined (Cutti et al., 2008). This study evaluated a single subject performing a number of uni-planar movements of the shoulder and elbow joints. The results from the inertial measurement units were compared with data from an optoelectronic system (Vicon) by the calculation of Root Mean Square (RMS) error and correlation coefficient. For the shoulder joint, the anatomical system of reference was established during a static trial, with the arms held in a neutral position with respect to the thorax. At the elbow joint a trial of repeated flexion and extension was used to estimate the flexion/extension axis and a trial of repeated pronation and supination used to estimate the pronation/supination axis. These estimations were then used to calculate elbow joint angle. In terms of measurement of main joint angles, the results demonstrated a correlation coefficient greater than 0.94 between the 2 measurement methods. The accuracy of MIMU's for upper limb measurement has also been tested against a camera based motion capture system, during an examination of 3 healthy participants (Hooke et al., 2009). At the shoulder joint, the study reported a RMS error of 3.97˚ for flexion/extension, 2.88˚ for abduction/adduction and 3.60˚ for internal and external rotation. At the elbow joint, the study reported a RMS error of 4.72˚ for flexion and extension, and 3.54˚ for pronation/supination at the radioulnar joint. MIMU's have also been used to assess the upper limb kinematics of experienced and inexperienced manual wheelchair users during agility and sprint tests (Starrs et al., 2012), but the mathematical method of joint angle calculation is not presented.

Whilst it is clear that MIMU's will not be able to provide the measurement accuracy of an optoelectronic system, it is apparent that they are able to provide a reasonably accurate measurement of the orientation of one body segment with respect to another, therefore providing a useful approximation of joint kinematics during 'real life' activities.

2.7.3 Surface EMG

Surface EMG is used in biomechanical analysis to measure muscle activation pattern, relative muscle activity and muscle fatigue (De Luca, 1997). Surface EMG can be used in the clinical setting as it is safe and easy to use in comparison to fine wire EMG.

2.7.3.1 Surface EMG: normalising the raw EMG signal

In the summary article by De Luca (1997), the author highlights the limitations of surface EMG measurements, in terms of quantification of muscle demand. An established relationship exists between EMG signal and muscle force during isometric contractions, but this is not the case during anisometric contractions.   This means that analysis of anisometric contractions, such as those measured during manual wheelchair propulsion, is limited to qualitative observation of whether a muscle is more active from task to task. For such comparison between participants, normalising the raw EMG signal to that recorded during a maximal voluntary isometric contraction (MVIC) is required.   Normalisation of the raw EMG signal (numerator) is completed by division by a reference value (denominator), which is commonly measured during the task, or from a MVIC. It has been debated how to normalise the raw EMG signal for between subject comparisons (Burden, 2010). Burden (2010) identifies 8 commonly used normalisation methods, and reviews their effect on the magnitude and inter and intra-individual variability of results. It is concluded that although using peak or mean values from the task to normalise the raw signal minimises inter-individual variability, this method should not be used for between task or individual comparison, as when the numerator rises, so will the denominator, so any increase in demand will be missed. It is therefore suggested that the MVIC method be used to provide information on how active a muscle is relative to its maximal capacity.

2.7.3.2 Surface EMG during manual wheelchair propulsion

EMG analysis has demonstrated that during the push phase of manual wheelchair propulsion, the muscles responsible for GH joint flexion and adduction (Anterior Deltoid (AD) and PM) and external rotation (IS) are active. During the recovery phase, the muscles responsible for extension (Posterior Deltoid (PD)), abduction (Middle Deltoid (MD)) and internal rotation (SSc) are active (Mulroy et al., 1996). At the elbow joint, during flexion in the early push phase the Biceps Brachii (BB) is active, and then from the middle of the push phase moving into the recovery phase, the Triceps Brachii (TB) muscle is active as the elbow joint extends (Mulroy et al., 1996). The SS muscle is also active during the push phase of manual wheelchair propulsion (Mulroy et al., 1996, Lighthall-Haubert et al., 2009).

2.7.3.3 Surface EMG during manual wheelchair propulsion: the rotator cuff

Assessing the activity level of the rotator cuff muscles is of particular interest during manual wheelchair propulsion. Rotator cuff injury is very common in manual wheelchair users (Akbar et al., 2010) and caused by repetitive overloading of the tendon (Soslowsky et al., 2000a, Nho et al., 2008). The anatomical position of the rotator cuff muscles mean that surface EMG reading may be altered by cross-talk from other over lying muscles, so it is important to consider whether recording rotator cuff activity using surface EMG is valid. The SS muscle is most commonly injured (Akbar et al., 2010), so it would be useful to measure demand placed upon the muscle. Previous research has demonstrated that surface EMG readings significantly over estimate fine wire readings for the SS muscle during resisted contractions (Waite et al., 2010). The IS muscle is the most accessible rotator cuff muscle for measurement using surface EMG. Surface EMG measurement of the IS has been shown to be valid in comparison to fine wire EMG when the muscle is moderately to highly active, but not when it is minimally active (Johnson et al., 2011). During moderate to high muscle activity level, surface and fine wire readings were similar, but during lower level muscle activity, the surface EMG recorded a significant overestimate. This suggests that that during the

push phase of wheelchair propulsion when the IS is known to be active, surface EMG measurement is valid. However determining activation pattern of the muscle may be inaccurate, as activity level during the recovery phase may be an overestimate.

2.7.3.4 Surface EMG during manual wheelchair propulsion: detecting muscle activation

Two methods have been previously used to detect muscle activation during manual wheelchair propulsion. The first records EMG during maximal voluntary isometric contraction (MVIC) of the muscle in question. During wheelchair propulsion, the muscle is considered to be active when it reaches 5% of MVIC for a time period of more than 5% of the propulsion cycle (Mulroy et al., 1996). This technique is limited as muscle activation during a task can exceed that recorded during the isometric test (Wilen et al., 2002). The second option is to calculate baseline 'noise' at rest and classify the muscle as active when the EMG signal increases above this baseline for a set period of time (Wilen et al., 2002, Hodges and Bui, 1996).

2.7.3.5 Surface EMG during manual wheelchair propulsion: previous research

Previous studies have used EMG to measure muscle activity during manual wheelchair propulsion. A number of studies assessed muscle activity using indwelling, fine-wire EMG assessment (Lighthall-Haubert et al., 2009, Mulroy et al., 1996, Mulroy et al., 2004, Requejo et al., 2008), whereas the majority use surface EMG. Studies have previously used EMG to quantify the effect of a variety of variables on muscle activity during manual wheelchair propulsion, including intensity of the task (Bernasconi et al., 2007, Chow et al., 2000, Qi et al., 2012a, Qi et al., 2012b), propulsion technique (Chow et al., 2001, Kwarciak et al., 2012), variable surfaces and slopes (Chow et al., 2009, Gagnon et al., 2015, Howarth et al., 2010, Kim et al., 2014), experience of the user (Dubowsky et al., 2009), type of chair (Howarth et al., 2010, Levy et al., 2004, Lighthall-Haubert et al., 2009) and wheelchair set-up (Louis and Gorce, 2010, Arnet et al., 2012).

The majority of studies assess wheelchair propulsion on an ergometer or treadmill. The studies assessing over ground propulsion (Chow et al., 2009, Howarth et al., 2010, Kim et al., 2014, Levy et al., 2004) differ in their methods of analysis and presentation of results.

The study by Chow et al., (2009) assesses the muscle activity levels of 10 paraplegic participants when climbing a 7.3m wooden ramp at self selected normal and fast speeds with progressive increases in slope. The raw EMG signal is normalised to MVIC and the average EMG for the muscles measured are presented. At 'normal' speed, the mean activity level of the Anterior/middle Deltoid (AMD) muscle is approximately 5% and the PM muscle approximately 4%. Muscle activity level increases as the slope increases to a maximum during the 12° slope when the AMD muscle is approximately 38% active and the PM muscle approximately 36% active. This study is limited in that it does not measure activity of the SS or IS muscle and AMD activity rather than isolated AD activity is measured so the result is likely to be lower than AD activity measured in isolation due to lower activity of the MD during the push phase. In addition, although the study measures trunk and upper extremity kinematics, and derives push style parameters, push rim force is not measured.

The study by Howarth et al., (2010) tested the effect on muscle activity of geared, non-geared and standard wheels during climbing up a 2.44m wooden ramp at 4 different slopes. All participants were able bodied. Raw data was normalised to MVIC, and peak normalised muscle activity and integrated activity calculated. Peak muscle activity increased with increasing slope and reduced with the geared wheel, but the specific results cannot be examined more closely as the results assessing the effect of wheel type combine all slopes, and the results assessing the effect of slope level combine all wheel types. This study was also limited to kinematic analysis.

A further study by Kim et al., (2014) assessed the muscle activity of 30 able bodied participants climbing wooden ramps of different gradients, dividing the participants into groups of varied muscle strength. It is difficult to compare

27

the results with other studies, as the authors calculated 'total EMG' by calculating average normalised EMG, multiplied by time, but did not report peak muscle activity levels. The study by Levy et al., (2004) also presented results that cannot be compared with those from other studies. This study assessed the potential benefit of a push rim activated power-assist wheelchair wheel on propulsion performance of 11 elderly wheelchair users on a level surface, carpet and an incline. The power-assist chair was associated with reduced activity in 5 of 8 muscles tested, but the EMG was presented as mean rectified signal, not normalised to MVIC.

2.7.3.6 Surface EMG during manual wheelchair propulsion: a summary

Many studies have used EMG as an outcome measure to assess the effect of interventions to optimise wheelchair propulsion and minimise risk of injury. The majority of these studies utilise wheelchair ergometers and treadmills for such experiments, which is understandable as this enables potentially confounding variables such as speed and rolling resistance to be controlled. Analysis of over ground propulsion is vital, both to provide information about the demand placed on wheelchair users during daily activity and also to assess whether suggested optimisation interventions apply in this environment. A number of studies have assessed over ground propulsion, but have some limitations to their methods. Further research is required to assess muscle activity during over ground propulsion over different terrain and tasks including cross slopes. In addition, integrated assessment including push rim parameters, kinematics and EMG is required so propulsion technique can be associated with muscle demand. It would also be useful to measure IS muscle activity, as it can be validly measured during the push phase of manual wheelchair propulsion using surface EMG, and therefore provides the best measure of rotator cuff muscle demand available using this technique.

2.7.4 Musculoskeletal modelling

Musculoskeletal modelling enables estimation of internal loading of the musculoskeletal system, including estimation of muscle forces, joint torques

and also magnitude and direction of joint contact forces (Delp et al., 2007). Both inverse and forward methods can be used to calculate musculoskeletal dynamics. In inverse dynamics, the motion of the system and external forces applied to it are known and the forces and moments required to generate that motion are calculated. In forward dynamics, these forces and moments are known and the resulting motions are calculated. Static optimisation techniques are commonly employed during inverse techniques, to solve the indeterminacy problem at the shoulder to provide muscle force estimations and enable calculation of joint contact forces (Morrow et al., 2010b). The main limitation of static optimisation is that it does not include the time dependent physiological properties of muscles (Morrow et al., 2014), whereas dynamic optimisation does (Anderson and Pandy, 2001). Anderson and Pandy (2001) compared the muscle forces derived from both static and dynamic optimization during simulation of a single cycle of normal gait. They reported similar results from both methods, and conclude that if aiming to measure muscle activity and joint contact forces, there is no reason to use dynamic ahead of static optimization. Morrow et al., (2014) performed a similar study, comparing static and dynamic optimization for predicting muscle force during a single push phase of manual wheelchair propulsion. The results demonstrated that overall, there was a good agreement in muscle forces predicted by dynamic and static optimization, although when analysed individually, some of the muscles demonstrated poor agreement. It is concluded that dynamic optimization may provide more accurate results for complex tasks.

The results suggest that when assessing manual wheelchair propulsion, despite its limitations, static optimisation is in agreement with dynamic optimisation in the overall estimation of muscle forces. In addition, the results of static optimisation can be combined with experimental data to estimate joint contact forces (Steele et al., 2012). The following section will introduce the inverse methods that can be used, and examine previous studies utilising inverse methods in the assessment of manual wheelchair propulsion. The studies using inverse dynamics will be summarised and those using joint contact analysis will be examined in detail.

2.7.4.1 Musculoskeletal modelling: Inverse dynamics

Inverse dynamics calculates the net generalised force at each degree of freedom in a musculoskeletal model. These generalised forces only account for the model motion and applied external force (OpenSim, 2012).

A number of studies have used inverse dynamic methods in the assessment of manual wheelchair propulsion. Mercer et al., (2006) reported an association between high shoulder joint forces and shoulder joint pathology. Increasing the speed of wheelchair propulsion has been shown to increase shoulder joint forces (Collinger et al., 2008), although fatigue was not found to lead to increases in shoulder joint forces or moments (Rodgers et al., 2003). In addition, significantly higher shoulder joint forces have been measured during over ground ramp propulsion (Morrow et al., 2010a). The major limitation of these studies is that force results from inverse dynamic methods do not represent joint surface loading, as they do not incorporate the contribution of muscle activity to this calculation.

2.7.4.2 Musculoskeletal modelling: static optimisation and joint reaction analysis

Other studies have advanced the accuracy of joint reaction force measurement with the addition of estimated muscle force contributions to inverse dynamic methods in the form of static optimisation. Static optimisation is an extension to inverse dynamics that further resolves the net joint moments into individual muscle forces at each instant in time (OpenSim, 2015a). Joint reaction analysis combines experimentally collected kinematics and external forces, with muscle forces required to generate joint torques calculated during static optimisation (Steele et al., 2012).

2.7.4.3 Musculoskeletal modelling joint reaction analysis of manual wheelchair propulsion: previous research

The table below summarises previous studies reporting GH joint contact forces during manual wheelchair propulsion.

Table 2.3: Summary of studies reporting GH joint contact force during manual wheelchair propulsion calculated using musculoskeletal modelling.

Author	Model used	Task description	Resultant GH joint contact force
Bregman et al., (2009)	Delft shoulder and elbow model	Level propulsion on wheelchair treadmill (0.83m·s^{-1})	340.6N
Dubowsky et al., (2008)	AnyBody software model (Based on Delft shoulder and elbow model)	Level propulsion on wheelchair ergometer (self selected speed)	334N
Morrow et al., (2010b)	Simm software model (Based on Holzbaur model)	Over ground propulsion: 10m level 10m ramp (1:12 incline) (5˚ gradient)	 702N 2555N
Sasaki et al., (2015)	nMotion musculoskeletal model	Level ergometer propulsion (0.56m.s^{-1}) Simulated 0˚ gradient Simulated 2˚ gradient Simulated 4˚ gradient	 863N 1519N 1827N
van Drongelen et al., (2005)	Delft shoulder and elbow model	Level propulsion on ergometer (0.83m·s^{-1})	350N
Veeger et al., (2002)	Delft shoulder and elbow model	Level propulsion on ergometer: 0.83m·s^{-1} at 10W 0.83m·s^{-1} at 20W 1.39m·s^{-1} at 10W 1.39m·s^{-1} at 20W	 800N 1050N 1000N 1400N

Each study used data gathered from an instrumented wheelchair wheel and motion capture system to run a musculoskeletal model to estimate GH joint contact force. The studies reported GH joint contact forces ranging from 334N during level ergometer propulsion (Dubowsky et al., 2008) to 2555N during over ground propulsion up a slope (Morrow et al., 2010c). The results for level propulsion vary widely; ranging from 334N (Dubowsky et al., 2008) to 1400N (Veeger et al., 2002). These differences are likely to be due to differences in peak push rim force application during the tasks; although this cannot be confirmed as the majority of studies did not report push rim kinetics (Dubowsky et al., 2008, Morrow et al., 2010c, van Drongelen et al., 2005). Differences in reported push rim kinetics can be used to explain the difference in GH joint contact forces measured between two of the studies. Bregman et al., (2009) reported a GH joint contact force of 340.6N during a propulsion task with a mean push force of 18.9N, whereas Veeger et al., (2002) reported a GH joint contact force of 1400N during a propulsion task with a mean peak force of 30.0N. The majority of the studies assessed wheelchair propulsion on either an ergometer or treadmill. Veeger et al., (2002) assessed 3 experienced manual wheelchair users during 4 different combinations of speed and power output. Increasing speed and power output resulted in increasing GH joint contact force. Morrow et al., (2010b) was the only study examined to investigate over ground wheelchair propulsion, assessing 12 experienced manual wheelchair users during level propulsion and when ascending a 1:12 incline ramp. This study demonstrated high contact forces during incline propulsion and demonstrates the necessity for further assessment of wheelchair propulsion biomechanics during more demanding tasks, including different slopes and inclines, for example bus access ramps.

2.7.5 Validity of musculoskeletal models

As with all simulated estimation of biomechanical data, it is important to consider whether the GH joint contact forces discussed in the previous section are valid. Bolsterlee et al., (2013) identified a number of weaknesses of the upper limb models available, including:

- Simplification of joint kinematics by reducing degrees of freedom
- Optimisation methods that ignore differences in muscle activation pattern
- Simplification of modelling or joint articulation around the shoulder girdle, including the highly complex interaction between scapular and thorax and AC and SC joints, due in part to the complexity of accurate kinematic analysis of the shoulder girdle.
- Limited modelling of GH joint stability.

In addition, before complex shoulder girdle kinematics can be applied to musculoskeletal models, modelling of the trunk, commonly represented as a rigid body, needs to be improved. Due to difficulties in model validation, the influences of these limitations on output data are hard to quantify, and absolute values should be interpreted with caution. Until models are validated, it is apparent that measuring relative change across different tasks, using the same model properties is most appropriate.

Attempts have been made to validate simulation data using data collected in vivo using instrumented prostheses. Westerhoff et al., (2011) examined GH joint contact forces during manual wheelchair propulsion of 6 participants with an implanted instrumented shoulder prosthesis. The participants propelled at different speeds and inclines up to a maximum of 7% on a treadmill. The results demonstrated that GH joint contact forces rarely exceeded 100% body weight during level and incline propulsion, although peak forces for one of the participants did reach 188% body weight (1568N). It is possible that GH joint contact forces during the tasks were not as high as those reported during simulations as the data was recorded from participants who required surgical intervention for GH joint degeneration. Is it possible that the force generating capacity of the muscles in these instrumented shoulders would be lower than that of healthy shoulders, so the joint contact forces would likely be lower. The participants may have transferred the demand to other muscles around the elbow joint and hip flexors.

In summary, it appears that whilst the data collected from a simulation should be interpreted with caution in absolute terms, an upper limb musculoskeletal model could be used to assess for relative change in joint loading during different manual wheelchair propulsion tasks.

2.8   Strategies for optimising manual wheelchair propulsion

The previous section introduced the biomechanical measures used by researchers to quantify upper limb demand during manual wheelchair propulsion.   The impact of propelling a manual wheelchair over different terrains and tasks on these measures of upper limb demand was then investigated.   The next section will investigate the literature reporting methods of reducing such demands during manual wheelchair propulsion. This will include a summary of optimisation of the wheelchair itself, in terms of type of chair and configuration to best suit the user.   The focus will be directed towards the research considering optimisation of technique, including the impact of wheelchair skills training and real time visual feedback to the user.   The review will also consider whether the beneficial effect of such strategies can be transferred to the variety of terrains and tasks experienced during over ground manual wheelchair propulsion.

2.8.1   Optimising manual wheelchair propulsion: the wheelchair, wheelchair set up and physical capacity of the user

There exists evidence to guide wheelchair users in terms of both type and set-up of the wheelchair components and also physical capacity of the user themselves.   Increased body weight is positively associated with shoulder forces during manual wheelchair propulsion (Collinger et al., 2008). Therefore manual wheelchair users are advised to maintain a healthy body weight and it is suggested that the lightest wheelchair possible is provided to the user.   In terms of wheelchair set-up, seat height leading to elbow joint extension ranging from 100˚ to 130˚ has been found to improve mechanical efficiency (van der Woude et al., 2009).   This lower seat position is beneficial as it enables propulsion with a greater push arc (Boninger et al., 2000).   A more forward axle position has been shown to reduce superiorly oriented

joint forces (Mulroy et al., 2005) and demand in the major propulsive muscles during the push phase of propulsion (Gutierrez et al., 2005). In terms of the wheelchair wheels, a wheel camber of 18˚ was found to improve propulsion force in wheelchair athletes (Mason et al., 2012b) and larger wheels (26-inch versus 24-inch) reduced physiological demand and resultant force (Mason et al., 2012a).

In terms of physical capacity, interventional studies with a strengthening component have reported a positive effect on reducing shoulder pain. Strengthening of the posterior shoulder musculature and stretching of the anterior shoulder soft tissue structures has been shown to result in a decrease in self reported pain among wheelchair users (Curtis et al., 1999). Strengthening and propulsion technique modification has also been shown to result in reduced pain and improved quality of life scores (Kemp et al., 2011). Mulroy et al., (2011) conducted a randomised controlled trial to assess the effect of an exercise and technique modification programme on pain, muscle strength and quality of life of manual wheelchair users with paraplegia. The twelve week strengthening regime focusing on adductor, external rotator and retractor muscles led to significant improvement in strength which is associated with a reduction in pain and improved quality of life.

2.8.2 Optimising wheelchair propulsion: propulsion pattern

A number of different propulsion patterns have been previously identified (See figure 2-8).

Semicircular   Arc   Single Loop Over   Double Loop Over
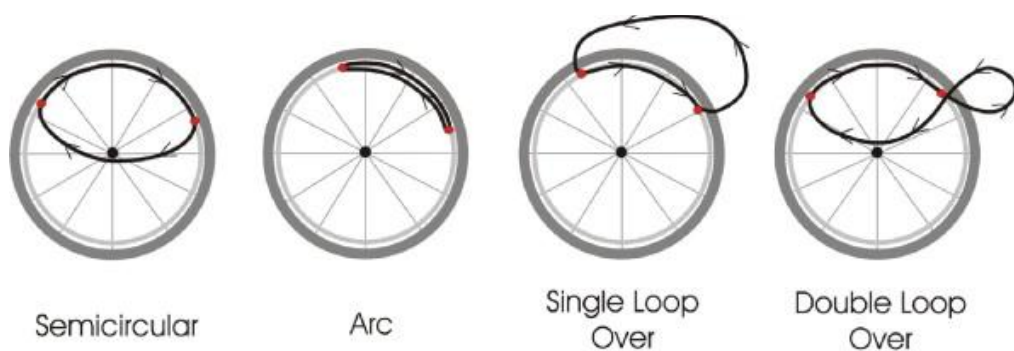
Figure 2-8: Examples of four different propulsion patterns (Koontz et al., 2009).

Manual wheelchair users are advised to use the semi-circular style of propulsion to minimise risk of injury (Boninger et al., 2005a) as this pattern has been associated with a reduction in push rate and greater propulsion efficiency (Boninger et al., 2002). However, research has demonstrated that during over ground propulsion, the semi-circular pattern is not always applied by wheelchair users (Koontz et al., 2009). During more challenging tasks such as climbing ramps, it may be more practical to follow and arcing pattern, keeping the hand close to the push rim to apply force as quickly as possible should the chair begin to roll backwards. It is apparent that enforcing a particular pattern may not be optimal for all terrains.

2.8.3 Optimising wheelchair propulsion: the influence of training and technique modification

Wheelchair skills training is provided to the majority of novice manual wheelchair users in the first year following SCI (Taylor et al., 2015). Morgan et al., (2015) conducted focus groups with both Health Care Professionals and experienced manual wheelchair users to investigate the importance of wheelchair skills for new wheelchair users. The focus groups identified the importance of instruction on optimal technique and education on negotiating accessibility barriers such as climbing curbs, ramps and also propelling the wheelchair over rough terrain. The groups also reported that the amount of wheelchair skills training provided is often too little, and failure to optimise skills can have a significant impact as improving manual wheelchair skills has been shown to be positively associated with participation in major life activities (Kilkens et al., 2005).

MacPhee et al., (2004) conducted a randomised controlled trial, assessing the influence of the wheelchair skills training programme. The study reported results from 35 wheelchair users, 20 with a musculoskeletal injury and 15 with neurological impairment, during the initial stages of rehabilitation. The intervention group received on average 4.5 sessions of wheelchair skills training lasting for 30 minutes, in addition to the standard rehabilitation received by the control group. The wheelchair skills training programme is

based on improving the participants' level of skill execution, based on their baseline aptitude for a variety of tasks, with instruction provided both by video demonstration and also verbal instruction. The outcome was quantified using the Wheelchair Skills Test (WST), a 32 point test recording a range of wheelchair skills. The results demonstrated a significantly greater improvement in the WST score in the intervention group in comparison to the control group. Ozturk and Ucsular, (2011) completed a similar randomized controlled study, analysing the impact of the wheelchair skills training programme on a group of experienced community-living manual wheelchair users who had on average been using a manual wheelchair for 9.3 years. The intervention group received skills training using the wheelchair skills training programme three times weekly for 4 weeks, and demonstrated significantly greater improvements in WST score than the control group. These results suggest that wheelchair skills training can be beneficial for both novice and experienced manual wheelchair users. Rice et al., (2014) completed a further randomised controlled trial, assessing the influence of an intervention based on the published clinical guidelines for the preservation of upper limb function following SCI (Boninger et al., 2005a). Participants in the early stages of rehabilitation were randomised either to receive standard care, or the intervention, with both therapists and participants educated in the manner of the guidelines. The results demonstrated no differences between groups in terms of choice of wheelchair, wheelchair setup, pain or quality of life. However, the results demonstrated improved propulsion biomechanics in the intervention group who demonstrated lower push frequency during propulsion on a tiled surface at the time of discharge and greater push arc during ramp propulsion at each follow-up.

2.8.3.1 Optimising propulsion technique: the use of real time feedback

Further studies have investigated the effect of real time feedback to modify propulsion technique using a variety of methods including visual, verbal and haptic feedback. A systematic review of the literature investigating the influence of real time feedback on wheelchair propulsion biomechanics is presented in Chapter 3.

2.9   Conclusions

It has been shown that shoulder injury in manual wheelchair users is common and can negatively impact functional independence. The evidence to directly link manual wheelchair propulsion to shoulder injury is limited. Rotator cuff injury is most common, and is associated with increasing age and time as a wheelchair user, linking to the theory of age related degeneration and repetitive tendon overload as causes of rotator cuff injury in the general population.   This also supports the guidelines suggesting minimising repetition and peak force of a propulsion task may minimise risk of injury.

The instrumented wheelchair wheels used in the biomechanical analysis of manual wheelchair propulsion are limited in that they add weight to the wheelchair.   There exists a requirement for a lightweight instrumented wheelchair wheel to improve the validity of biomechanical analysis.

In terms of quantifying shoulder joint demand, measuring muscle activity level and joint contact forces are a suitable area of focus. Further research is required to assess the demands placed on the ageing shoulder during wheelchair propulsion and also to further estimate the demands placed on the shoulder during over ground propulsion, similar to that experienced during daily propulsion.

It has also been shown that the wheelchair set up and propulsion technique modification can reduce the measures linked to an increased risk of shoulder injury. Further research is required to apply such technique training to over ground wheelchair propulsion.

Chapter 3 A systematic review: The influence of real time feedback on wheelchair propulsion biomechanics

3.1 Overview

A systematic review was completed to examine whether real time feedback can influence manual wheelchair propulsion biomechanics. The electronic databases Web of Science, PubMed, Science Direct, Cochrane Database of Systematic Reviews and IEEE Xplore were searched, including their full archive history to December 2015. All English language clinical trials and case series comparing the use of real time verbal, visual or haptic feedback with no feedback were included. A general review was performed and methodological quality assessed by two independent practitioners using the Downs and Black checklist. Six papers including 123 participants were included in the review. There were significant changes in propulsion biomechanics with the addition of visual feedback, including changes in push arc, push rate, peak force and Mechanical Effective Force (MEF) / Fraction of Effective Force (FEF). Haptic feedback resulted in changes in MEF. Methodological assessment identified weaknesses in external validity. The addition of visual and haptic feedback resulted in changes in propulsion biomechanics. The results demonstrated that visual feedback could be used to consistently increase push arc and decrease push rate, and may be the best focus for feedback training. Further investigation is required to assess such intervention during outdoor propulsion, including identification of the most practical form of real time feedback.

3.2 Introduction

As discussed in section 2.8 of the background chapter, published clinical guidelines suggest that manual wheelchair users should aim to minimise peak force and repetition during completion of a task (Boninger et al., 2005a). To achieve this, in terms of propulsion biomechanics, manual wheelchair users are commonly advised to propel with a semicircular pattern (Boninger

et al., 2002) at a push rate of 1 push per second and push arc in the range of 85˚ to 100˚ (Sawatzky et al., 2015).

As introduced in section 2.8.3, wheelchair skills training has demonstrated benefit to manual wheelchair users, leading to an improvement in ability to complete a variety of functional tasks (MacPhee et al., 2004, Ozturk and Ucsular, 2011). Tracking and modification of specific propulsion parameters can be optimised with the use of instrumented wheelchair wheels, which have the capacity to measure the temporal parameters of propulsion in addition to the 3-dimensional forces and moments applied by the user to the wheelchair push rim (Cowan et al., 2008). The output from such devices has the potential to provide real time feedback during manual wheelchair propulsion.

The aim of this systematic review is to examine the current knowledge about the benefit of using real time feedback to modify wheelchair propulsion biomechanics. The review will consider different types of feedback and their impact on both temporal and kinetic propulsion parameters. As instrumented wheelchair wheels and other rehabilitation devices become more widely available, it is important to identify how optimising methods of real time feedback could improve propulsion efficiency and minimise injury risk.

3.3   Materials and Methods

3.3.1   Study selection process

A systematic review was completed to assess the influence of real time feedback on wheelchair propulsion biomechanics. The electronic databases Web of Science, PubMed, Science Direct, Cochrane Database of Systematic Reviews and IEEE Xplore were searched, including their full archive history to December 2015, using the following search terms:

Manual wheelchair propulsion AND feedback

The titles and abstracts of all studies identified were reviewed, and if matching the review inclusion and exclusion criteria full text articles were obtained. The reference list of each selected full text study was also reviewed.

The inclusion criteria for the review were as follows:

- Clinical trials and case series comparing the effect of real time feedback and no real time feedback on wheelchair propulsion biomechanics
- Clinical trials including real time verbal, visual and haptic feedback
- Full text, English language publications
- Experienced and novice wheelchair users of any age

The exclusion criteria for the review were as follows:

- Case studies, editorials and review articles
- Studies not comparing real time feedback to no real time feedback
- Non-English language articles
- Unpublished theses and dissertations

3.3.2 Study review process

A general review of the literature was completed, including assessment of study design, study population, the type of real time feedback provided, the outcome measures used and whether the main findings were statistically significant. In addition, the methodological quality of each of the studies was assessed using a modified version of the checklist published by Downs and Black, (1998). The checklist has been previously used to assess the methodological quality of similar studies (Kloosterman et al., 2013). The checklist scores methodological quality under the headings reporting, external validity, internal validity bias, internal validity confounding and power. The question relating to study power was simplified to determine whether a power calculation was performed. If the answer was 'yes' one point was awarded and if 'no', zero points were awarded. Each article was

reviewed against the checklist by two people working independently. Results were then compared, and disagreements were resolved during a face to face discussion.

3.4 Results

3.4.1 Study selection

The systematic review identified 281 citations. On review of the title and abstract of these citations, 18 articles were considered appropriate for full review and full text versions obtained. 12 of these articles were excluded. One was a case study, four studies did not assess an intervention, and seven provided an intervention to improve wheelchair propulsion but did not examine the implementation of real time feedback. Six articles met the inclusion and exclusion criteria for the review.
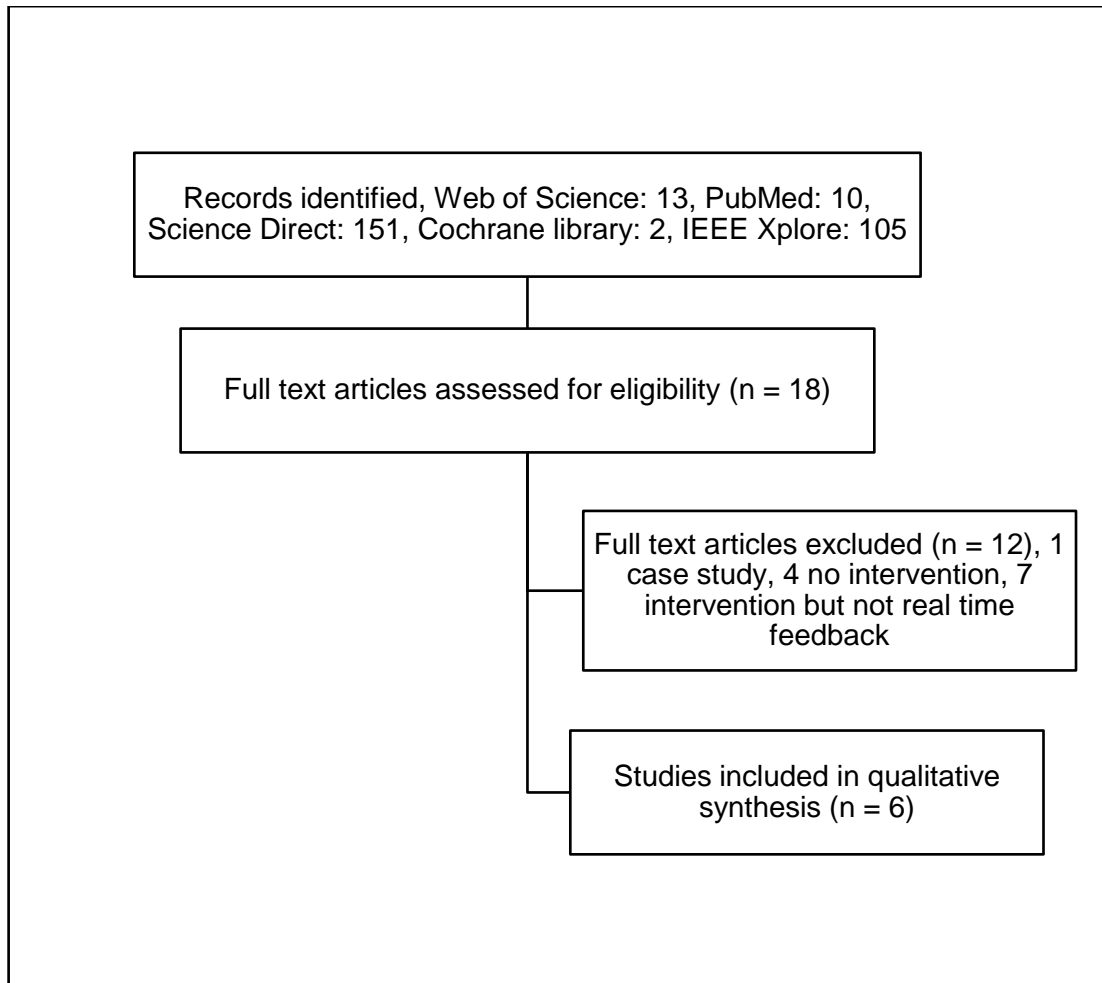
Figure 3-1: Flow chart showing the literature search process investigating the influence of real time feedback on wheelchair propulsion biomechanics

Table 3.1: Summary of studies selected for full review investigating the influence of real time feedback on manual wheelchair propulsion biomechanics

Study	Design	Population	Intervention	Outcome measures	Results	When outcome measured
Blouin et al., (2015)	Cross-over trial with repeated measures	18 SCI (range C7-L1), 16 male, 2 female	Haptic feedback provided by wheelchair simulator: MEF Visual feedback to guide maintenance of velocity	Mechanical effective force (MEF) Mean Linear velocity	Mean linear velocity remained equivalent Significant increase in MEF with haptic feedback	Immediately post intervention
de Groot et al., (2002)	Randomised controlled trial	20 able-bodied male participants	Control group (n=10) no visual feedback: wheelchair propulsion on stationary ergometer Intervention group (n=10) visual feedback: wheelchair propulsion on a stationary ergometer with visual feedback to guide FEF and velocity	Mean velocity Fraction of effective force (FEF)	Significant increase in FEF at 3 levels of power output (0.15 $W^.kg^{-1}$, 0.25 $W^.kg^{-1}$ and 0.40 $W^.kg^{-1}$)	During intervention
Degroot et al., (2009)	Case-series with repeated measures	9 manual wheelchair using adults	Visual feedback: push rate, push arc, push force	Push rate Push arc Push force	Significant reduction in push rate Significant increase in push arc Significant increase in push force	Immediately post intervention

Study	Design	Population	Intervention	Outcome measures	Results	When outcome measured
Kotajarvi et al., (2006)	Controlled trial	18 SCI (range T4-L2), 16 male, 2 female	Visual feedback: FEF, propulsion velocity, power output	FEF Velocity	No significant difference in FEF at 2 levels of power output	During intervention
Rice et al., (2013)	Randomised controlled trial	27 SCI (range C7-L3), 24 male, 3 female	Control group (n=9): Wheelchair propulsion on a dynamometer Instruction group (n=9): Multimedia presentation then propel on dynamometer Real-time visual feedback group (n=9): Multimedia presentation then propel on dynamometer with real-time visual feedback: push rate, push arc, propulsion velocity	Push rate Push arc Propulsion velocity	Push rate: significant decrease vs. control group at short and long term follow up and vs. instruction group at long term follow up Push arc: significant increase in push arc vs. control group at short and long term follow up and vs. instruction group at long term follow up	Immediately post intervention and at three months follow up
Richter et al., (2011)	Case-series with repeated measures	31 manual wheelchair users (SCI, Spina Bifida, CP, Spinal lipoma), 27 male, 4 female	Visual feedback: push rate, push arc, peak force, braking moment, push distance, smoothness (separate trial for each variable aiming for maximum and 10% change)	Push rate Push arc Peak force Braking moment Push distance Smoothness	Maximum change trials: significant improvements in all parameters except smoothness 10% change trials: change to within 1% of goal for all parameters except peak force	During intervention

3.4.2 Participants

In total, 123 participants were assessed in the six studies, 109 being male and 14 female. The mean age across the six studies calculated from the mean values presented was 35.5 years. 5 studies examined a total of 103 experienced manual wheelchair users (Blouin et al., 2015, Rice et al., 2013, Richter et al., 2011, DeGroot et al., 2009, Kotajarvi et al., 2006), the other study examined 20 novice non wheelchair users (de Groot et al., 2002). The 103 experienced manual wheelchair users comprised 92 participants with a diagnosis of SCI (Injury level range C6-L3), six with a diagnosis of Spina Bifida, two with a diagnosis of Cerebral Palsy and single participants with a diagnosis of Spinal Lipoma, Multiple Sclerosis and Spinal Muscular Atrophy. The mean time as a manual wheelchair user calculated from these 103 experienced participants was 14.6 years.

3.4.3 Study characteristics

3.4.3.1 Study design

Two of the studies were randomised controlled trials (Rice et al., 2013, de Groot et al., 2002). The remainder of the studies employed a repeated measures design, assessing the change in propulsion biomechanics following intervention with respect to pre-intervention 'control' biomechanical results (Blouin et al., 2015, Richter et al., 2011, DeGroot et al., 2009, Kotajarvi et al., 2006).

3.4.3.2 Intervention

The studies used interventions including haptic and visual feedback. Only one of the studies examined haptic feedback (Blouin et al., 2015). This was delivered by a wheelchair simulator, on to which a wheelchair was positioned. Haptic feedback was delivered via an increase in resistance to propulsion when participants deviated from the suggested MEF. Participants were also provided with visual feedback to ensure maintenance of propulsion velocity.   One of the randomised controlled trials divided participants in to three groups; a control group, an instruction only group that received a

multimedia presentation and an intervention group that received real time visual feedback on push frequency, push arc and propulsion velocity in addition to the multimedia presentation (Rice et al., 2013). The other randomised controlled trial divided the participants into two groups, a control group receiving only real time visual feedback on propulsion velocity and an intervention group receiving real time visual feedback on both propulsion velocity and FEF (de Groot et al., 2002). The remaining studies investigated real time visual feedback focusing on a range of variables. Richter investigated the influence of single variable visual feedback including braking moment, push rate, push arc, push force, push distance and smoothness (Richter et al., 2011). DeGroot et al., (2009) provided visual feedback on push rate, push arc and push force and Kotajarvi et al., (2006) provided visual feedback on FEF, propulsion velocity and power output.

3.4.3.3 Setting and measurement of outcome

Each of the studies was completed in a laboratory setting. Blouin et al., (2015) provided both feedback and measured outcome during propulsion on a simulator. Rice et al., (2013) provided visual feedback during propulsion on a dynamometer and measured outcome during over ground propulsion. DeGroot et al., (2009) provided visual feedback during propulsion on an ergometer and measured outcome during both ergometer and over ground propulsion. The remaining three studies provided both visual feedback and measured outcome during propulsion on an ergometer (Richter et al., 2011, Kotajarvi et al., 2006, de Groot et al., 2002). Four of the studies measured outcome during the intervention (Blouin et al., 2015, Richter et al., 2011, Kotajarvi et al., 2006, de Groot et al., 2002). Three of the studies measured outcome immediately post intervention (Blouin et al., 2015, Rice et al., 2013, DeGroot et al., 2009) and only one of the studies presented results from longer term (three months) follow up (Rice et al., 2013).

3.4.4 Outcome measures

The direct influences of feedback on propulsion biomechanics are reported, when feedback on a variable was delivered and reported as an outcome measure.

3.4.4.1 Temporal parameters

Push rate is defined as the number of push cycles per second. The aim of the interventions reported was to decrease push rate. Three of the studies provided feedback on push rate and recorded it as an outcome measure (Rice et al., 2013, Richter et al., 2011, DeGroot et al., 2009). Rice et al., (2013) reported a decrease in push rate in the intervention versus control group at both short term follow up (0.82 s^{-1} vs. 1.10 s^{-1}, P<0.05) and long term follow up (0.87 s^{-1} vs. 1.10 s^{-1}, P<0.05). Although the visual feedback group demonstrated no significant reduction in push rate compared to the instruction only group in the short term, at longer term follow up a significant reduction was demonstrated (0.87 s^{-1} vs. 0.93 s^{-1}, P<0.05). Richter et al., (2011) demonstrated a significant reduction in push rate when both aiming for a maximum reduction (64% decrease, P<0.005) and also a 10% reduction (9% decrease, P<0.005). DeGroot et al., (2009) reported a significant reduction in push rate with the addition of visual feedback (0.68 s^{-1} vs. 0.99 s^{-1}, P<0.01). Kotajarvi et al., (2006) used push rate as an outcome measure, but did not provide real time feedback on push rate as an intervention.

Push arc is defined as the angle over which force is applied to the wheelchair push rim. The aim of the interventions was to increase push arc. Three of the studies provided feedback on push arc and recorded it as an outcome measure (Rice et al., 2013, Richter et al., 2011, DeGroot et al., 2009). Rice et al., (2013) reported an increase in push arc in the intervention versus control group at both short term follow up (107.7˚ vs. 97.9˚, P<0.05) and long term follow up (111.8˚ vs. 97.9˚, P<0.05). Although the visual feedback group demonstrated no significant increase in push arc compared to the instruction only group in the short term, there was a significant increase at longer term follow up (111.8˚ vs. 104.6˚, P<0.05). Richter et al., (2011)

demonstrated a significant increase in push arc when both aiming for a maximum increase (31% increase, P<0.005) and also a 10% increase (10% increase, P<0.005). DeGroot et al., (2009) reported a significant increase in push arc with the addition of visual feedback (86.1° vs. 67.0°, P<0.05).

3.4.4.2 Kinetic parameters

Peak resultant propulsion force describes the total force applied to the wheelchair push rim. The aim of the intervention is to minimise this force. Two of the studies provided feedback on peak force and recorded peak force as an outcome measure (Richter et al., 2011, DeGroot et al., 2009). Richter et al., (2011) reported that participants were able to significantly reduce peak forces when aiming for maximum reduction (-11%, P<0.005), but not when aiming for a 10% reduction. DeGroot et al., (2009) reported a significant increase in peak push force (61.79N vs. 52.89N, P<0.05), despite the aim of the feedback being to reduce peak force.

Braking moment is defined as the 'minimum (negative) moment about the axle from the end of the previous push phase to the end of the current push phase' (Richter et al., 2011). Richter et al., (2011) reported a significant reduction in braking moment as a result of visual feedback (-44%, P<0.005).

MEF/FEF are defined as the effective component of the propulsion force which drives the wheels forward (Kotajarvi et al., 2006). Three of the studies provided feedback on MEF/FEF and record MEF/FEF as an outcome measure (Blouin et al., 2015, Kotajarvi et al., 2006, de Groot et al., 2002). Blouin et al., (2015) reported a significant increase in MEF with the addition of haptic feedback (P<0.02). Kotajarvi et al., (2006) reported no significant change in FEF at 2 different intensity levels. Contrary to this, de Groot et al., (2002) reported significantly greater levels of FEF with feedback at three different levels of power output, 0.15 $W^{.}kg^{-1}$ (90.22% vs. 79.26%, P<0.01), 0.25 $W^{.}kg^{-1}$ (97.47% vs. 83.04%, P<0.01) and at 0.40 $W^{.}kg^{-1}$ (96.56% vs. 83.14%, P<0.01).

Push distance is defined as the distance travelled during one propulsion cycle (Richter et al., 2011). Richter et al., (2011) reported a significant increase in push distance with visual feedback when aiming for both maximum increase (255%, P<0.005) and also a 10% increase (11%, P<0.005).

Smoothness is calculated by dividing the mean force applied to the push rim during the push phase by the peak force measured during the same push phase (unit less variable) (Richter et al., 2011). Richter et al., (2011) reported no significant improvement in smoothness with the addition of visual feedback.

Four of the studies also provided visual feedback on propulsion velocity (Blouin et al., 2015, Rice et al., 2013, Kotajarvi et al., 2006, de Groot et al., 2002). This feedback was provided to enable participants to control their velocity, rather than alter it.

3.4.4.3 Cross variable effects

One of the studies directly compared the cross variable effect of modifying single variables with visual feedback (Richter et al., 2011). Minimising push rate was associated with an increase in contact angle and push distance, but a 154% increase in peak force. Maximising push arc was associated with a significant reduction in push rate and an increase in push distance, but a 34% increase in peak force.

3.4.5 Methodological quality

The Downs and Black study quality scores are presented in table 3.2. The highest score was 19/28 (de Groot et al., 2002) and the lowest 12/28 (Blouin et al., 2015). Across each of the six studies, the scores were particularly low for the section measuring external validity, with all studies completed in the laboratory setting.

Table 3.2: Methodological quality of papers reviewed to examine the influence of real time feedback on wheelchair propulsion biomechanics

Paper	Reporting	External validity	Internal validity		Power	Total
			Bias	Confounding		
Maximum score	**11**	**3**	**7**	**6**	**1**	**28**
Blouin et al., (2015)	7	0	4	1	0	12
De Groot et al., (2002)	9	0	6	4	0	19
DeGroot et al., (2009)	8	0	4	2	0	14
Kotajarvi et al., (2006)	8	1	6	1	0	16
Rice et al., (2013)	8	1	4	4	0	17
Richter et al., (2011)	7	0	4	1	1	13

3.5   Discussion

This systematic review aimed to determine whether the use of real time feedback could lead to changes in manual wheelchair propulsion biomechanics. The results suggest that real time visual feedback can be used to alter push rate (DeGroot et al., 2009, Rice et al., 2013, Richter et al., 2011), push arc (DeGroot et al., 2009, Rice et al., 2013, Richter et al., 2011), push force (Richter et al., 2011), MEF (de Groot et al., 2002), braking moment (Richter et al., 2011) and push distance (Richter et al., 2011). The results also suggest that real time haptic feedback can be used to alter MEF (Blouin et al., 2015). There is limited evidence to support the carryover of such interventions, and further research is required to enable useful application of real time feedback away from the laboratory during day to day wheelchair propulsion.

3.5.1 Outcome measures

3.5.1.1 Temporal parameters

Reducing push rate has been associated with a reduction in upper extremity total muscle power during a study utilising forward dynamic simulations (Rankin et al., 2012) and also preservation of median nerve function at the wrist (Boninger et al., 1999, Boninger et al., 2004). Increasing push arc has been advised, to enable greater power generation for a set force by applying this force over a greater angle (Boninger et al., 2005b).   Providing real time visual feedback to reduce push rate and increase push arc demonstrated beneficial effects during the intervention (Richter et al., 2011), immediately following the intervention (DeGroot et al., 2009, Rice et al., 2013) and at three months follow up (Rice et al., 2013), indicating that they may be successful parameters to target as part of an initial training program and also during real time feedback via an instrumented wheelchair wheel. This thesis reports such a study in chapter 8.

3.5.1.2 Kinetic parameters

Higher push rim forces have been associated with both progressive shoulder joint pathology (Boninger et al., 2003) and reduced median nerve function (Boninger et al., 1999). Guidelines suggest that peak force applied to the push rim should be minimised to preserve upper limb function (Boninger et al., 2005a, Sawatzky et al., 2015). The results of the review demonstrated conflicting evidence regarding the use of visual feedback to minimise peak force. DeGroot et al., (2009) reported a significant increase in push force. During this study, visual feedback was provided on three variables at the same time (push rate, push arc and peak force) and it was concluded that push force may have increased to compensate for a reduction in push rate to maintain the same push length. Richter et al., (2011) reported a significant reduction in push force when participants were attempting to minimise it, but participants were not able to control a reduction in push force of 10%. This study investigated single variable feedback and discussed the difficulty in minimising peak force, suggesting that providing visual feedback on the

whole force curve rather that peak value may be beneficial. The review also identified contrasting results from the studies reporting MEF/FEF as an outcome measure. Blouin et al., (2015) reported a significant increase in MEF with the addition of haptic feedback and de Groot et al., (2002) reported significant increases in FEF at three levels of power output with the addition of visual feedback. However, Kotajarvi et al., (2006) reported no significant increase in FEF at two levels of power output with the addition of visual feedback. In addition to these inconsistencies, the validity of aiming for an increase in MEF/FEF to minimise upper limb injury risk has been questioned. Previous research has highlighted that increased application of tangential force can lead to increased forces and moments at the GH joint (Desroches et al., 2008b) and also increased GH joint muscle demand (Bregman et al., 2009). In addition to the greater stresses placed on the upper limb, increasing MEF has been associated with a greater physiological cost (de Groot et al., 2002).

3.5.2 Cross variable effects

The success of optimising a single variable cannot be measured in isolation of the cross effect on other variables. Only one of the studies reviewed measured statistically the impact of altering a single variable on others measured (Richter et al., 2011). The results of this study demonstrated that while inducing a desired change such as reducing push rate, there may be a resultant undesirable change, in this case an increase in push force.

To highlight the balance between minimising task repetition and peak force application, it is useful to apply the examples of reducing push rate and increasing push arc to the average daily activity of a manual wheelchair user. Previous data tracking activity levels of manual wheelchair users has reported the average distance travelled per day to be 1600m (Sonenblum et al., 2012). Using the baseline data and percentage change values for single variable feedback presented by Richter et al., (2011):

Minimising push rate to 18.87 stokes per minute increased push arc to 108.79˚, increasing peak force to 145.75N with an average distance per push increasing to 4.27m, the manual wheelchair user would make 374 pushes during the day. Reducing push rate by 10% to 47.69 strokes per minute increased push arc to 87.90˚, increasing peak force to 61.97N with an average distance per push increasing to 1.48m, the manual wheelchair user would make 1082 pushes per day.

Maximising push arc to 114.00˚ reduced push rate to 36.69 strokes per minute, increasing peak force to 76.89N with an average distance per push of 2.19m, the manual wheelchair user would make 729 pushes per day. Increasing push arc by 10% to 95.73˚ reduced push rate to 45.07 strokes per minute, increasing peak force to 63.12N with an average distance per push of 1.61m, the manual wheelchair user would make 994 pushes per day.

Minimising the push rate leads to the requirement of fewer pushes, but the peak forces are very high, equivalent to climbing a 12% ramp, which are associated with higher GH joint contact forces and theoretically greater risk of injury (Holloway et al., 2015). Maximising push arc leads to the requirement of fewer pushes, with less increase in peak force, but increasing the push arc such an extent may lead to injury due to the upper limb moving to greater extremes of movement, which should be avoided (Boninger et al., 2005a). Inducing a 10% reduction in push rate lead to an increase in peak force and push distance, whereas inducing a 10% increase in push arc lead to a slighter greater increase in push force than during the push rate reduction, but also a greater increase in push distance and therefore reduced pushes during daily activity. These results suggest that optimising push arc towards 100˚ may result in the best balance between peak force and task repetition, although such an assumption needs to be tested during more challenging propulsion tasks away from the laboratory, whilst maintaining the required chair velocity.

3.5.3 Methodological review

The results revealed that a key future development would be to improve external validity. Each of the studies was completed within a laboratory, with the real time feedback provided during propulsion on an ergometer or treadmill. Propelling a wheelchair outdoors provides a different challenge, negotiating terrain including cross slopes (Holloway and Tyler, 2013) and inclines (Chow et al., 2009, Morrow et al., 2010c) has been shown to increase upper limb demand. Further research is required not only to assess whether real time feedback can be successful in a changing environment, but also to determine how best to apply this feedback. Providing real time visual feedback is possible in a laboratory experiment, but not practical during outdoor propulsion when negotiating the environment requires visual focus on the terrain. The acceptability and effectiveness of other forms of feedback such as auditory and haptic feedback, which could potentially be applied via vibration to the skin surface, require investigation. Both auditory (Meardon and Derrick, 2014) and haptic feedback via vibration (Wheeler et al., 2011) have been shown to influence the biomechanics of gait. The review demonstrates the success of real time feedback in improving propulsion biomechanics in both complete novices (de Groot et al., 2002) and also experienced manual wheelchair users (Blouin et al., 2015, DeGroot et al., 2009, Rice et al., 2013, Richter et al., 2011). This indicates that real time feedback may be beneficial both in the early stages of wheelchair skills training and also to optimise an established technique. However, only one of the studies included in the review reported outcome at longer term follow up (Rice et al., 2013). Therefore it is not possible to establish whether a single period of intervention is sufficient to influence technique in the long term. In addition, only one of the studies reports statistical power (Richter et al., 2011).

3.5.4 Limitations

The main limitation of the review is that due to the small number of articles included and the differences in terms of population recruited, type and form of intervention applied and outcome measures recorded, a meta-analysis

was not possible. In addition, the articles selected only consider the direct impact of real time feedback on temporal and kinetic push rim parameters. For further insight into minimising injury risk, the secondary impact of altering push rim variables on participant kinematics (joint angle and muscle activity levels) should be considered.

3.6 Conclusions

The findings of this review suggest that real time visual and haptic feedback can be used to modify wheelchair propulsion biomechanics. These results in conjunction with previous research investigating wheelchair propulsion and upper limb injury risk suggest that push arc and push rate may be the best parameters to target to optimise the fine balance between minimising peak force and task repetition. In addition, it appears that applying single variable feedback may be more successful than multiple variable feedbacks. However, these conclusions are drawn from data collected in the laboratory, mainly investigating the use of real time visual feedback. In reality, real time visual feedback is not a practical or safe option for the wheelchair user negotiating journeys outdoors. Further investigation is required to determine if the findings of the review can be applied during journeys outdoors and also if other forms of real time feedback, including auditory of haptic (vibration) can be successfully applied.

Chapter 4 The Sensewheel design and function

4.1 Overview

The aim of this chapter is to introduce the design and function of the Sensewheel. The chapter begins by discussing the requirement for such a device, in the context of the technologies currently available. The hardware, software, calibration process, data capture and post processing steps are then described.   The benefits and limitations of the device are then discussed, with reference to ongoing design improvements.

4.1.1 Acknowledgements

The concept and design of the Sensehweel hardware and software, including the finite element analysis to inform strain gauge position, were the work of Dr Stephen Taylor and Dr Catherine Holloway. Both the physical set-up and mathematical methods of the load cell calibration were the work of Dr Stephen Taylor. The work of Andrew Symonds in the development of the Sensewheel was limited to the physical process of load cell calibration and building the load cells on to the wheel.   In addition, Andrew Symonds established the post processing methods.

4.2 Introduction

As introduced in chapter 2, section 2.7.1, instrumented wheelchair wheels have been used to analyse wheelchair propulsion biomechanics. The major limitation of the instrumented wheelchair wheels currently available is that they add additional weight to the wheelchair.   Previous research has demonstrated a statistically significant strong positive correlation between peak propulsion force and body weight ($r = 0.59$, $P < 0.01$), during a study of manual wheelchair users propelling at a controlled speed on a dynamometer (Boninger et al., 1999). Estimating from the line of best fit on the scatter plot in this paper, a 100N increase in weight leads to approximately a 10N increase in peak force. This suggests that using instrumented wheelchair wheels that add additional weight to the wheelchair will influence the

biomechanics of propulsion and will not be fully representative of the demand experienced by wheelchair users during daily propulsion. There exists a need for a lightweight instrumented wheelchair wheel, to improve the validity of biomechanical analysis of manual wheelchair propulsion. In addition, as technologies develop, an instrumented wheelchair wheel adding no additional weight to the wheelchair could be used as a research tool during longer bouts of propulsion, without increasing the risk of injury.

The Sensewheel is a lightweight instrumented wheelchair wheel measuring three-dimensional forces applied to the push rim and torque about the wheel axle. The Sensewheel can be used interchangeably with a standard wheelchair wheel, the Mark 1 version, including the wheel itself and three load cells weighs 2.25kg. The additional weight of the Sensewheel over the standard wheel being adapted is less than 100g. It has 3 aluminium load cells interconnecting the push rim and the wheel and a master controller and telemeter mounted at the wheel hub. Figure 4-1 (A) shows the Sensewheel Mark 1 and figure 4-1 (B) an individual Sensewheel Mark 1 load cell. Figure 4-2 shows the position of the 3 load cells and master controller.
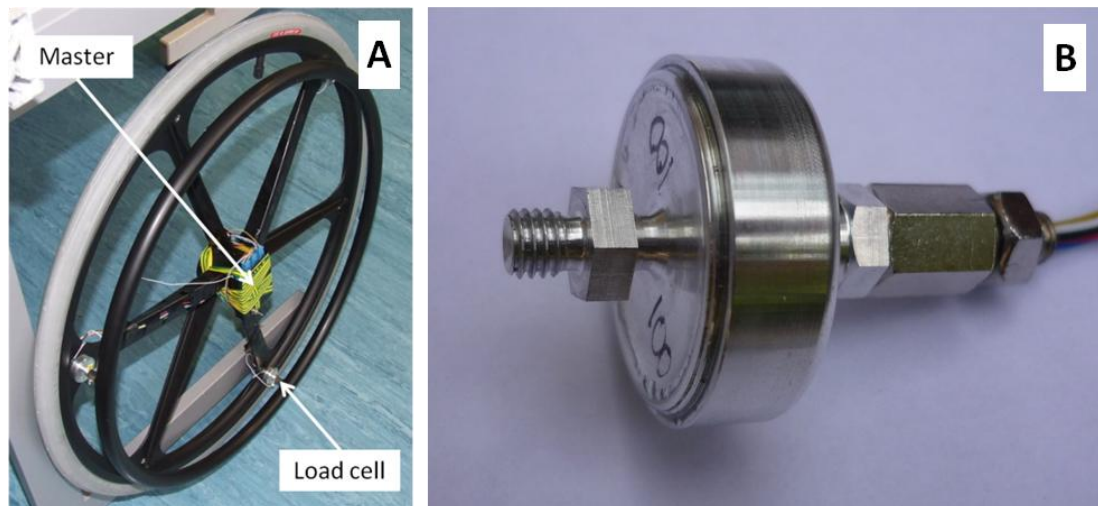
Figure 4-1: The Sensewheel Mark 1 (A) and an individual Sensewheel load cell (B).
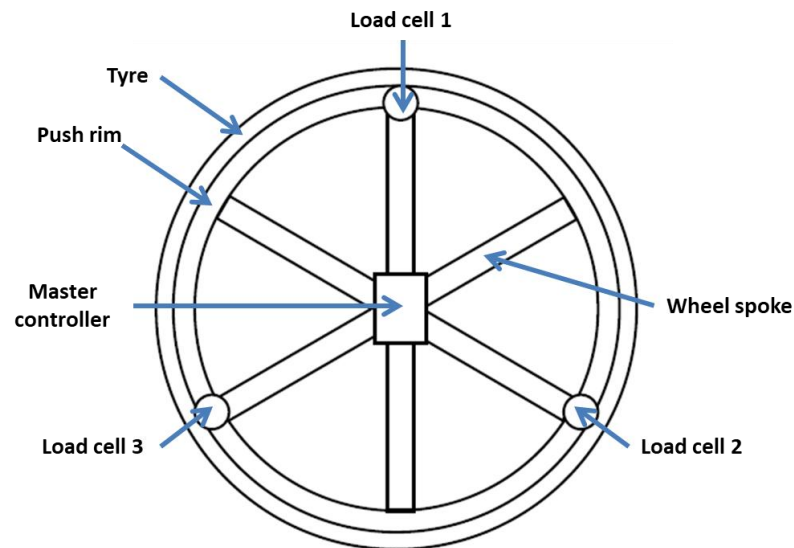
Figure 4-2: A schematic representation of the Sensewheel.

4.3 The Sensewheel hardware

4.3.1 The load cell

Each load cell contains four pairs of strain gauges (Vishay, Basingstoke, UK) connected in a half bridge formation (see figure 4-3), a three axis accelerometer, and contains local amplification and data processing, and connects to a master controller mounted at the wheel hub via an i^2C serial digital data connection.
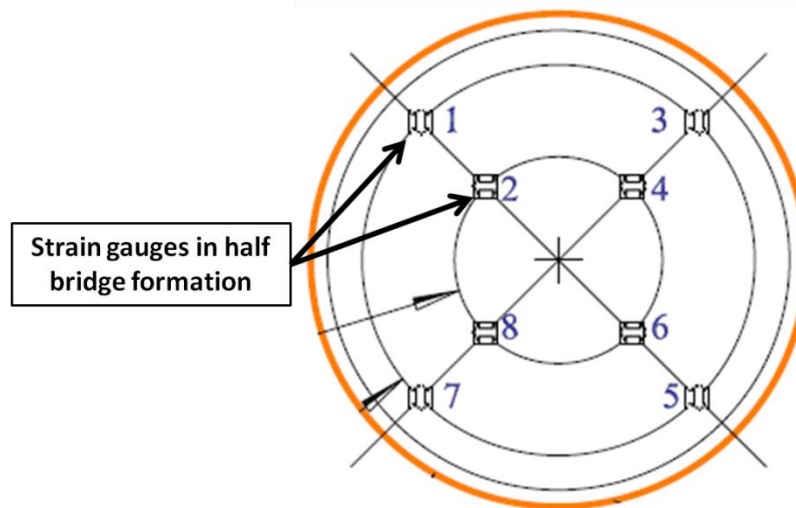
Figure 4-3: A schematic representation of the position of the strain gauges on the Sensewheel load cell diaphragm.

The position of the strain gauges was informed by finite element analysis. Using the software COMSOL Multiphysics 4.4, simulations to apply axial and shear forces, torque and bending moments to the load cell were completed, with sensitivities to these loads analysed at 0.5mm increments across the load cell diaphragm. As axial and bending loads are applied to the diaphragm, the diaphragm deforms, with peak sensitivities to loads measured either side of the point of inflection. The strain gauges for each pair are mounted either side of the point of inflection. The half bridge formation of strain gauges enables measurement of a greater relative difference in voltage for a given load, as when one strain gauge is compressed resistance increases, whereas the other is stretched and resistance decreases. Change in voltage for each half bridge is assessed with respect to a common reference. Each strain gauge is connected to a flexible printed circuit. This small change in signal differential with respect to the common reference is passed through an amplifier with a gain of 64. The amplifier passes the signal to an analogue to digital convertor (sigma delta), which forms part of the microcontroller (ADuC7061). Figure 4-4 (A) shows the flexible printed circuit and figure 4-4 (B) shows the flexible printed circuit positioned in the Sensewheel load cell.
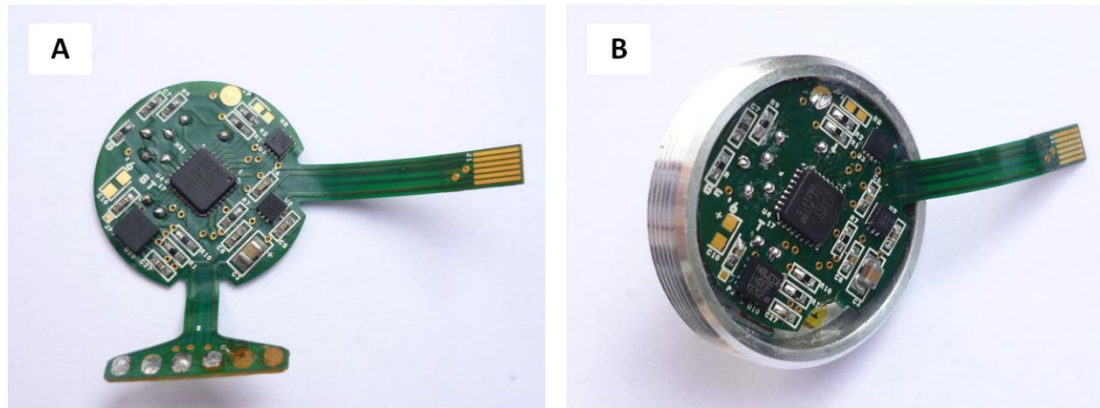
Figure 4-4: The flexible printed circuit (A) and the flexible printed circuited mounted in the Sensewheel load cell (B).

The microcontroller program cycles through the channels carrying data from the strain gauges and digitises each channel at a rate of 1 sample every 20ms, producing 4 24-bit digital numbers for every sample. This output is encoded in a serial data protocol called I^{2}C that is read by the master controller on the wheel hub.

Each load cell measures local axial, torque, tangential and radial forces. These are then combined in the GUI, knowing the 120° spacing of the load cells around the wheel, to find the overall tangential, radial and axial force applied by the hand to the push rim.

4.3.2 The master controller

The master controller houses a three-axis digital gyroscope (L3G4200D) and a 3-axis digital accelerometer (LIS331DLH). The gyroscope and accelerometer are connected onto the I^{2}C bus. Data from the 3 load cells are serially multiplexed into the master micro-controller. The master requests and packs data, to enable transmission of data at 38000 Baud via ultra-high frequency (UHF) radio (RADIOMETRIX TX2A-433-64-3V) to the receiver connected to the personal computer. Figure 4-5 (A) shows the wired connection of the load cell to the master and figure 4-5 (B) the radio receiver. The Z axis of the gyroscope is used to find the rotational speed about the

wheel axis. The accelerometer provides the reference wheel angle to enable alignment of the load cell coordinate systems.
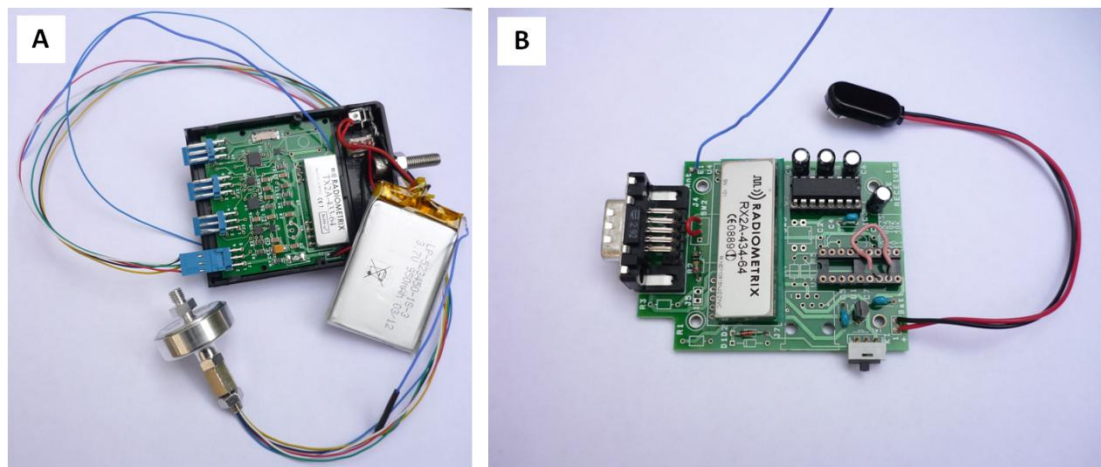
Figure 4-5: The wired connection of the load cell to the master (A) and the radio receiver (B).

4.3.3 Load cell calibration

Each load cell was individually calibrated, at ambient temperature. In order to minimise the effect of an angle error in applying loads, an arrangement was used whereby the load cell was held in a motorised chuck which was rotated at slow speed (1 revolution per 90 seconds). The motor/chuck/load cell was aligned at angle α (about 20˚) to the vertical such that with a load suspended by a string from the axis of the load cell both an axial load component and a shear component were applied (See figure 4-6).
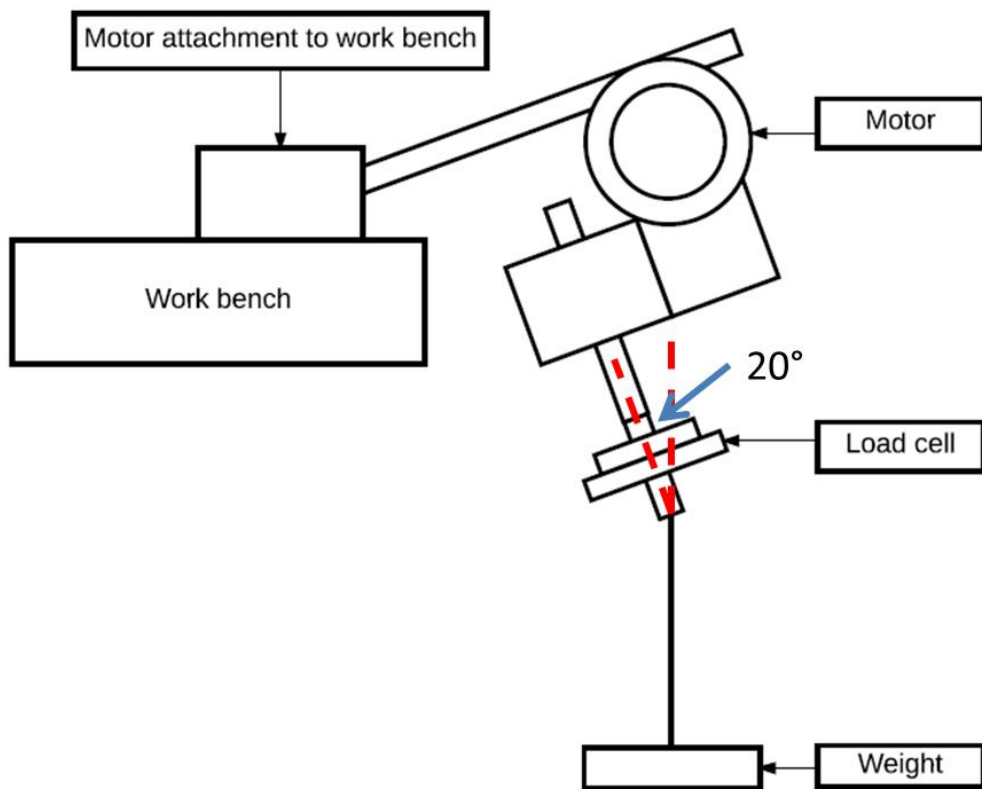
Figure 4-6: Schematic of the load cell calibration rig.

In this way a sinusoidally-varying load was experienced by each half bridge, allowing a best-fit sinusoid to be fitted to the data for determining the sensitivities at any given axial angle.

The accelerometer also included on the load cell flexi circuit allowed this sinusoidal profile to be referenced to the accelerometer axes (which were in turn used to determine the load cell angle at any given point in time in service). The slow speed of revolution minimised any applied torque due to inertial effects in the load application, and gave many data points for the curve fitting. The sinusoidal variation was due only to the shear force; the axial component was constant, and the mean value thus represented an offset from the unloaded condition, proportional to the axial component. A further record was made with no load applied, to obtain the zero load counts. The resulting data, obtained over one complete revolution of the motor,

represented the sinusoidally varying shear force at (90- α) degrees to its normal direction on the load cell, and constant axial force at α degrees to the load cell axis.

In order to separate the axial from the shear component, each strain channel was curve fitted to a sinusoid formed by the orthogonal components of the load cell accelerometer, and thus phase referenced to it. The mean value (subtracted from the zero load value) represented the axial component attenuated by 1/cos α, and the peak amplitude with respect to the mean value represented the maximum shear force sensitivity attenuated by 1/sin α. From these data, the axial and shear components and the shear phase shift with respect to the accelerometer 0 degrees, were calculated.

Torque was applied in a separate setup using a bending bar and dead weights. The sensitivity of each half bridge to each applied load (axial, shear at 0 degrees, shear at 90 degrees, torque) was thus obtained, and these values arranged in a 4x4 calibration matrix, which when inverted became the measurement matrix for that load cell, referenced to the load cell accelerometer axes.

When mounted onto Sensewheel, each load cell's accelerometer was used to find its local angle at a known position of the wheel (load cell 1 at the top). These 3 angles were used to rotate the shear components about the axis of symmetry, X, to find the shear forces along any given axis system, principally those tangential to, and radial to, the push rim.

4.4 The Sensewheel software

When received at the PC for the master controller, a LabView (National Instruments Inc, Texas, USA) interface program written in C (LVi program) decodes the serial data and compiles it for processing in LabView. The LabView program performs a matrix multiplication on each load cell to convert the data received in counts from the load cells to forces, aligns load cells 2 and 3 to the axis system of load cell 1 by axis transformation, and summates these forces for the whole wheel.

4.5 The Sensewheel: data collection and processing

4.5.1 Data collection: step by step guide

Figure 4-7: Sensewheel GUI.

The Sensewheel Graphical User Interface (GUI) enables real time propulsion data to be viewed simultaneously from right and left wheels. The GUI displays tangential force, linear velocity and push arc (Figure 4-7). In advance of data capture, the wheel is positioned with load cell one on each wheel positioned at the top dead centre. The 'set zero' function is executed to record the angle of each load cell with respect to the coordinate system of the wheel. By selecting the tab 'Real time' data can be recorded for a specified trial period and assigned an appropriate file name, and the raw data file is saved automatically. The raw data file includes the accelerometer data for each load cell, the data from the strain gauges presented in 'counts' and

the raw data from the gyroscope. The raw data file is then processed under the 'Data from file' tab, to enable application of the calibration data to the strain gauge data to enable output of the force and moment data. Data processing creates an output file, including tangential, radial and axial forces and moment about the wheel axle. The header of an example output file is presented in figure 4-8.

	A	B	C	D	E	F	G
1	Patient Name						
2	Test, GEN6						
3	Patient Number						
4	0						
5	Recording Date						
6	10-Jul-13						
7	Activity						
8	1						
9	Session Number						
10	6						
11	Left Master Name						
12	M0						
13	Left Wheel Slaves Name						
14	s1	s2	s3	s4			
15	Right Master Name						
16	M1						
17	Right Wheel Slaves Name						
18	s5	s6	s7	s8			
19	Time [sec]	WR Fx	WR Fy	WR Fz	WR Mx	WR My	WR Mz
20	0	-0.127	-1.058	-0.778	0	0	0.055
21	0.02	-0.177	-0.896	-0.775	0	0	0.056
22	0.04	-0.224	-1.212	-0.794	0	0	0.059
23	0.06	-0.073	-0.998	-0.5	0	0	0.07

Figure 4-8: An example Sensewheel data output file.

4.5.2 Data collection: post processing

The Sensewheel uses measurements of 3-dimensional forces, torque about the wheel axle and angular velocity of the wheel to calculate push rate, push arc, percentage push phase, velocity, wheel moment, peak force, angular velocity and power. Figures 4-9 (A) and 4-9 (B) display example raw data output for tangential force and angular velocity respectively.
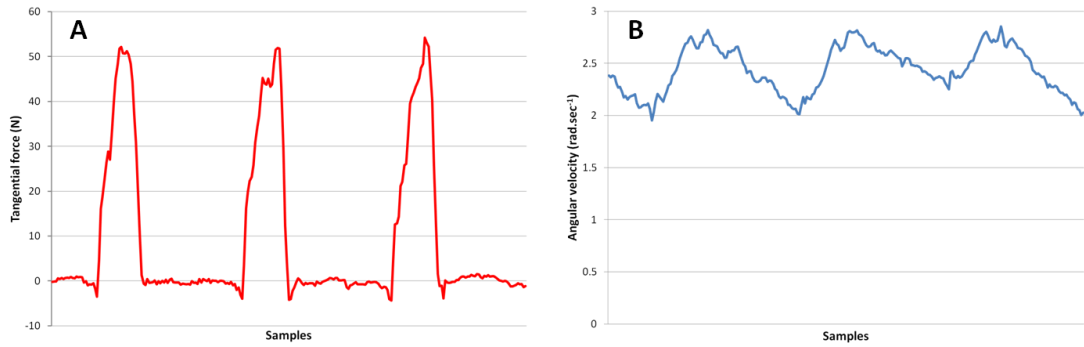
Figure 4-9: Example raw data output for tangential force (A) and angular velocity (B).

In advance of post processing, the raw data are prepared. Missing data up to 8 samples (0.16 seconds) are accounted for via linear interpolation and any offest in the tangential, radial and axial force measurements is accounted for by subtracting the baseline unloaded 'noise' from the signal. Each push cycle is measured from the start of one push phase to the start of the next, and is divided in to the push phase and recovery phase. The phases of the push cycle are presented in figure 4-10, with the red line depicting the threshold for defining the push phase, for example when the wheel moment is in excess of 0N·m.
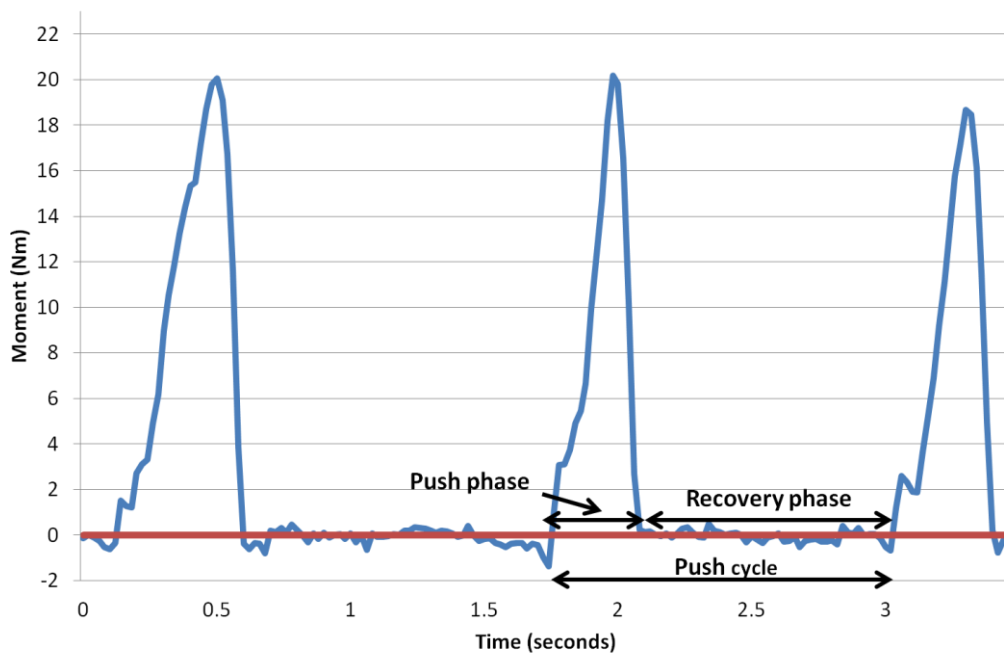
Figure 4-10: Identification of the push and recovery phases within the push cycle.

67

The parameters used in this thesis to analyse wheelchair propulsion biomechanics are calculated as follows:

a) Push rate is defined as the number of push cycles per second. Push rate is calculated as:

$$Push\ rate\ (s-1) = \frac{Number\ of\ pushes}{Time\ (s)}$$

b) Push arc is defined as the change in the angle of the wheel during the push phase. Push arc is calculated as:

$$Push\ arc\ (°) = mean\ angular\ velocity\ (°.s-1) \times time(s)$$

c) Percentage push phase is the percentage of the push cycle spent in the push phase. Percentage push phase is calculated as:

$$Percentage\ push\ phase\ (\%) = \frac{Push\ phase\ time\ (s)}{Push\ cycle\ time\ (s)} \times 100$$

d) Mean velocity is calculated as:

$$Mean\ velocity\ (m.s-1) = \frac{Distance(m)}{Time(s)}$$

e) Resultant propulsion force is defined as the total force applied by the wheelchair user to the push rim. It is calculated from the tangential (F_x), radial (F_y) and axial (F_z as follows):

$$Resultant\ force\ (N) = \sqrt{(Fx^2 + Fy^2 + Fz^2)}$$

f) Wheel moment is defined as the torque applied about the wheel axle. It is calculated as follows:

$$Wheel\ moment\ (N.m) = Tangential\ force\ (N) \times Wheel\ radius\ (m)$$

g) Power output is defined as the mean power generated during the push. Power output is calculated as:

$$Power\ (W) = Wheel\ moment\ (N.m) \times \omega\ (rad.s-1)$$

4.6   Summary of Sensewheel technical specifications

Table 4.1 presents a summary of the technical specifications of the Sensewheel, for comparison with those of the SmartWheel and OptiPush

presented in chapter 2 section 2.7.1. The main advantage possessed by the Sensewheel is that it is lighter than the alternatives, adding no additional weight to the wheelchair wheel. The Sensewheel Mark 1 has a number of limitations which need to be addressed if it is to be adopted more widely as a research tool or provided to healthcare professionals and wheelchair users in the clinical setting. These limitations are listed below, along with the planned developments for the Mark 2 version of the wheel.

Table 4.1: Table showing the technical specification of the Sensewheel.

	Sensewheel
Total wheel weight	2.25Kg
Forces measured	Tangential, radial, axial, wheel moment
Available wheel sizes	60cm diameter
Sampling frequency	50Hz
Communication type	UHF radio
Battery type	rechargeable lithium ion 3.7V, 950mAh
Battery life	>10 hours
Cost	£1500

4.7 The Sensewheel: current limitations and future developments

The main limitations of the Mark 1 Sensewheel are:

- Data loss due to method of data transmission
- Insufficient mechanical strength of the load cell
- Lower sampling frequency than alternative instrumented wheelchair wheels
- Lack of adaptability of the load cell for application to different wheel types
- Additional width added by the load cell to the push rim connection
- Complexity of the GUI

These limitations and proposed future developments to address them are presented in Appendix 1.

4.8 Summary

This chapter introduces the Sensewheel, a novel lightweight instrumented wheelchair wheel, with the potential of improving the validity of the

biomechanical analysis of wheelchair propulsion biomechanics. The current limitations to the system have been introduced, and the strategies planned to account for these limitations have been discussed. The studies presented in the experimental chapters 5 to 8 provide the proof of concept for the clinical application of the Sensewheel. Potential clinical applications are introduced both in terms of tracking demand and identifying technique differences during manual wheelchair propulsion and also in terms of using the Sensewheel as a training tool via the application of real time feedback to minimise risk of injury.

Chapter 5 The effect of age on muscle activity level during manual wheelchair propulsion

5.1 Overview

Manual wheelchair propulsion can lead to rotator cuff injury, which is associated with increasing age and time as a wheelchair user. As the population ages and the number of wheelchair users increases, it is important to understand age related differences in manual wheelchair propulsion biomechanics to protect users from injury and optimise function. Eight younger and six older healthy volunteers propelled a manual wheelchair on a wheelchair ergometer. During the task push rim parameters and surface EMG around the shoulder and elbow were measured. The older group were able to maintain the required velocity with no significant differences in push rim parameters. The older group demonstrated a trend towards higher muscle activity levels, but these differences were not statistically significant. Although the results of this study were not conclusive, in theory as muscles age they are at greater risk of injury.   Further assessment, during more challenging over ground propulsion tasks is required.

5.2 Introduction

As discussed in section 2.2, rotator cuff degeneration is the most commonly reported shoulder injury among manual wheelchair users (Akbar et al., 2010). The frequency of rotator cuff degeneration and tears increases naturally with age (Ozaki et al., 1988) and these injuries can be accelerated by the repetitive loading of the shoulder joint during manual wheelchair propulsion (Boninger et al., 2005a). As the population ages and the number of manual wheelchair users increases (Hers et al., 2015), it is important to investigate the age-related effects of manual wheelchair propulsion (Requejo et al., 2015), so injuries can be prevented and function maximised.

Previous research has identified age related differences during wheelchair propulsion. During wheelchair propulsion tests on a dynamometer, older

participants demonstrated a higher push rate to achieve a lower average velocity (Mercer et al., 2006). A further study assessing propulsion on a treadmill showed that older participants propelled with lower mechanical effectiveness, and were not able to generate such high peak power output as younger participants (Hers et al., 2015). There is little evidence available assessing age related differences in muscle activity level during manual wheelchair propulsion. Greater rotator cuff muscle activity has been reported in older participants during a study measuring surface EMG during tasks such as pulling, pushing and throwing (Gaur et al., 2007). It is likely that this is related to the reduction in shoulder joint muscle strength demonstrated with ageing (Hughes et al., 1999), so for the same force requirement an older participant is likely to have to work relatively harder than a younger participant.

5.2.1 Aims and hypothesis

The aim of this study was to quantify the effect of age related differences in shoulder joint function on the biomechanics of manual wheelchair propulsion. It was hypothesised that:

- The older group would demonstrate lower GH joint internal rotation and external rotation muscle strength than the younger group during the baseline assessment.
- The older group would demonstrate a significantly greater push rate that the younger group to maintain the required velocity during the wheelchair propulsion task.
- The older group would demonstrate greater GH joint and elbow joint peak muscle activity than the younger group during the wheelchair propulsion task.

5.3   Materials and Methods

5.3.1   Study participants

The study received ethical approval from the University College London (UCL) Research Ethics Committee.   University staff and students and previous study participants at the UCL Pedestrian Accessibility and Movement Environment Laboratory (PAMELA) were contacted and asked to participate.   Healthy participants were recruited if they were aged either between 18 and 40 years (younger group) or 60 and 85 years (older group), were able to propel a manual wheelchair, and reported no history of shoulder surgery and no pain within the previous 3 months.   Potential participants were not invited to participate if they reported a history of shoulder pain or surgery, were unable to propel a manual wheelchair, presented with implanted electronic devices including cardiac pacemakers and similar assistive devices (due to potential interference with the EMG signal), reported irritated skin or open wounds.   All participants provided written informed consent in advance of data collection.

5.3.2   Experimental protocol

Participants were required to attend UCL PAMELA.   They were subject to a baseline physical examination to assess shoulder joint range of motion and muscle strength.   Participants were positioned in a manual wheelchair, which was mounted on a wheelchair ergometer.   The position of the participant within the chair was adjusted to ensure that when the hand was placed at the top centre of the push rim, the elbow joint flexion angle was in the range of 100˚ to 120˚ (Boninger et al., 2000).   In advance of the test, each participant was provided with a familiarisation period, with instruction to aim for a semi-circular propulsion pattern (Boninger et al., 2002).   Participants then propelled for 60 seconds, using visual feedback from the ergometer to maintain a velocity of $1.2 m \cdot s^{-1}$.   During the propulsion task, push rim parameters, propulsion velocity and surface EMG were recorded for 10 steady state pushes.

5.3.3 Baseline strength testing

Shoulder joint internal and external rotation muscle strength was measured using a handheld dynamometer (Lafayette Manual Muscle Testing system, Lafayette, IN, USA). The participant was seated with the shoulder joint in neutral, the elbow flexed to 90° and the superior radio-ulnar joint in neutral. The sensor pad was placed immediately proximal to the ulnar styloid, with muscle strength recorded using a 'make contraction' technique (Turner et al., 2009). The participants were provided with the following instruction:

> 'participants were asked to build their force gradually to a maximum voluntary effort over a 2 second period and hold the maximum voluntary effort' (Riemann et al., 2010).

A single trial was used for this measurement of muscle strength, due to the reported similarity between a single trial and maximum and mean values of multiple repeats (Bohannon and Saunders, 1990).

5.3.4 Wheelchair ergometer

The wheelchair ergometer utilises a double roller system. The wheelchair is positioned on the roller and fixed to the ergometer from behind (Figure 5-1). As the wheelchair wheels are propelled, the ergometer roller moves at the same time. Rotation of the ergometer roller causes rotation of the tachometers at the same angular velocity as the wheelchair wheel.
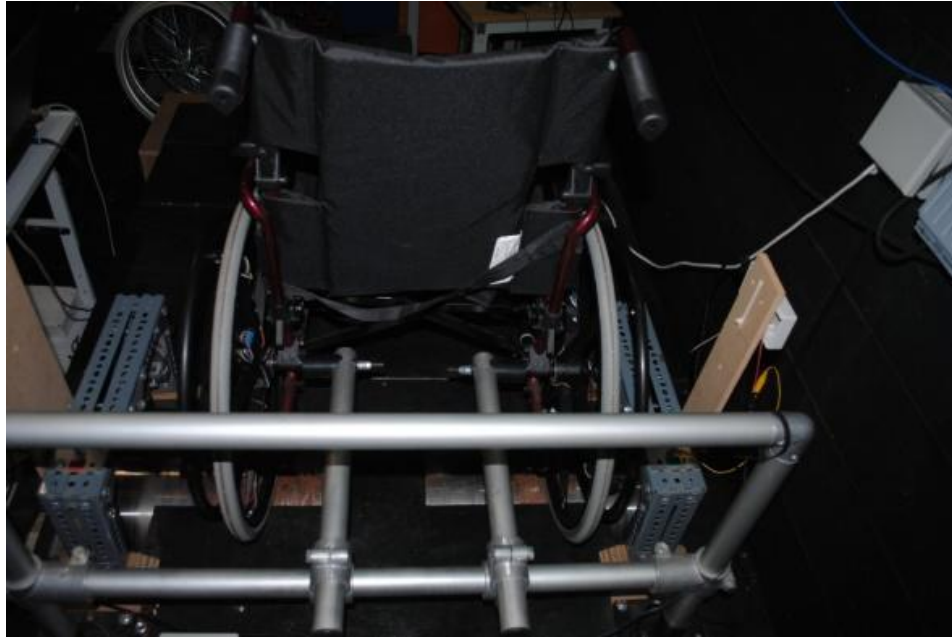
Figure 5-1: Wheelchair mounted on the ergometer.

The output wires of the tachometers were connected to an analogue to digital convertor (PCI DT3000, Data translation). The data acquisition was carried out in LabView. During the wheelchair test, tachometer data were sampled at 500Hz. The participants were able to view the LabView GUI during the test (Figure 5-2). The average speed of wheelchair propulsion was calculated for the period of the test.
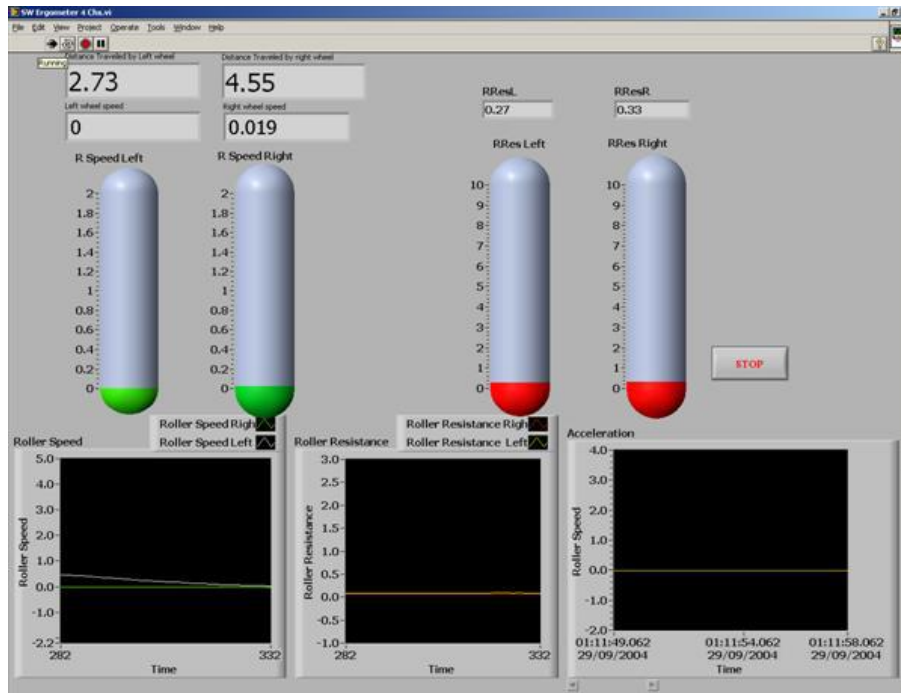
Figure 5-2: The LabView GUI viewed by the participants during the wheelchair propulsion task.

5.3.5 Synchronisation

The Sensewheel, surface EMG system and ergometer were synchronised via a TTL pulse, which triggered data capture of the surface EMG system and ergometer and presented as an 'event' in the Sensewheel record at that time.

5.3.6 Outcome measures

5.3.6.1 The Sensewheel

Push rim parameters were recorded using the Sensewheel Mark 1. The Sensewheel was positioned on the left side of the wheelchair, data was sampled at 50Hz and analysed using Matlabr2012b (Mathworks Inc, MA, USA). The push phase of the propulsion cycle was defined by measurement of the application of a positive moment about the wheel axle above a threshold of 0N.m. Push rate, push phase percentage and peak resultant propulsion force were calculated for the push phase of each of the measured push cycles, and the average of these values calculated.

5.3.6.2 Surface EMG

Surface EMG was recorded from the AD, PM, IS, BB and TB muscles using the Delsys Trigno™ Wireless System (Delsys Inc, MA, USA). Each sensor contains four contacts, 99.9% silver, dimensions 5 x 1mm, with 2 active contacts and 2 stabilising references. Skin surface EMG is amplified by 1000, with a signal bandwidth ranging from 20-450Hz. Baseline noise is reported as <750nV RMS, with a Common Mode Rejection Ratio of >80db. Data were sampled at 2000Hz.

Sensors were attached to the left upper limb using medical grade double sided tape, in accordance with the Surface Electromyography for the Non-Invasive Assessment of Muscles (SENIAM) guidelines for sensor placement (Hermens et al., 2000). Data were recorded from MVIC for each of the muscles and then during each of the pushing tasks. The MVIC tests for the shoulder used the functional tests described previously (Boettcher et al., 2008) (Table 5.1).

The sensors were positioned as follows:

- PM: sensor placed 2cm medial to the anterior axillary fold in a direct vertical line with the coracoid process, oriented parallel to the muscle fibres.
- AD: starting position sitting with the arms hanging vertically and the palm pointing inwards, sensor placed one finger width distal and anterior to the acromion and the thumb.
- IS: starting position sitting with arms at rest, sensor placed parallel and approximately four centimetres below the spine of the scapula in the infrascapular fossa.
- BB: starting position sitting with the elbow flexed to 90˚ and the dorsal side of the forearm in a horizontal downwards position, sensor placed on the line between the medial acromion and the cubital fossa, one third from the cubital fossa.

- TB: sitting with the shoulder at approximately 90˚ abduction with the elbow flexed to 90˚ and the palm of the hand pointing downwards, sensor placed at the half way point on the line between the posterior crista of the acromion and the olecranon at 2 finger widths medial to the line.

Table 5.1: Starting positions and test instruction for MVIC measurements.

Muscle	Starting position and test
Pectoralis Major	Shoulders flexed 90˚ bilaterally with heel of hands together and elbows flexed 20˚ as arms are horizontally adducted
Anterior Deltoid/Infraspinatus	Shoulder flexion at 125˚ as resistance applied above elbow and at inferior angle of the scapula attempting to de-rotate the scapula
Biceps Brachii	Shoulder joint neutral, elbow joint 90˚ flexion, forearm supination, resistance applied to the forearm in direction of extension
Triceps Brachii	Shoulder joint neutral, elbow joint 90˚ flexion, forearm supination, resistance applied to the forearm in direction of flexion

The data were exported to Matlabr2012b (Mathworks Inc, MA, USA) for analysis. All data were full wave rectified, and low pass filtered using a fourth order Butterworth filter with a cut-off frequency of 5Hz. The pushing task data for each muscle were normalised using the values obtained from the MVIC tests. The peak values for each muscle were obtained from the push phase of the 10 push cycles measured, and the mean of these peak values calculated. Data were excluded if the peak values were significantly in excess of 100% MVIC.

5.3.7 Statistical analysis

Statistical analysis was completed using IBM SPSS Statistics version 22 (IBM Corp, NY, USA). The Shapiro-Wilk test was used to assess whether each data set followed a normal distribution. When data were normally distributed, differences between the younger and older groups were assessed using the independent samples t-test. When data were not

normally distributed, the Mann Whitney-U test was used. The significance level was set at P<0.05.

5.4 Results

5.4.1 Participant characteristics

The younger and older groups demonstrated no significant difference in terms of stature (t(12) = -0.030, P = 0.977) or weight (t(12) = -0.410, P = 0.689). The younger group demonstrated greater shoulder internal rotation muscle strength than the older group, but this difference was not statistically significant (t(12) = 0.632, P = 0.270). The younger group also demonstrated greater external rotation muscle strength than the older group, but this difference was also not statistically significant (t(12) = 1.399, P = 0.094). Table 5.2 presents the study participant characteristics.

Table 5.2: Participant characteristics: Differences between the younger and older groups. Data are mean (SD).

	Younger group	Older group	P value
Sex (Male/Female)	4/4	5/1	n/a
Age (years)	31.13 (4.12)	67.17 (5.98)	n/a
Stature (cm)	171.81 (6.50)	172.00 (14.15)	0.977
Weight (kg)	70.25 (11.50)	73.25 (16.00)	0.689
Internal rotation strength (kg)	9.98 (3.06)	8.97 (2.80)	0.270
External rotation strength (kg)	7.96 (2.60)	6.25 (1.70)	0.094

5.4.2 Push rim parameters

During the propulsion test, both groups were able to maintain the goal velocity of $1.2m.s^{-1}$. There was no significant difference in any of the push rim parameters during the propulsion task between the younger and older groups (Table 5.3), including push phase percentage (t(12) = -0.271, P = 0.795), peak resultant force (t(12) = 0.245, P = 0.811) and body weight normalised peak resultant force (t(12) = 0.600, P = 0.556). As hypothesised,

the older group demonstrated a greater push rate, but this was not statistically significant (t(12) = -0.817, P = 0.430),

Table 5.3: Comparison of push rim parameters between the younger and older groups during the wheelchair propulsion task. Data are mean (SD).

	Younger group	Older group	P value
Push rate (s^{-1})	0.95 (0.20)	1.04 (0.22)	0.430
Velocity (m·s^{-1})	1.28 (0.18)	1.26 (0.17)	0.809
Push phase percentage (%)	35.14 (5.30)	36.54 (11.79)	0.795
Peak resultant force (N)	46.06 (15.25)	44.23 (11.67)	0.811
Peak resultant force (%BW)	6.59 (1.32)	6.17 (1.23)	0.560

5.4.3 Surface EMG

Surface EMG data was excluded from the statistical analysis if peak values significantly exceeded 100% MVIC. For the PM muscle, the data was excluded for 1 participant in the older group. For the AD muscle, the data was excluded for 2 participants in the younger group and 1 in the older group. For the IS muscle, the data was excluded for 1 participant in the younger group and 1 in the older group. No data was excluded for the BB or TB muscles. During the propulsion task, the older group demonstrated greater surface EMG amplitude as a percentage of MVIC that the younger group (Figure 5-3) in each of the muscles tested at both the GH joint and elbow joint. However, these differences were not statistically significant.
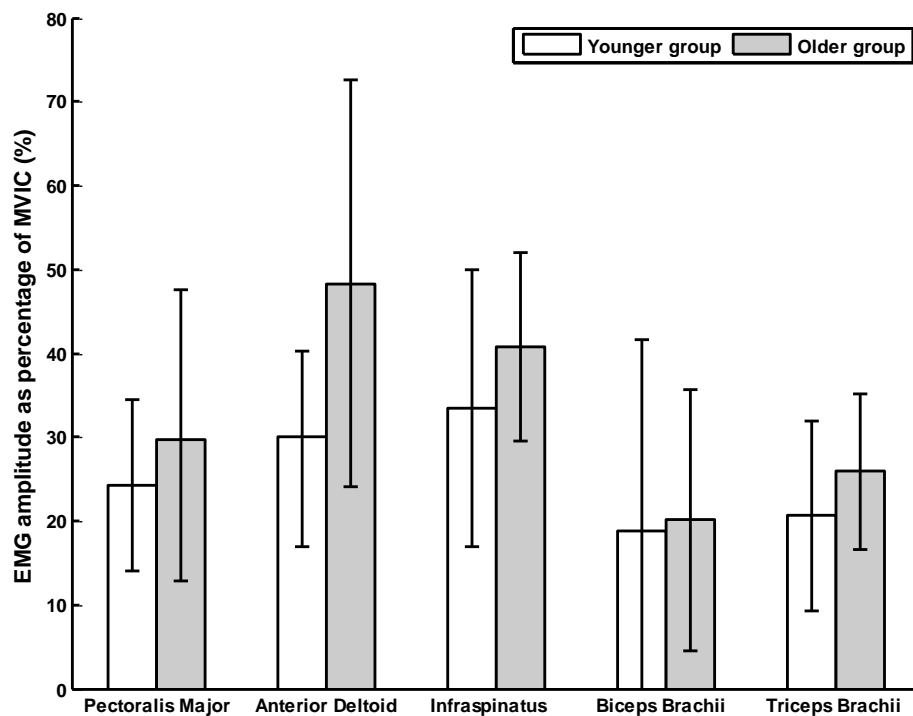
Figure 5-3: Differences in EMG amplitude between younger and older groups during wheelchair propulsion.

5.5 Discussion

The results demonstrated no significant differences in push rim parameters during the wheelchair propulsion task. To maintain the required velocity, the older group demonstrated higher muscle activity levels around the shoulder and elbow joint, although these differences were not statistically significant.

5.5.1 Demographics and baseline assessment

The younger and older groups were matched in terms of stature and body weight. The mean age of the younger group was 31.13 years with the mean age of the older group 67.17 years. The age related inclusion criteria was selected to reflect an expected distinction in muscle strength due to the reported progressive muscular deterioration that has been shown to manifest during the seventh decade of life (Ozaki et al., 1988). Focussing on the rotator cuff muscles, this cadaveric study has demonstrated a significant

increase in muscle degeneration and related muscle tears during the seventh decade. The results of the isometric strength tests performed during this study revealed that the younger group were stronger in terms of shoulder joint internal and external rotation strength, but these differences were not statistically significant. However, the differences presented supported the results of previous studies, which reported participants over 60 years of age with external rotation strength of 71.4% relative to a group of participants aged between 30 and 39, and internal rotation strength 83.3% that of the younger group (Hughes et al., 1999).

5.5.2 Push rim parameters

The results demonstrated no significant differences in push rim parameters during the wheelchair propulsion test. The older group were able to maintain the required velocity of $1.2 m^. s^{-1}$ without a significant difference in push rate, percentage push phase or peak force application. These results differ from previous research, which reported older participants using a higher push rate to achieve a lower velocity (Mercer et al., 2006). It is possible that these results differ as the propulsion task used during this study is of low intensity, with an average peak resultant force application of 44N (6.17% body weight). The velocity of $1.2 m.s^{-1}$ was chosen as the test speed for this study as this is the velocity required to safely negotiate a pedestrian crossing (Hoxie and Rubenstein, 1994). In reality, daily over ground wheelchair propulsion is much more demanding. Peak resultant forces have been demonstrated to be higher during propulsion on surfaces such as carpets and grass (Koontz et al., 2005), and can rise to values over 200N during incline tasks (Gagnon et al., 2014). It is likely that more demanding activities would highlight age related differences, similar to the findings that older participants generated significantly lower power than younger during wheelchair sprint testing (Hers et al., 2015).

5.5.3 Muscle activation

The results support the finding that the AD, PM, IS, BB and TB are active during the push phase of manual wheelchair propulsion (Mulroy et al., 1996).

The older group demonstrated higher peak muscle activity level for each muscle tested during the wheelchair propulsion task, although these differences were not statistically significant. These results cannot be used to support the findings of previous research which reported an increase in shoulder muscle activity level in older participants during tasks such as pulling, pushing and throwing (Gaur et al., 2007). The greatest difference between the groups existed for the AD muscle. However, it must be noted that the AD values of 2 of the younger group were excluded due to results in excess of 100% MVIC.

Clinically, the demand placed on the IS muscle during manual wheelchair propulsion is of particular interest. Although during this study the older group did not demonstrate a significantly greater activity level of the IS muscle than the younger group, the theory suggests that further investigation is warranted. The IS forms part of the rotator cuff, which is commonly injured in manual wheelchair users (Akbar et al., 2010). Although rarely injured in comparison to the SS muscle (Akbar et al., 2010), the IS muscle is accessible for measurement using surface EMG. During the push phase of wheelchair propulsion, the IS muscle is active, and when the IS muscle is active measurements have been shown to be valid when compared to intramuscular EMG (Johnson et al., 2011). Therefore, it provides the best measure of rotator cuff muscle activity. The natural age related degeneration of the rotator cuff (Ozaki et al., 1988) may increase the relative demand of a task and put older manual wheelchair users at increased risk of injury. Alternatively, it may be that relative activity (% MVIC) is not the optimal measure of injury risk. It may be that absolute load is a better measure, linking to the theory of repeated loading of a degenerate tendon leading to soft tissue damage (Nho et al., 2008). Further testing with a larger number of participants during more demanding over ground tasks is required to determine whether older wheelchair users may be at greater risk of injury. Additionally, although the older group demonstrated lower external rotation muscle strength, this difference was not significant. Testing an older group of participants with a significant reduction in muscle strength may have highlighted differences more clearly.

5.5.4 Limitations

Testing a larger sample of participants is required to assess whether the trends demonstrated are significant. As previously mentioned, this study was completed on a wheelchair ergometer and the task was of low intensity. Assessing more challenging over ground propulsion tasks may highlight further any age related differences. In addition, the wheelchair ergometer test was limited in that the wheelchair was fixed from behind to sit straight on the wheelchair ergometer. This completely eradicates the necessity for the user to control the direction in which the wheelchair travels, which can be particularly demanding during over ground propulsion during tasks involving cross slopes (Holloway and Tyler, 2013).

5.6 Conclusions

Although not statistically significant, the older group presented with reduced shoulder strength during baseline assessment. The older group were able to maintain the required velocity with no difference is push rim parameters, and did not demonstrate significantly greater muscle activity levels. Although the results were not conclusive, the known fact of age related rotator cuff degeneration suggests that further investigation is warranted during more demanding wheelchair propulsion tasks to identify age related risk of muscle injury.

Chapter 6 Linking wheelchair kinetics to GH joint demand during everyday accessibility tasks

6.1 Overview

The aim of the study was to investigate GH joint demand and injury risk during manual wheelchair accessibility tasks. The study also aimed to investigate if push rim kinetics could be used as markers of GH joint demand during manual wheelchair accessibility activities. Propulsion forces, trunk and upper limb kinematics and surface EMG were recorded during four propulsion tasks (level, 2.5% cross slope, 6.5% incline and 12% incline). Kinetic and kinematic data were applied to an OpenSim musculoskeletal model of the trunk and upper limb, to enable calculation of GH joint contact force. Propulsion forces increased as the task became more challenging. Participants demonstrated increases in trunk flexion angle as the requirement for force application increased, significantly so in the 12% incline task. There were significant increases in both resultant GH joint contact forces and peak normalised muscle activity levels during the incline tasks. In addition, results demonstrated a strong positive association between propulsion forces and GH joint contact forces. This study demonstrated the high demand placed on the GH joint during accessibility tasks, especially as the gradient of incline increases. A lightweight instrumented wheelchair wheel has potential to guide the user to minimise upper limb demand during daily activity.

6.2 Introduction

The previous chapter investigated the influence of ageing on the risk of rotator cuff injury. As introduced in section 2.5.2 of the background chapter, in addition to ageing, it is theorised that rotator cuff injury among manual wheelchair users is caused by repetitive loading of the joint. Therefore it is important to understand the extent of this loading during daily propulsion activity.

Wheelchair users must tackle a number of difficult footway conditions as they move around the environment. Previous research highlights increased upper

limb demand during cross-slope (Holloway and Tyler, 2013) and incline propulsion (Hurd et al., 2009). Specifically, negotiating an incline has been shown to require an increase in both muscle activity (Chow et al., 2009) and GH joint contact force (Morrow et al., 2010b) compared to level propulsion. Therefore, there is a need to measure the effect of these different obstacles and how people overcome them. This study develops on the work of Morrow et al., (2010b), with measurement of GH joint contact force during cross-slope propulsion and incline propulsion to simulate a bus access ramp.

There exists limited evidence highlighting a direct link between push rim kinetics and shoulder joint injury (see chapter 2, section 2.6). The association between push rim kinetics and measures of upper limb demand have been reported. Higher values of mechanical fraction of effective force and mechanical use have been associated with higher net shoulder joint moments, calculated using an inverse dynamic model (Desroches et al., 2008a). Reducing cadence and peak propulsion force has been associated with a reduction in total muscle power during a study utilising forward dynamic simulations (Rankin et al., 2012). However, this reduction in cadence was associated with higher net muscle stress.

The guidelines for preservation of upper limb function following spinal cord injury suggest that wheelchair users should aim to minimise push frequency and peak resultant propulsion force (Boninger et al., 2005a). These suggestions are based on studies linking such propulsion parameters with median nerve function and carpal tunnel syndrome (Boninger et al., 1999). Each of the studies linking push rim kinetics to upper limb demand assessed propulsion on a dynamometer.

6.2.1 Aims and hypothesis

The aims of the study were:

1) To quantify upper limb demand during over ground wheelchair propulsion tasks, using a combination of wireless inertial measurement and surface EMG sensors and the Sensewheel, to

provide a method of biomechanical assessment of manual wheelchair propulsion that could be used in any environment.

2) To examine whether any correlation existed between push rim kinetics and GH joint contact force during over ground wheelchair propulsion tasks, with a view to using the instrumented wheelchair wheel to track daily upper limb demand and optimise propulsion style.

It was hypothesised that:

- There would be a significant increase in peak and mean resultant propulsion force as the gradient of the footway increased
- There would be a significant increase in percentage push phase as the force application required to complete the task increased
- There would be a significant increase in push rate as the force application required to complete the task increased
- There would be a significant increase in peak muscle activity level as the force application required to complete the task increased
- There would be a significant increase in peak and mean resultant GH joint contact force as the force application required to complete the task increased
- There would be a significant positive correlation between peak and mean resultant propulsion force and peak and mean resultant GH joint contact force respectively

6.3 Materials and Methods

6.3.1 Study participants

The study was approved by the London Stanmore Research Ethics Committee. Participants were eligible for recruitment if they had suffered a SCI below the spinal level of the first thoracic vertebra, were able to propel a manual wheelchair, reported no history of major shoulder injury or surgery and had capacity to provide written informed consent. Potential participants were excluded if they reported upper limb pain that prohibited the propelling of a manual wheelchair, reported any medical condition deemed to have a

high risk of being exacerbated by the study protocol (angina, exercise induced asthma, uncontrolled hypertension), had a history of shoulder surgery, implanted electronic devices or irritated skin or open wounds. Participants were recruited through the London Spinal Cord Injury Centre, based at the Royal National Orthopaedic Hospital, Stanmore. Potential participants were pre-screened by a rehabilitation consultant and then sent a study information sheet and asked to make contact if they were interested in participating. If they made contact, participants were screened by a physiotherapist and invited to attend UCL PAMELA on a single occasion. All participants provided written informed consent in advance of the experiments.

7 male SCI subjects participated in the study (SCI level range T5-L1), mean age 42.7 years, mean weight 83.1 kg, mean time since injury 8.9 years (Table 6.1).

Table 6.1: Participant characteristics. M = male, T = Thoracic, L = Lumbar.

Subject	Gender	Age	Weight (kg)	SCI Level	Years since SCI
1	M	63	85	T12	9
2	M	58	77	T9	7
3	M	27	89	T8	2
4	M	31	73	T12	6
5	M	38	75	L1	17
6	M	39	93	T5	10
7	M	43	90	T5	11

6.3.2 Experimental protocol

The study was completed at UCL PAMELA. PAMELA houses a modular platform that can be adjusted to simulate different surface profiles (Figure 6-1). For this study participants were required to complete 4 different

propulsion tasks; level (8.4m), 2.5% cross slope (7.2m, instrumented side on the down slope), 6.5% incline (7.2m) and 12% incline (1.5m). A 2.5% cross slope was chosen to simulate the recommended cross slope for footways in the UK to aid surface water drainage. The choice of the 6.5% incline was dictated by the capacity of the platform to enable an incline over a longer distance, and the length and 12% incline of the ramp set to mimic a London Bus access ramp.
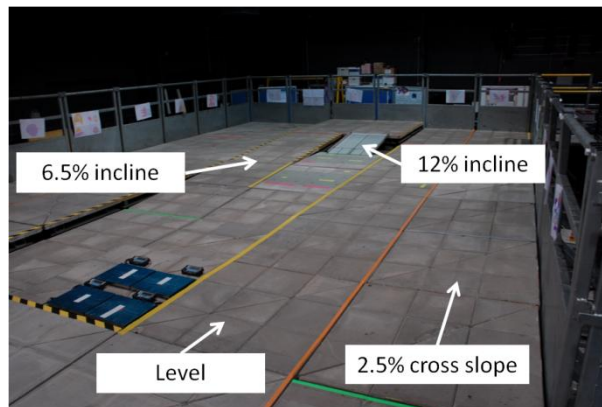
Figure 6-1: The UCL PAMELA platform

All participants transferred into the same wheelchair to complete the experiment. The wheelchair was a Van Os Excel G6 High Active 'Sports Edition'.

6.3.3 Synchronisation

The Sensewheel, surface EMG system and inertial measurement system were synchronised using the same method reported in section 5.3.5.

6.3.4 Outcome measures

6.3.4.1 Push rim forces

Push rim forces were measured with the Sensewheel. Peak and mean resultant propulsion force, percentage push phase and push rate were calculated for a representative steady state push phase for each of the

propulsion tasks. Sensewheel data were used to animate a musculoskeletal model of the trunk and upper limb.

6.3.4.2 Trunk and upper limb kinematics

The Xsens MTw^{TM} (Xsens Technologies, NL) is a wireless inertial measurement system comprising units with 3D accelerometers, gyroscopes and magnetometers. Application of a kalman filter enables measurement of real time 3D orientation in addition to measurement of linear acceleration and angular velocity. Each Xsens unit measures 34.5 x 57.8 x 14.5mm (W x L x H) and weighs 27g, with a reported 2˚ RMS error dynamic accuracy when used to measure orientation (XSens, 2016).

When removed from the base station the units were placed in alignment on a stable flat surface at rest for 2 minutes. Units were attached to the participant using medical grade double sided tape and micropore, to the following anatomical locations:

1) The thorax (sternum)
2) Left humerus (on the lateral border superior to the lateral epicondyle)
3) Left radius (dorsal surface superior to the radial styloid)

To position the units, and align the coordinate systems of the units to the 'anatomical' coordinate system, the participant was positioned in a 'neutral position'. From distal to proximal, the anatomically 'neutral' position was maintained as follows:

1) Neutral position at the pelvis
2) Neutral scapula-thoracic position
3) GH joint – neutral
4) Elbow joint - 90˚ flexion
5) Radio-ulnar joint – neutral
6) Radio-carpal joint – neutral

The unit on the thorax was placed on the flat portion of the sternum, with the unit z-axis pointing horizontally forwards and the unit x-axis vertically upwards (see Figure 6-2). The unit on the upper arm was placed on the lateral border of the humerus, with the unit x-axis pointing horizontally forwards and the unit y-axis vertically upwards. The unit on the lower arm was placed on the distal radius, with the unit x-axis pointing horizontally forwards and the unit y-axis vertically upwards.

Figure 6-2: XSens unit and unit coordinate system.

Once the sensors were attached, the participant transferred into the test wheelchair and re-positioned in a 'neutral position' to enable alignment reset of the sensors.

The alignment reset function aligns the co-ordinate systems of each unit, and subsequently orientation data is output with respect to this new 'anatomical' co-ordinate system. Following triggering of the measurement devices and in advance of the propulsion test, the participant maintained the neutral anatomical position for 5 seconds, and when the propulsion test was completed the participant re-assumed the neutral anatomical position. This step enabled the investigators to check for any sensor drift. Data were sampled at 50Hz and exported as a .csv file using the rotation matrix (direction cosine matrix) orientation output mode.

Post processing was completed in Matlab. Matrix multiplication to calculate the relative position of the sensors, and then conversion to Euler angles to represent joint angles was completed using a previously published method

(Kobrick et al., 2012). The OpenSim model was constrained to allow trunk lean, 3 degrees of freedom at the GH joint and elbow joint flexion and extension. Accordingly, flexion and extension of the thorax were calculated by measurement of the relative orientation of the sensor on the thorax with respect to its neutral starting position. The relative orientation of the sensor on the humerus with respect to the sensor on the thorax was used to calculate the 3 degrees of freedom at the shoulder joint. As per the OpenSim model used, this technique calculated thoraco-humeral angle (rather than GH joint angle), as a sensor was not positioned on the scapular. The relative orientation of the sensor on the radius with respect to the orientation of the sensor of the humerus was measured to calculate elbow joint flexion and extension (constrained to uniplanar movement).

Maximum, minimum and change in inclination angle for each degree of freedom was calculated from a representative steady state push cycle for each of the propulsion tasks. For the trunk, flexion was recorded as a positive angle and extension a negative angle. For the thoraco-humeral measurements, flexion was recorded as a positive angle and extension a negative angle, abduction a positive angle and adduction a negative angle and internal rotation a positive angle and external rotation a negative angle. At the elbow joint, flexion was assigned a positive angle, with respect to 0˚ at full elbow joint extension.

6.3.4.3 Surface EMG

Muscle activity was recorded from the AD, PM and IS muscles using the Delsys Trigno^{TM} System. For each muscle the data collected during the wheelchair propulsion tasks was normalised to the peak value gained from functional MVIC tests (Boettcher et al., 2008). Peak normalised EMG values were calculated for a representative steady state push phase for each of the propulsion tasks. A detailed description of the surface EMG system and muscle activity calculation is provided in the methods section of chapter 5, section 5.3.6.2.

6.3.5 Musculoskeletal model

The OpenSim model used was called 'Dynamic Arms 2013', an adapted version of the Stanford VA upper extremity model (Holzbaur et al., 2005) downloaded from OpenSim (Delp et al., 2007) (See figure 6-3). The model is a rigid body model of the trunk and both upper limbs. The mass of the unscaled model is 34.04kg. The thorax is 26.63kg, the humerus 2.03kg, the radius and ulna both 0.61kg and the hand 0.46kg. In terms of joints, the model has 6 available degrees of freedom at the joint between the ground and thorax (rotation and translation), 3 degrees of freedom at the GH joint, 2 degrees of freedom at the elbow joint (elbow joint flexion and extension and superior radio-ulnar joint pronation and supination) and 2 degrees of freedom at the radio-carpal joint. For this study, the model was constrained to allow trunk lean, 3 degrees of freedom at the GH joint and elbow joint flexion and extension. All other joints/coordinates were locked in a neutral position.
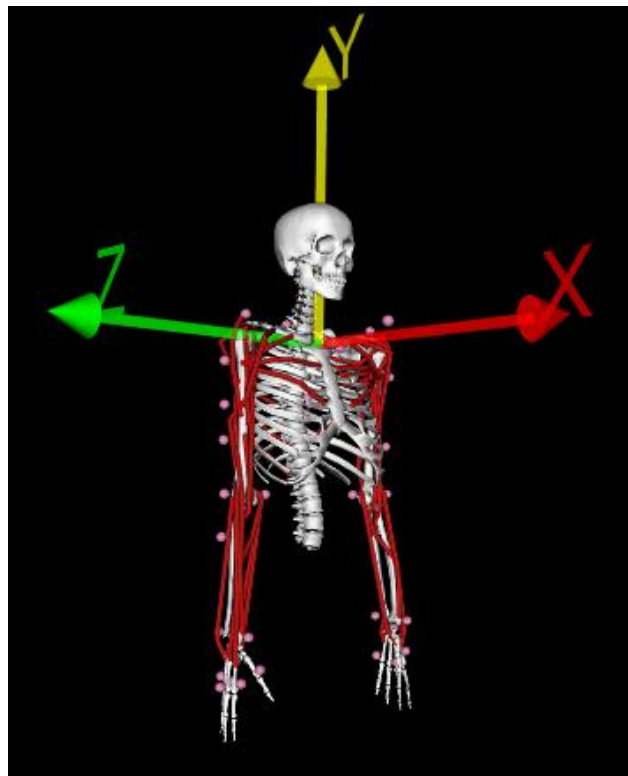
Figure 6-3: The OpenSim model.

The ground to thorax, shoulder and elbow joints are classified as 'custom joints' in OpenSim, allowing up to 6 user defined coordinates. The joint between the thorax and ground (ground_thorax joint) allows 3-dimensional rotation and 3-dimensional translation. Rotation about the x-axis represents thoracic side flexion, rotation about the y-axis thoracic rotation and rotation about the z-axis thoracic flexion and extension. For this study, the model was constrained to allow only rotation about the z axis, with no translation.

The joint between the humerus and thorax (shoulder2 joint) allows 3-dimensional rotation. Rotation about the x-axis (shoulder_elv) represents anatomical GH joint abduction, rotation about the y-axis (shoulder_rot) GH joint rotation and rotation about the z-axis GH joint flexion/extension.

The joint between the radius and the humerus (elbow joint) allows uni-planar rotation, with rotation about the y-axis representing elbow joint flexion and extension.

The model included 29 muscle actuators; each created using the Thelen muscle model (OpenSim, 2015c). The muscle properties are tabulated in appendix 2 (maximum isometric force, optimal muscle fibre length, maximum contraction length and pennation angle). As described, the Thelen muscle model consists of a contractile element, a parallel element and a series element. The muscle force generated is a function of three factors, the activation value, normalised length of the muscle unit and normalised velocity of the muscle unit. The active length curve describes the contractile element and the passive length curve the parallel element. The model was uniformly scaled to participant mass, using the model scaling tool within the OpenSim software.

The degrees of freedom of the model were constrained whilst the full actuator set was retained. Although the model elbow joint was constrained to allow only flexion and extension, the actuators of pronation and supination were retained as they also perform a role in flexion and extension:

- Anconeus: extends the elbow joint in addition to stabilising the ulna during pronation and supination
- Brachioradialis: flexes the elbow joint and assists in pronating and supinating the forearm
- Pronator teres: pronates the forearm and assists in flexion of the elbow joint

The actuators of the wrist were also retained, despite the model wrist joint being constrained to a neutral position. Constraining the wrist resulted in a minimal contribution by the wrist actuators to the static optimisation force output file. It is possible that this may have resulted in greater force generating requirements for the elbow and shoulder joint actuators, although wrist joint moments have previously been shown to be much lower than those at the shoulder and elbow during wheelchair propulsion (Rankin et al., 2010).

6.3.5.1 Preparation of experimental data to animate the OpenSim model

To prepare the experimental data for application to the model, the kinematic and kinetic data were converted to the model coordinate system:

x-axis points forward from the model (positive forwards)

y-axis points upwards from the model (positive upwards)

z-axis points to the right of the model (positive to the right)

Kinematic output data for each trial were collated in Microsoft Excel 2007 (Microsoft Corporation, WA, USA), with the joint angles recorded represented by the following coordinate headers for application to the model.

Trunk lean (flexion negative) = thorax_ry

Thoraco-humeral flexion/extension (flexion positive) = elv_angle

Thoraco-humeral abduction/adduction (abduction positive) = shoulder_elv

Thoraco-humeral internal rotation/external rotation (internal rotation positive) = shoulder_rot

Elbow joint flexion/extension (flexion positive) = elbow_flexion

The .mot file created by the developers of SIMM (Software for Interactive Musculoskeletal Modelling) is compatible with OpenSim, and requires a specific global header and column headers.

To apply push rim reaction forces to the model, a .mot file with forces and coordinates of point of force application was created. The coordinates of point of force application were calculated using the 'Point kinematic' function available in the software, which outputs the 3-dimensional coordinates of a marker positioned on the palmar surface of the right radio-carpal joint, during the model motion created by the trial specific kinematic .mot file. The flow diagram for the Point kinematic function is presented in Appendix 3 (OpenSim, 2014). All OpenSim set up files were processed using Notepad++.

To create a .mot file to apply push rim reaction forces, the software specific general and column headers were created. The 'ground_force_v' columns represent forces applied to the model along the x, y and z axes. The 'ground_force_p' columns represent the x, y and z coordinates of the point of force application on the radio-carpal joint.

6.3.5.2 Visualising data in advance of simulation

In advance of performing the static optimisation analysis, the push rim reaction force during the animated motion was visually checked in the OpenSim GUI using the 'Associate Motion Data' function. As the push rim force was consistently anterior, inferior and medially oriented with respect to the wheelchair push rim, the resultant push rim reaction force was posterior,

superior and lateral with respect to the point of force application on the model.

6.3.5.3 Static optimisation

The static optimization function within OpenSim 3.1 was used to resolve the net joint moments into individual muscle forces at each time point. The model was animated with a trial specific .mot file, and push rim reaction forces applied using the OpenSim set-up file (OpenSim, 2015b). To account for dynamic inconsistencies, a reserve actuator was added to the single degree of freedom at the ground thorax joint. This was necessary as the model did not include a pelvis or hip joints, or associated actuators (OpenSim, 2016).

In this study, the force-length-velocity muscle parameters were used and apart from the addition of an actuator at the ground thorax joint, model muscle properties were maintained. The static optimisation tool calculates muscle forces by applying an objective function to minimise the sum of muscle activation, assuming a non-elastic tendon. The flow diagram for the OpenSim static optimisation function is presented in appendix 4 (OpenSim, 2013b).

6.3.5.4 Joint reaction analysis

The Joint Reaction Analysis function in OpenSim 3.1 was used to calculate the GH joint contact forces (Steele et al., 2012). The results were calculated as the force applied by the humerus on the glenoid (fixed scapula on the thorax), presented in the ground reference system (equal to that of the thorax). The flow diagram for the OpenSim joint reaction analysis is presented in appendix 5 (OpenSim, 2013a).

6.3.5.5 Post processing of OpenSim data

For analysis of GH joint contact forces, resultant force was calculated from the x, y and z components. Peak values for the x, y and z forces and peak

and mean values for the resultant forces were calculated for the push phase of a representative steady state push for each of the propulsion tasks.

6.3.6 Statistical analysis

To assess for differences in push rim kinetics, surface EMG, kinematics and GH joint contact forces between the 4 propulsion tasks, a repeated measures ANOVA was used using SPSS. When Mauchly's tests indicated that the assumption of sphericity had been violated, degrees of freedom were corrected using the Greenhouse-Geisser estimates. When the results were significant, the Bonferroni post hoc test was applied and adjusted for multiple comparisons, and results reported in the results tables to demonstrate differences relative to the level propulsion task. Correlation was measured between peak and mean resultant propulsion forces and peak and mean resultant GH joint contact forces respectively, using Spearman's correlation coefficient. Statistical significance was set at $P < 0.05$ for all tests.

6.4 Results

6.4.1 Propulsion forces

Peak resultant propulsion force was significantly affected by task, $F_{(3,18)} = 103.97$, $P < 0.05$. The Bonferroni post hoc test demonstrated significant differences between each pushing task. There was a significant increase in peak resultant propulsion force between level and 2.5% cross slope (50.36N vs. 67.48N, $P<0.05$), 2.5% cross slope and 6.5% incline (67.48N vs. 106.90N, $P<0.05$) and 6.5% incline and 12% incline (106.90N vs. 139.63N, $P<0.05$). Mean resultant propulsion force was also significantly affected by task, $F_{(3,18)} = 179.09$, $P < 0.05$. The Bonferroni post hoc test demonstrated significant differences between each pushing task. There was a significant increase in mean resultant propulsion force between level and 2.5% cross slope (14.69N vs. 22.28N, $P<0.05$), 2.5% cross slope and 6.5% incline (22.28N vs. 39.79N, $P<0.05$) and 6.5% incline and 12% incline (39.79N vs. 65.12N, $P<0.05$).

Percentage push phase was significantly affected by task, $F(3,18) = 23.24$, P < 0.05. The Bonferroni post hoc test demonstrated significant differences with significant increases between level propulsion and 6.5% incline (43.63% vs. 56.97%, P<0.05) and level propulsion and 12% incline (46.63% vs. 65.21%, P<0.05). A significant increase between 2.5% cross slope and 12% incline was also evident (48.77% vs. 65.21%, P<0.05). Push rate was not significantly affected by task, $F(3,18) = 1.22$, P > 0.05.

Table 6.2: Sensewheel parameters during the different manual wheelchair propulsion tasks. Data are mean (SD), statistically significant results in bold.

	Conditions					Post hoc comparisons		
Level	2.5% cross slope	6.5% incline	12% incline	ANOVA	Level vs. 2.5% cross slope	Level vs. 6.5% incline	Level vs. 12% incline
Push rate (s^{-1})							
0.97 (0.16)	1.04 (0.16)	1.07 (0.11)	1.12 (0.22)	0.332	-	-	**-**
Push phase (%)							
43.63 (4.60)	48.72 (5.95)	56.97 (6.33)	65.21 (5.36)	**0.000**	0.449	**0.034**	**0.003**
Peak resultant propulsion force (N)							
50.36 (12.38)	67.48 (11.41)	106.90 (20.53)	139.63 (15.30)	**0.000**	**0.018**	**0.001**	**0.000**
Mean resultant propulsion force (N)							
14.69 (3.29)	22.28 (4.12)	39.79 (6.35)	65.12 (6.37)	**0.000**	**0.002**	**0.000**	**0.000**

6.4.2 Trunk and upper limb kinematics

6.4.2.1 Trunk inclination

Maximum trunk flexion angle was significantly affected by task, $F_{(3,18)} = 33.96$, $P < 0.05$. The Bonferroni post hoc test demonstrated that maximum trunk flexion angle was significantly greater in the 12% incline condition than the other tasks, level and 12% incline (4.88˚ vs. 35.33˚, P<0.05), 2.5% cross slope and 12% incline (6.67˚ vs. 35.33˚, P<0.05) and 6.5% incline and 12% incline (22.04˚ vs. 35.33˚, P<0.05). Minimum trunk flexion angle was significantly affected by task, $F_{(3,18)} = 4.99$, $P < 0.05$. The Bonferroni post hoc test demonstrated that although there was an overall effect of task, there was no significant effect between tasks. Trunk excursion was also significantly affected by task, $F_{(3,18)} = 35.66$, $P < 0.05$. The Bonferroni post hoc test demonstrated that total trunk excursion angle was significantly greater in both incline tasks when compared to the level and 2.5% cross slope tasks. Level and 6.5% incline (6.54˚ vs. 21.57˚, P<0.05), level and 12% incline (6.54˚ vs. 29.97˚, P<0.05). 2.5% cross slope and 6.5% incline (9.32˚ vs. 21.57˚, P<0.05), 2.5% cross slope and 12% incline (9.32˚ vs. 29.97˚, P<0.05).

6.4.2.2 Thoraco-humeral joint

Maximum thoraco-humeral extension was not significantly affected by task, $F_{(3,18)} = 0.31$, $P > 0.05$. Minimum thoraco-humeral extension was not significantly affected by task, $F_{(3,18)} = 0.93$, $P > 0.05$. Thoraco-humeral excursion in the sagittal plane was also not significantly affected by task, $F_{(3,18)} = 1.25$, $P > 0.05$.

Maximum thoraco-humeral abduction was not significantly affected by task, $F_{(3,18)} = 0.19$, $P > 0.05$. Minimum thoraco-humeral abduction was not significantly affected by task, $F_{(3,18)} = 0.96$, $P > 0.05$. Total thoraco-humeral excursion in the frontal plane was also not significantly affected by task, $F_{(3,18)} = 0.49$, $P > 0.05$.

Maximum thoraco-humeral internal rotation was not significantly affected by task, $F_{(3,18)} = 0.88$, $P > 0.05$. Minimum thoraco-humeral internal rotation (external rotation) was not significantly affected by task, $F_{(3,18)} = 0.11$, $P > 0.05$. Total thoraco-humeral excursion in the transverse plane was also not significantly affected by task, $F_{(3,18)} = 1.37$, $P > 0.05$.

6.4.2.3 Elbow joint

Maximum elbow flexion was significantly affected by task, $F_{(3,18)} = 11.83$, $P < 0.05$. The Bonferroni post hoc test demonstrated that maximum elbow flexion was greater in both incline tasks compared to the level task, level and 6.5% incline (59.07˚ vs. 68.65˚, $P<0.05$) and level and 12% incline (59.07˚ vs. 73.12˚, $P<0.05$). Minimum elbow flexion was not significantly affected by task, $F_{(3,18)} = 0.22$, $P > 0.05$. Total excursion of the elbow joint was significantly affected by task, $F_{(3,18)} = 7.01$, $P < 0.05$. The Bonferroni post hoc test demonstrated that total excursion of the elbow joint was significantly different between the level and 6.5% incline (24.41˚ vs. 32.08˚, $P<0.05$).

Table 6.3: Trunk, thoraco-humeral and elbow kinematics during the different manual wheelchair propulsion tasks. Data are mean (SD), statistically significant results in bold.

		Conditions					Post hoc comparisons		
		Level	2.5% cross slope	6.5% incline	12% incline	ANOVA	Level vs. 2.5% cross slope	Level vs. 6.5% incline	Level vs. 12% incline
	Trunk – Flexion(+ve) Extension(-ve)								
	Maximum	4.88 (8.16)	6.67 (6.65)	22.04 (11.13)	35.33 (8.98)	**0.000**	1.000	0.073	**0.001**
	Minimum	-1.65 (6.54)	-2.65 (6.14)	0.46 (3.02)	5.36 (2.97)	**0.011**	1.000	1.000	0.097
	Excursion	6.54 (3.09)	9.32 (5.84)	21.57 (12.09)	29.97 (9.72)	**0.000**	0.664	**0.036**	**0.001**
	Sagittal thoraco-humeral angle – flexion (+ve) extension (-ve)								
	Maximum	-43.39 (9.78)	-44.55 (10.43)	-44.09 (10.58)	-43.46 (7.93)	0.992	-	-	-
	Minimum	1.24 (8.06)	2.31 (8.81)	3.08 (11.44)	8.37 (7.46)	0.445	-	-	-
	Excursion	44.62 (8.01)	46.85 (12.36)	47.17 (5.58)	51.82 (7.30)	0.323	-	-	-
	Frontal thoraco-humeral angle – abduction (+ve) adduction(-ve)								
	Maximum	28.10 (9.43)	29.48 (9.06)	27.89 (7.15)	27.74 (9.43)	0.901	-	-	-
	Minimum	11.15 (4.73)	10.73 (5.99)	8.63 (8.19)	8.56 (8.79)	0.433	-	-	-
	Excursion	16.95 (5.74)	18.75 (5.95)	19.27 (1.61)	19.18 (2.99)	0.697	-	-	-
	Transverse thoraco-humeral angle – IR(+ve) ER(-ve)								
	Maximum	18.00 (6.59)	26.04 (10.99)	27.23 (14.06)	21.94 (16.89)	0.469	-	-	-
	Minimum	-14.68 (10.01)	-13.06 (10.31)	-13.23 (13.94)	-15.93 (12.56)	0.900	-	-	-
	Excursion	32.68 (9.13)	39.10 (9.13)	40.48 (6.37)	37.88 (9.04)	0.292	-	-	-
	Elbow – flexion(+ve) extension(-ve)								
	Maximum	59.07 (10.96)	61.58 (10.13)	68.65 (7.21)	73.12 (6.84)	**0.000**	1.000	**0.026**	**0.007**
	Minimum	34.66 (5.94)	35.26 (9.81)	36.57 (5.09)	36.32 (5.89)	0.878	-	-	-
	Excursion	24.41 (9.39)	26.32 (8.36)	32.07 (8.54)	36.81 (10.48)	**0.003**	1.000	**0.013**	0.071

Segment angles (°)

6.4.3 Surface EMG

Peak AD activity was significantly affected by task, $F_{(1.1, 6.66)} = 11.84$, $P < 0.05$. The Bonferroni post hoc test demonstrated significant increases in peak AD activity between the level and 12% incline (22.12% vs. 92.10%, $P<0.05$) and between the 2.5% cross slope and 12% incline (27.26% vs. 92.10%, $P<0.05$).

Peak PM activity was significantly affected by task, $F_{(3,18)} = 16.92$, $P < 0.05$. The Bonferroni post hoc test demonstrated significant increases in peak PM activity between the level and 12% incline (15.41% vs. 58.85%, $P<0.05$) and between the 2.5% cross slope and 12% incline (20.44% vs. 58.85%, $P<0.05$).

Peak IS activity was significantly affected by task, $F_{(1.96, 11.77)} = 5.68$, $P < 0.05$. The Bonferroni post hoc test demonstrated that although there was an overall effect of task, there was no significant difference between each task.

Table 6.4: Peak EMG (% MVIC) of Anterior Deltoid, Pectoralis Major and Infraspinatus muscles during the different manual wheelchair propulsion tasks. Data are mean (SD), statistically significant results in bold.

		Conditions				Post hoc comparisons		
	Level	2.5% cross slope	6.5% incline	12% incline	ANOVA	Level vs. 2.5% cross slope	Level vs. 6.5% incline	Level vs. 12% incline
Anterior Deltoid								
	22.19 (15.42)	27.26 (13.06)	87.97 (64.42)	92.10 (51.68)	**0.011**	0.318	0.105	**0.025**
Pectoralis Major								
EMG (%MVIC)	15.41 (7.39)	20.44 (11.86)	43.26 (21.29)	58.85 (22.12)	**0.000**	0.469	0.064	**0.010**
Infraspinatus								
	38.98 (24.29)	36.50 (21.92)	57.78 (31.24)	79.30 (42.24)	**0.019**	1.000	1.000	0.092

6.4.4 GH joint contact forces

Peak resultant GH Joint contact force was significantly affected by task, $F_{(1.33, 7.96)} = 17.51$, $P < 0.05$. The Bonferroni post hoc test demonstrated significant increases between level propulsion and 12% incline (521.00N vs. 2031.55N, $P<0.05$), cross-slope and 12% incline (684.20N vs. 2031.55N, $P<0.05$) and 6.5% incline and 12% incline (1297.38N vs. 2031.55N, $P<0.05$). Mean resultant GH Joint contact force was also significantly affected by task, $F_{(3,18)} = 45.63$, $P < 0.05$. The Bonferroni post hoc test demonstrated significant increases between level propulsion and 6.5% incline (267.08N vs. 537.39N, $P<0.05$), level propulsion and 12% incline (267.08N vs. 887.51N, $P<0.05$), cross-slope and 6.5% incline (352.67N vs. 537.39N, $P<0.05$), cross-slope and 12% incline (352.67N vs. 887.51N, $P<0.05$) and also 6.5% incline and 12% incline (537.39N vs. 887.51N, $P<0.05$).

Peak posterior GH Joint contact force was not significantly affected by task, $F_{(1.22, 7.32)} = 4.59$, $P > 0.05$. Peak superior GH Joint contact force was significantly affected by task, $F_{(1.16, 6.99)} = 19.93$, $P < 0.05$. The Bonferroni post hoc test demonstrated significant increases in peak superior GH Joint contact force between level and 6.5% incline (196.20N vs. 486.31N, $P<0.05$), level and 12% incline (196.20N vs. 912.70N, $P<0.05$), 2.5% cross-slope and 12% incline (288.32N vs. 912.70N, $P<0.05$), and between 6.5% incline and 12% incline (486.31N vs. 912.70N, $P<0.05$). Peak medial GH Joint contact force was also significantly affected by task, $F_{(1.37,8.19)} = 13.04$, $P < 0.05$. The Bonferroni post hoc test demonstrated significant increases between level and 12% incline (430.69N vs. 1765.70N, $P<0.05$) and between 2.5% cross slope and 12% incline (625.77N vs. 1765.70N $P<0.05$).

Table 6.5: GH joint contact forces during the different manual wheelchair propulsion tasks. Data are mean (SD), statistically significant results in bold.

	Conditions					Post hoc comparisons		
	Level	2.5% cross slope	6.5% incline	12% incline	ANOVA	Level vs. 2.5% cross slope	Level vs. 6.5% incline	Level vs. 12% incline
GH Joint contact force (N)	**Peak posterior**							
	186.84 (85.10)	257.04 (64.11)	407.21 (296.91)	675.92 (493.71)	0.063	-	-	-
	Peak superior							
	196.20 (83.63)	288.32 (80.65)	486.31 (209.32)	912.70 (411.44)	**0.002**	0.188	**0.023**	**0.015**
	Peak medial							
	430.69 (117.10)	625.77 (126.77)	1160.03 (621.77)	1765.70 (874.93)	**0.005**	0.150	0.124	**0.041**
	Peak resultant							
	521.00 (54.87)	684.20 (44.32)	1297.38 (251.03)	2031.55 (322.91)	**0.002**	0.244	0.121	**0.017**
	Mean resultant							
	267.08 (70.74)	352.67 (34.48)	537.39 (111.54)	887.51 (230.69)	**0.000**	0.062	**0.002**	**0.001**
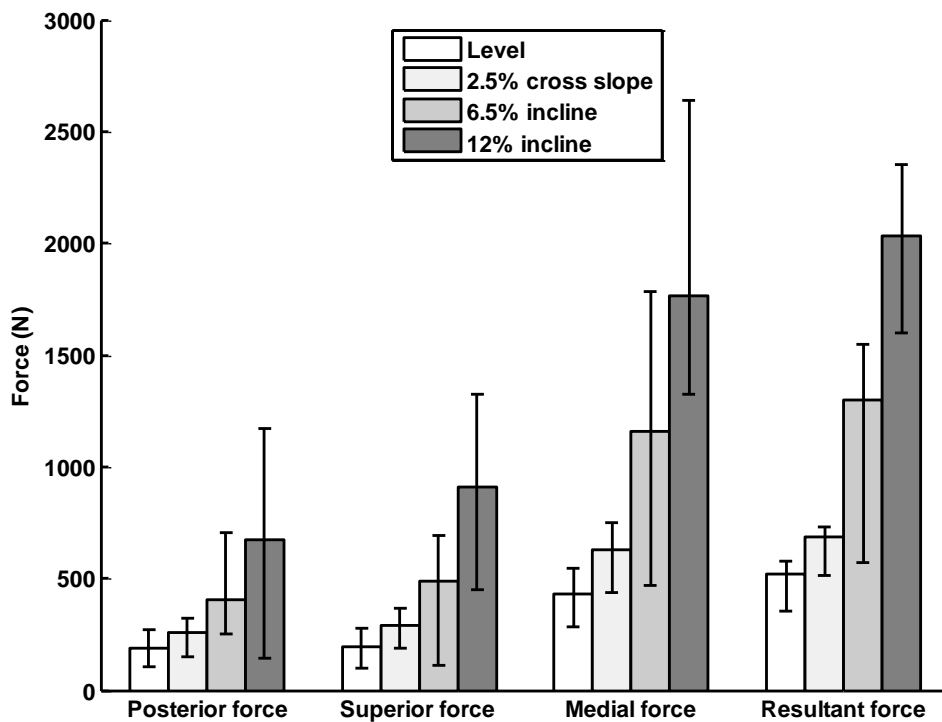
Figure 6-4: Peak GH joint contact forces during different manual wheelchair propulsion tasks.

6.4.5 Association between propulsion parameters and GH joint contact force

There was a strong significant positive correlation between peak resultant propulsion force and peak resultant GH joint contact force (r = 0.88, p<0.01) (Figure 6-5). There was also a strong significant positive correlation between mean resultant propulsion force and mean GH joint contact force (r = 0.93, p<0.01) (Figure 6-6).
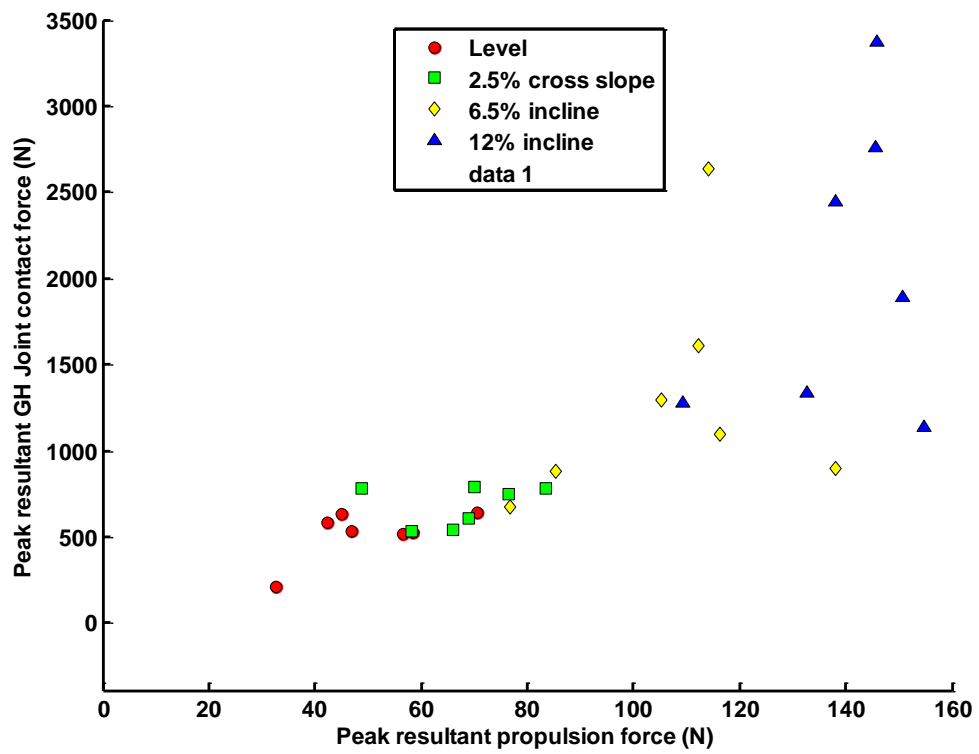
Figure 6-5: Association between peak resultant propulsion force and peak GH joint contact force during the propulsion tasks.
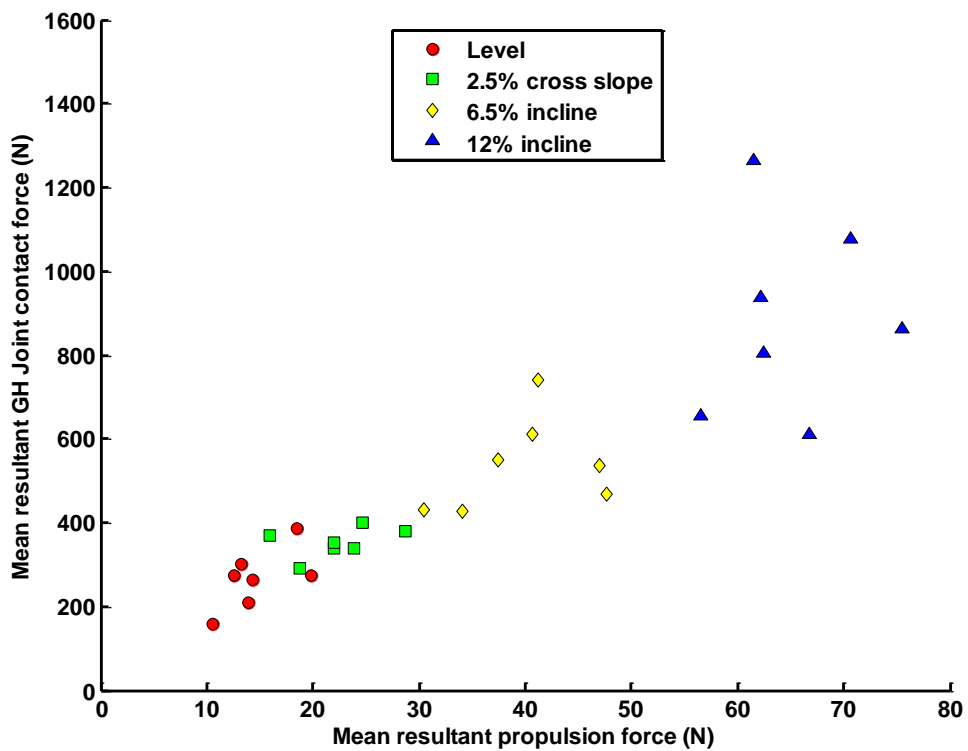
Figure 6-6: Association between mean resultant propulsion force and mean GH joint propulsion force during the propulsion tasks.

6.5 Discussion

This study investigates the potential to use a lightweight instrumented wheelchair wheel to monitor upper limb demand during over ground manual wheelchair propulsion. Participants were required to complete 4 different propulsion tasks to represent conditions that may be experienced during every day journeys. During these tasks, propulsion forces, GH joint contact forces and muscle activity levels were calculated to quantify upper limb demand. It has been suggested that propulsion force should be minimised to protect the upper limb during wheelchair propulsion. The study examined whether a correlation existed between resultant propulsion forces and resultant GH joint contact forces.

The results demonstrated an increased GH joint demand as the propulsion tasks became more challenging, in terms of propulsion forces, muscle activity levels and GH joint contact forces.

111

6.5.1 Propulsion forces

The 4 tasks were distinct from each other in terms of requirement of force application, representing a sample of the varied propulsion activities performed by manual wheelchair users on a daily basis. Propulsion forces increased as the task became more challenging and these increases in force application were associated with an increase in percentage push phase. Peak resultant propulsion force was significantly greater in the 2.5% cross slope than the level task. The peak resultant propulsion value 67.48N is in line with previous data which reported a peak resultant propulsion force of 62.8N on a treadmill set at approximately 5% cross slope (Richter et al., 2007a). Peak resultant propulsion forces were also significantly greater in the incline tasks than the level propulsion tasks, with a peak value of 106.9N (13% body weight) in the 6.5% incline and 139.63N (17% body weight) in the 12% incline. These results closely match previous results of 13% body weight in ~5% incline and 17% body weight in ~10.5% slope during a treadmill test (Richter et al., 2007b). Higher values of peak resultant propulsion force have been reported in another study of treadmill incline propulsion, with the greatest value reported 205.1N during a 12.5% incline task (Gagnon et al., 2014).

6.5.2 Trunk and upper limb kinematics

The only kinematic differences demonstrated during this study were an increase in trunk flexion and elbow joint flexion, significantly so for the 12% incline task. This strategy has previously been reported during incline propulsion (Gagnon et al., 2008), and moving the centre of gravity forward in the chair enables the user to prevent the wheelchair from tipping backwards on steeper inclines. There were no significant differences in thoraco-humeral angle as the tasks became more challenging.

6.5.3 Muscle activity

Peak muscle activity levels increased as the propulsion task became more challenging. The 2.5% cross slope and 6.5% incline tasks did not result in a

significant increase in peak muscle activity in any of the muscles tested. Muscle activity levels were significantly greater in the 12% incline task for peak AD (92.10%) and PM (58.85%). The IS muscle was also highly active relative to its maximum at 79.30%. Previous studies have demonstrated similarly high levels of muscle activity during equivalent incline treadmill propulsion, including AD (68%) and PM (101%) (Gagnon et al., 2015). The results show that manual wheelchair users experience highly demanding tasks during daily activity that are significantly more challenging than standard level propulsion. In future, studies attempting to link wheelchair biomechanics with direct measures of muscle injury such as real time US scanning should include such demanding tasks rather than just focusing on level propulsion. Aside from the risk of injury associated with tasks as demanding as climbing a bus access ramp, the impact that such designs may have on the accessibility of the environment to wheelchair users should also be considered. Not every wheelchair user is able to climb a ramp of such an incline and such accessibility barriers have been shown to reduce confidence and lead to social isolation (Velho et al., 2016). A tool such as the Sensewheel could be used in collaborative design to improve environmental accessibility.

6.5.4 GH joint contact forces

Peak and mean GH joint contact forces increased as the propulsion tasks became more challenging. Peak GH joint contact force during the 2.5% cross slope was not significantly greater than the level task. Peak GH joint force was significantly greater in the 12% incline condition when compared to the level propulsion condition.

In terms of level propulsion, the GH joint contact force results were in the range of those previously reported (Table 2.3). The GH joint contact forces reported in this study were lower than those reported in the only previous study measuring over ground propulsion (Morrow et al., 2010c). Although direct comparison is difficult as the study by Morrow et al., (2010c) does not report peak propulsion forces, peak GH joint contact force during level

propulsion was 702N, greater than the results from the level propulsion task in this study (521.00N). The peak GH joint contact force during the 8% incline was 2555N, which is greater than the values from this study of 1297.34N (6.5% incline) and 2031.55N (12% incline).

The force files generated by the OpenSim static optimisation function were reviewed to check whether the AD, PM and IS muscles were active during the push phase of each of the simulations. As reported in the EMG results section, these muscles were consistently active during the push phase of the experimental tasks. The review of the static optimisation output files demonstrated that the AD and PM muscles were active during the push phase in 100% of the simulations. The IS muscle was active during the push phase in 25 of the 28 simulations (89%). In the three simulations when IS was not active during the push phase, the IS was active during the early recovery phase. On review of the kinematic files of these 3 simulations, there was little GH joint external rotation during the push phase. These differences between the experimental and simulation data are likely due to the fact that the EMG will have recorded the role of IS as both stabiliser and prime mover, whereas the model used only considers the role of IS as an actuator of external rotation. The model could be improved by allowing translation of the GH joint, with calculation of co-contraction by the stabilising muscles during motion.

As discussed in section 2.7.5, it is not possible to quantify the impact of the model limitations on the accuracy of the absolute values presented. Although the simplified kinematics used in this model, including a simplified shoulder girdle may limit the validity of the absolute GH joint contact forces, relative change is unlikely to have been effected as there was little difference in thoraco-humeral kinematics demonstrated across the tasks. It is possible that the results from different studies analysing GH joint contact forces during manual wheelchair propulsion with a variety of models are broadly similar, as the task is kinematically constrained to the push rim during the push phase, so if the position of the participant within the chair is controlled, kinematic variability is relatively low. Using the same model properties each time, the

simplified model enabled calculation of relative change in demand between the tasks and has the potential to be used as such as an outcome measure. An example of the use of musculoskeletal modelling in this manner is presented by Sasaki et al., (2015), who used relative difference in GH joint contact force as an outcome measure to analyse differences between hand rim and lever wheelchair propulsion with respect to injury risk. It is clear that to have confidence in absolute muscle and joint contact force values for informing clinical decision making, upper limb models require improvement both in terms of improved kinematics and also representation of the biological and physiological properties of soft tissue.

6.5.5 Injury risk

In this study, shoulder muscle activity level and GH joint contact forces were measured to quantify GH joint demand and injury risk during wheelchair propulsion. Although negotiating the 2.5% cross slope required a significantly increased propulsion force, there was not a significant increase in load at the GH joint. Both incline conditions resulted in significant increases in GH joint demand, particularly during the 12% incline task. Significant increases in AD muscle activity and GH joint contact forces were observed, both of which may cause superior migration of the humeral head. IS activity was also increased, due in part to its contribution to external rotation during the push phase (Mulroy et al., 1996), but also as part of the rotator cuff muscle group, which works to stabilise the humeral head in response to these superior forces (Terry and Chopp, 2000). The high muscle activity levels in the IS muscle highlight how with repetitive loading, rotator cuff injury may occur (Bunker, 2002). Linking back to the models of rotator cuff degeneration presented in Chapter 2, this risk of injury would be greater for older wheelchair users. As introduced in section 2.4.3 of the background section, rotator cuff injury leads to a loss of the dynamic stabilising mechanism at the GH joint. Further repetitive wheelchair use is likely to exacerbate the problem, leading to the secondary effects of rotator cuff damage including degenerative joint conditions, which have also been observed in manual wheelchair users (Mercer et al., 2006).

6.5.6 Correlation between push rim force application and GH joint contact force

Across the different propulsion tasks, there was a strong positive correlation between resultant propulsion forces and resultant GH joint contact forces. This supports the suggestion that resultant propulsion forces should be minimised to preserve upper limb function (Boninger et al., 2005a). Although this study did not control for variables that may influence force such as velocity and push rate, the correlations between propulsion forces and GH joint contact forces were still strong. This indicates in simple terms, as you might expect, that the greater the force applied to the push rim, the greater load experienced at the GH joint. Although there will likely be variation in GH joint contact forces experienced, for example when applying a similar force to the push rim at a different angular velocity, reduction in the requirement for force applied to the push rim is likely to reduce load experienced at the GH joint. The results demonstrate the potential benefit of using a lightweight instrumented wheelchair wheel capable of transferring propulsion data to a mobile device, to track propulsion characteristics and upper limb demand during day to day propulsion activities. Strategies can then be implemented to minimise forces applied to the push rim, and therefore injury risk.

The correlation demonstrated between resultant propulsion force and resultant GH joint contact force is a useful finding, but it should be remembered that upper limb demand during wheelchair propulsion is a combination of force and frequency of application. This study did not account for the number of pushes required to complete each task, or average velocity during the task. It is possible participants may have used more pushes of lower peak force during the tasks. In reality, total upper limb demand during daily propulsion is a combination of number of pushes/repetitions and force application. Further research investigating the optimal balance between frequency of pushes and peak force application to maintain a required velocity, and demand placed on the upper limb throughout the course of the day would be useful.

6.5.7 Limitations

In terms of kinematic analysis, the method was used to record thoraco-humeral angle, not GH joint angle. An inertial measurement unit was not positioned on the scapular, so no analysis of the influence of scapular stability on propulsion biomechanics can be made. The main limitations of the musculoskeletal model used were that the GH joint was modelled as a ball and socket joint with a fixed scapula and the superior radio-ulnar was locked in a neutral position. These limitations were dictated by the method of kinematic analysis used to enable analysis of functional tasks, and the fact that model did not have musculature for the scapula-thoracic joint.

6.6 Conclusions

The results of the study demonstrate the importance of measuring wheelchair propulsion during functional tasks. The 12% incline task resulted in high GH joint contact forces and muscle activity levels in comparison to level propulsion, supporting a potential mechanism by which rotator cuff injury may occur with increasing age and time using a manual wheelchair. Resultant propulsion forces demonstrated a significant strong positive correlation with resultant GH joint contact forces. This suggests that the Sensewheel is potentially useful for both tracking upper limb demand during day to day propulsion activity, and also informing strategies to reduce injury risk.

Chapter 7 Identifying key experience related differences in over ground manual wheelchair propulsion biomechanics to inform real time feedback

7.1 Overview

The purpose of this study was to investigate technique differences between expert and novice manual wheelchair users during over ground wheelchair propulsion, to identify key parameters to guide real time feedback for propulsion training. 7 experts (SCI level between T5 and L1) and 6 novices (non wheelchair users) pushed a manual wheelchair over level ground (8.4m length), a 2.5% cross slope and up a 6.5% incline (7.2m length) and 12% incline (1.5m length). Push rim kinetics, trunk and shoulder kinematics and muscle activity level were measured. The results demonstrated that during the level and cross slope tasks, the experts completed the tasks with fewer pushes than the novices by applying a similar push rim moment over a greater push arc, demonstrating a trend towards lower muscle activity. During the incline tasks, the experts required fewer pushes and maintained a greater average velocity than the novices, generating greater power by applying a similar push rim moment over a greater push arc with greater angular velocity, demonstrating greater trunk flexion and a trend towards higher shoulder muscle activity.

7.2 Introduction

Chapter 6 highlighted the high demand placed on the GH joint during over ground manual wheelchair propulsion and discussed how rotator cuff injuries may occur. In view of this, it is apparent that optimising propulsion technique to minimise risk of injury is vital. As discussed in section 2.8.3, wheelchair skills training has been shown to improve propulsion biomechanics (Rice et al., 2013). An instrumented wheelchair wheel capable of providing real time feedback to the user has the potential to improve propulsion biomechanics. To guide the use of such devices, the key parameters of effective push rim biomechanics during over ground propulsion need to be understood.

Previous research has examined differences in propulsion technique between novice and expert wheelchair users. Rodgers et al., (2003) examined experts and novices propelling on a wheelchair ergometer when both fresh and fatigued. The experts applied a lower hand rim moment to maintain the required velocity, with a significantly higher push rate and lower contact time. Another study examined biomechanical differences between novices and experts during propulsion at different speeds on a dynamometer (Hwang et al., 2013). The expert users maintained a greater average velocity than the novices, generating greater power without an increase in application of torque, achieved in part by application of force over a greater push arc. A further study examined muscle activity levels of experts and novices, demonstrating higher muscle activity levels in the expert paraplegic users, who chose to propel at a higher velocity than the novices (Louis and Gorce, 2010).

These ergometer based studies demonstrate that the expert users are able to propel more effectively than novices, either by applying torque to the push rim over a greater push arc at a greater angular velocity or at a higher push rate, but that higher muscle activity levels may be required to achieve this. This study aimed to develop on this previous research to examine whether such differences in propulsion technique are evident during over ground propulsion, particularly when tasks become more challenging. In particular, it is important to examine whether expert users are able to maintain the suggested optimal technique to complete more challenging propulsion tasks at a greater velocity with fewer pushes, and what impact this has on muscle activity level. With the availability of low cost, lightweight instrumented wheelchair wheels capable of providing real time feedback, such findings have the potential to guide manual wheelchair users to modify their propulsion technique during daily activity away from the clinical environment.

7.2.1 Aims and hypothesis

The aim of this study was to compare manual wheelchair propulsion technique between experts and novices during a variety of over ground

tasks, by examining push rim kinetics, trunk and upper limb kinematics and also shoulder muscle activity level. It was hypothesised that:

- The expert users would be able to achieve each task with fewer pushes than the novices during each of the propulsion tasks.
- The expert users would be able to achieve each task at a greater average velocity than the novices during each of the propulsion tasks.
- The expert users would demonstrate a greater peak muscle activity level than the novices during each of the propulsion tasks.

7.3   Materials and Methods

7.3.1   Participants

13 participants were recruited, 7 experienced wheelchair users with a history of SCI (experts) and 6 novices without mobility impairment (Table 7.1). The study was approved by the London Stanmore Research Ethics committee and UCL Ethics committee. The SCI participants were recruited if they used a wheelchair as a primary form of mobility, had a history of SCI below T1 with no previous history of shoulder pain or major shoulder surgery. The able bodied participants were recruited if they reported no history of shoulder pain or surgery. Participants provided written informed consent in advance of study participation.

Table 7.1: Participant characteristics: Differences between the expert SCI manual wheelchair users and novices.

	SCI participants	Non SCI participants
Participants (number)	7	6
Mean age ± SD (years)	42.71 ± 13.26	34.67 ± 8.56
Mean time since injury ± SD (years)	8.85 ± 4.67	n/a
Sex (M/F)	7/0	5/1
Injury level (range)	T5 – L1	n/a
Mean weight ± SD (kg)	83.14 ±8.05	71.25 ± 12.29

7.3.2 Experimental protocol

The participants attended UCL PAMELA for a single visit. Participants transferred into the test wheelchair, the Van Os Excel G6 High Active 'Sport Edition'. The chair was adjusted to enable an elbow joint angle in the range of 100-130° when the hand was placed on the top dead centre of the push rim. The participants performed 4 pushing tasks, level surface (8.4m), 2.5% cross slope (7.2m, instrumented side on the down slope), 6.5% incline (7.2m) and 12% incline (1.5m ramp). During each of the tasks, push rim kinetics, trunk and upper limb kinematics and surface EMG were recorded.

7.3.3 Push rim kinetics

Push rim kinetics were recorded using the Sensewheel Mark 1. The Sensewheel was positioned on the left side of the wheelchair, data were sampled at 50Hz and analysed using Matlab.

The push phase of the propulsion cycle was defined by measurement of the application of a positive moment about the wheel axle. The number of pushes to complete the task was calculated from detection of the first push phase, until detection of the braking phase. Mean velocity and push rate were calculated for the same time period. Power was calculated using measurement of the moment applied to the wheel (tangential force x wheel radius) and angular velocity of the wheel, and the mean value for the whole task was calculated (Mason et al., 2012c) (Section 4.5.2).

The mean moment value was calculated from the whole task. Peak resultant force, mean angular velocity, percentage push phase and push arc were calculated as an average of each push phase from the whole task.

7.3.4 Trunk and upper limb kinematics

Trunk and left thoraco-humeral kinematics were measured using the Xsens MTw inertial measurement system. A detailed description of the inertial measurement system and kinematic measurement protocol is provided in the

methods section of chapter 6 (section 6.3.4.2). For each push of each task, maximum, minimum and change in trunk flexion and thoraco-humeral extension, abduction and internal rotation were calculated. Average values of each measurement were calculated for statistical analysis.

7.3.5 Surface EMG

Surface EMG was recorded from the AD, PM and IS muscles using the Delsys Trigno^{TM} Wireless System. A detailed description of the surface EMG system, measurement protocol used and muscle activity calculation is provided in the methods section of chapter 5 (section 5.3.6.2). The peak values for each muscle were obtained for each push phase of each propulsion cycle for each of the tasks. A mean value for peak muscle activity level for each muscle was calculated for each of the pushing tasks, using the peak value from every push of each task.

7.3.6 Statistical analysis

Statistical analysis was completed using SPSS. Homogeneity of variance was analysed in advance of the between group comparisons using Levene's test. Between groups differences in age and body weight were assessed using the independent samples t-test. A split plot ANOVA with two groups (novice and expert) and four repeated measures (level, cross slope, 6.5% incline, 12% incline) was performed for each push rim parameter and kinematic and surface EMG variable. For the repeat measures component of the analysis, when Mauchly's tests indicated that the assumption of sphericity had been violated, degrees of freedom were corrected using the Greenhouse-Geisser estimates.   Between group differences for each outcome measure during each of the tasks was assessed using the independent samples t-test. Significance level for all tests was set at P < 0.05.

7.4 Results

7.4.1 Participant demographics

The results demonstrated no statistically significant difference in age ($t(11)$ = -1.268, 42.71 years vs. 34.67 years, $P = 0.231$) or body weight ($t(11)$ = -2.096, 83.14kg vs. 71.25kg, $P = 0.060$).

7.4.2 Push rim kinetics

Table 7.2 summarises the push rim kinetics measured using the Sensewheel. Analysis of the Sensewheel data revealed a significant experience level by task interaction for a number of the push rim parameters, with the two groups adopting significantly different techniques to negotiate the more challenging incline tasks.

Table 7.2: Differences in Sensewheel parameters between the novice and expert users during each of the manual wheelchair propulsion tasks. Data are mean (SD), statistically significant results in bold.

| | Task | | | | Between group comparisons | | | | |
	Level	2.5% cross slope	6.5% incline	12% incline	ANOVA	Level	2.5% cross slope	6.5% incline	12% incline
Number of pushes									
Novice	8.67 (1.63)	7.83 (1.33)	8.83 (2.14)	5.17 (1.47)	0.111	0.098	0.516	**0.028**	0.060
Expert	7.29 (1.11)	7.14 (2.19)	6.29 (1.50)	3.57 (1.27)					
Mean velocity (m·s^{-1})									
Novice	0.87 (0.11)	0.91 (0.07)	0.61 (0.10)	0.41 (0.11)	**0.006**	0.945	0.952	**0.009**	**0.012**
Expert	0.87 (0.15)	0.91 (0.15)	0.81 (0.12)	0.59 (0.11)					
Mean power (W)									
Novice	10.76 (2.54)	19.55 (4.89)	21.98 (5.29)	17.67 (4.18)	**0.000**	0.984	0.942	**0.033**	**0.003**
Expert	10.80 (4.06)	19.35 (4.97)	30.45 (6.96)	33.27 (9.26)					
Wheel moment (N.m)									
Novice	4.39 (0.82)	6.92 (1.44)	10.87 (2.08)	14.26 (4.67)	0.328	0.867	0.828	0.773	0.357
Expert	4.30 (1.04)	6.78 (0.81)	11.19 (1.76)	16.19 (2.36)					
Mean angular velocity (°·s^{-1})									
Novice	162.91 (18.54)	176.75 (10.32)	110.46 (19.06)	77.67 (20.62)	**0.001**	0.849	0.506	**0.007**	**0.023**
Expert	165.63 (29.46)	169.48 (23.93)	150.48 (23.61)	107.37 (19.94)					
Push rate (s^{-1})									
Novice	0.92 (0.10)	1.00 (0.10)	0.98 (0.13)	0.95 (0.11)	0.075	0.292	0.277	0.872	0.165
Expert	0.82 (0.18)	0.92 (0.14)	0.97 (0.15)	1.02 (0.06)					
Percentage push phase (%)									
Novice	41.28 (5.25)	48.02 (5.73)	58.09 (3.81)	74.83 (7.73)	0.104	0.065	0.176	0.225	0.433
Expert	47.21 (5.14)	51.93 (4.00)	60.43 (2.72)	72.14 (3.89)					

		Task					Between group comparisons		
	Level	2.5% cross slope	6.5% incline	12% incline	ANOVA	Level	2.5% cross slope	6.5% incline	12% incline
			Push arc (°)						
Novice	71.04 (14.83)	80.75 (10.05)	65.15 (10.03)	59.74 (26.05)	0.309	**0.013**	0.188	**0.002**	0.137
Expert	93.83 (13.01)	91.25 (15.71)	94.32 (14.34)	78.23 (14.86)					
			Peak resultant force (N)						
Novice	69.40 (7.50)	93.70 (10.18)	107.14 (10.73)	113.02 (13.66)	**0.008**	0.306	0.198	0.087	0.061
Expert	62.88 (13.11)	84.17 (14.18)	125.81 (22.15)	139.96 (28.87)					

The expert group required fewer pushes compared to the novice group when negotiating each of the propulsion tasks. Although not significantly different, the expert users required fewer pushes to complete the level and cross slope tasks by applying a similar moment over a greater push arc, using a greater percentage of the push cycle.

The reduction in the number of pushes required by the experts was significant during the 6.5% incline task (6.29 pushes vs. 8.83 pushes, P = 0.028) and also lower during the 12% incline task (3.57 pushes vs. 5.17 pushes, P = 0.060). The results also demonstrated a significant experience level by task interaction for mean velocity (F(1.908) = 6.9, P = 0.006), with the experts maintaining a significantly greater mean velocity during the 6.5% incline task (0.81m.s^{-1} vs. 0.61m.s^{-1}, P = 0.009) and 12% incline task (0.58m.s^{-1} vs. 0.41m.s^{-1}, P = 0.012) (Figure 7-1 (A)). This result was associated with a significant experience level by task interaction for mean power (F(1.586) = 14.14, P = 0.000) with the experts generating greater mean power during the 6.5% incline (30.45W vs. 21.98W, P = 0.033) and the 12% incline task (33.27W vs. 17.67W, P = 0.003) (Figure 7-1 (B)). This increased power generation can in part be explained by the experience level by task interaction demonstrated for mean angular velocity (F(3) = 7.42, P = 0.001), with the expert group applying force to the push rim at a greater mean angular velocity during both the 6.5% incline task (150.48°.s^{-1} vs. 110.46°.s^{-1}, P = 0.007) and also during the 12% incline task (107.37°.s^{-1} vs. 77.67°.s^{-1}, P = 0.023) (Figure 7-1 (C)). The differences in propulsion technique are examined in detail for the 6.5% incline task later in the chapter.

The experience level by task interaction for the key propulsion differences is highlighted in figure 7-1. The figure highlights the change in technique adopted between the novices and experts, from the level and cross slope tasks to the incline tasks, in addition to the consistently greater push arc demonstrated by the experts (Figure 7-1 (D)).
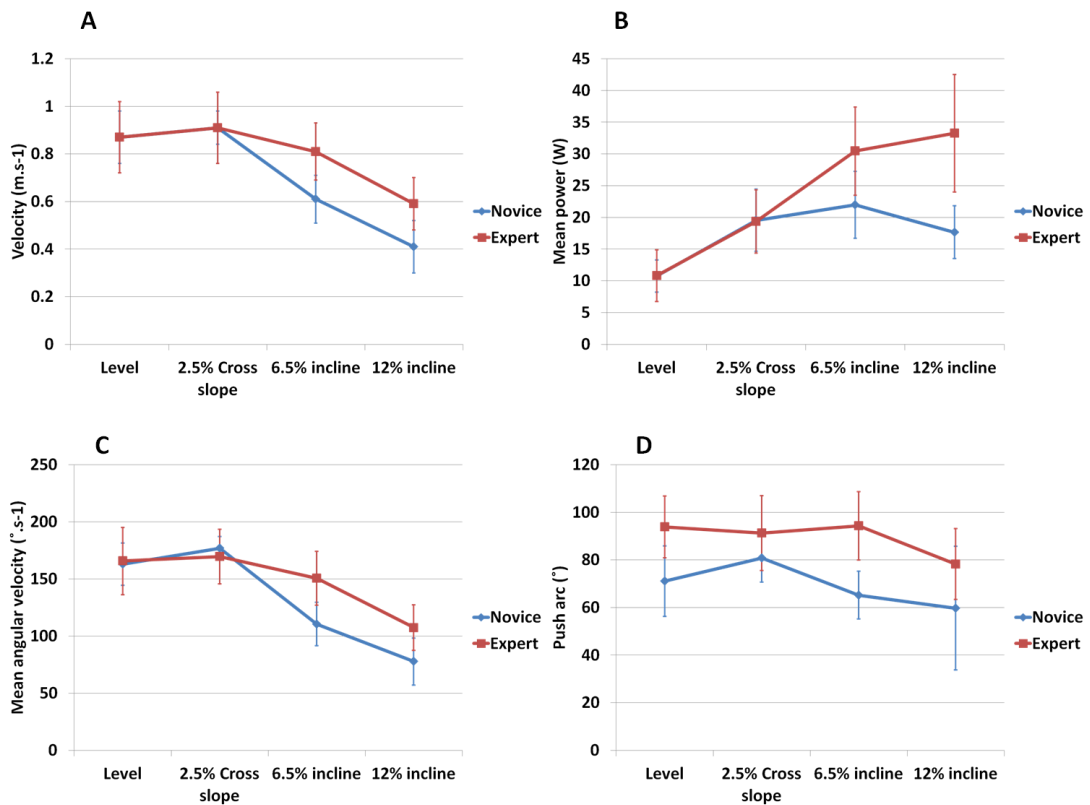
Figure 7-1: Experience level by task interaction of key push rim parameters.

7.4.3 Trunk and upper limb kinematics

Tables 7.3 and 7.4 demonstrate the kinematic results calculated using the Xsens inertial measurement system. The kinematic analysis did not demonstrate a significant experience level by task interaction for maximum, minimum or change in thoraco-humeral angle (in each of the three planes of movement).

The results demonstrated a significant experience level by task interaction for change in trunk flexion angle (F(1.292) = 11.55, P = 0.003). During both incline tasks, the expert group demonstrated a significantly greater change in trunk flexion angle compared to the novice group, 6.5% incline (19.96˚ vs. 7.85˚, P = 0.020) and 12% incline (21.26˚ vs. 8.99˚, P = 0.006).

Table 7.3: Thoraco-humeral kinematics of novices and experts during different manual wheelchair propulsion tasks. Data are mean (SD), statistically significant results in bold.

| | Task | | | | | Between group comparison | | | |
	Level	2.5% cross slope	6.5% incline	12% incline	ANOVA	Level	2.5% cross slope	6.5% incline	12% incline
	Maximum extension (˚)								
Novice	41.58 (8.20)	44.54 (10.13)	40.10 (6.99)	35.45 (8.44)	0.235	0.566	0.552	0.718	0.365
Expert	43.92 (6.09)	41.02 (10.50)	41.48 (6.45)	39.36 (6.45)					
	Minimum extension (˚)								
Novice	-2.46 (8.23)	-2.43 (6.61)	-1.91 (6.67)	-1.07 (10.09)	0.492	0.422	0.570	0.417	0.834
Expert	0.63 (4.96)	-5.17 (9.67)	-5.69 (9.06)	-2.07 (6.60)					
	Change in extension (˚)								
Novice	44.04 (8.97)	46.97 (5.46)	42.01 (6.18)	36.53 (10.23)	0.257	0.868	0.837	0.141	0.305
Expert	43.29 (6.74)	46.19 (7.55)	47.17 (5.57)	41.43 (5.97)					
	Maximum abduction (˚)								
Novice	41.12 (6.76)	43.59 (6.76)	43.44 (16.04)	39.11 (17.47)	0.635	**0.033**	**0.026**	**0.031**	0.114
Expert	29.23 (10.15)	27.81 (9.11)	25.92 (9.07)	24.67 (12.83)					
	Minimum abduction (˚)								
Novice	21.44 (4.81)	19.23 (9.54)	21.34 (10.70)	18.87 (12.03)	0.504	**0.006**	**0.040**	**0.024**	0.068
Expert	11.87 (5.19)	9.45 (5.35)	7.57 (8.25)	6.73 (9.67)					
	Change in abduction (˚)								
Novice	19.69 (5.11)	24.36 (12.58)	22.10 (16.77)	20.24 (15.31)	0.554	0.476	0.267	0.573	0.707
Expert	17.36 (6.09)	18.35 (4.90)	18.36 (3.25)	17.94 (3.99)					
	Maximum internal rotation (˚)								
Novice	16.44 (8.11)	28.75 (16.50)	16.05 (27.64)	14.13 (25.28)	0.468	0.751	0.127	0.566	0.518
Expert	14.83 (9.48)	16.02 (11.19)	9.22 (12.39)	7.01 (11.79)					
	Minimum internal rotation (˚)								
Novice	-26.01 (10.23)	-21.42 (12.38)	-28.09 (17.19)	-25.19 (11.60)	0.433	0.483	0.768	0.858	0.693
Expert	-22.31 (8.16)	-23.27 (9.74)	-29.54 (11.21)	-27.72 (10.84)					
	Change in rotation (˚)								
Novice	42.44 (8.55)	50.17 (11.04)	44.13 (13.17)	39.32 (14.91)	0.652	0.277	0.078	0.368	0.516
Expert	37.14 (8.15)	39.29 (9.19)	38.76 (8.10)	34.73 (9.62)					

Table 7.4: Difference in trunk kinematics between novice and expert users during different manual wheelchair propulsion tasks. Data are mean (SD), statistically significant results in bold.

| | Task | | | | | Between group comparisons | | | |
	Level	2.5% cross slope	6.5% incline	12% incline	ANOVA	Level	2.5% cross slope	6.5% incline	12% incline
	Minimum trunk flexion (˚)								
Novice	1.12 (6.76)	1.32 (9.38)	3.48 (12.81)	9.77 (13.58)	0.671	0.547	0.466	0.953	0.507
Expert	-0.91 (4.99)	-1.69 (4.49)	3.18 (4.18)	6.16 (3.18)					
	Maximum trunk flexion (˚)								
Novice	8.78 (4.91)	8.49 (7.32)	11.34 (14.68)	18.76 (16.21)	0.062	0.468	0.960	0.126	0.262
Expert	6.46 (6.00)	8.66 (4.09)	23.14 (11.04)	27.42 (9.97)					
	Change in trunk flexion (˚)								
Novice	7.66 (3.00)	7.17 (3.18)	7.85 (2.18)	8.99 (3.27)	**0.003**	0.874	0.197	**0.020**	**0.006**
Expert	7.37 (3.26)	10.34 (4.80)	19.96 (10.64)	21.26 (8.37)					

7.4.4 Surface EMG

For each of the trials, data from one participant for each muscle was excluded due to anomalous results. For the AD and IS muscles, data from one participant in the expert group was excluded. For the PM muscle, data from one participant in the novice group was excluded.   For these participants, normalised peak muscle activity was significantly in excess of 100% MVIC, indicating that that the MVIC test was not completed effectively or that the EMG measurement during the tasks was not accurate.

The results demonstrated a significant experience level by task interaction for the AD and PM muscles (Table 7.5). During the level and 2.5% cross slope tasks, the expert group demonstrated trends towards lower muscle activity levels than the novice group for each of the muscles tested, although there were no significant differences between the groups. During the incline tasks, the expert group demonstrated trends towards higher muscle activity levels than the novice group for each of the muscles tested, with significantly greater peak activity in the AD muscle during the 12% incline task (65.73% vs. 30.25%, P = 0.039). The experience level by task interaction in peak muscle activity level is highlighted in figure 7-2 for each of the muscles. The figure highlights the relative difference in muscle activity level change between the novices and experts, from the level and cross slope tasks to the incline tasks.
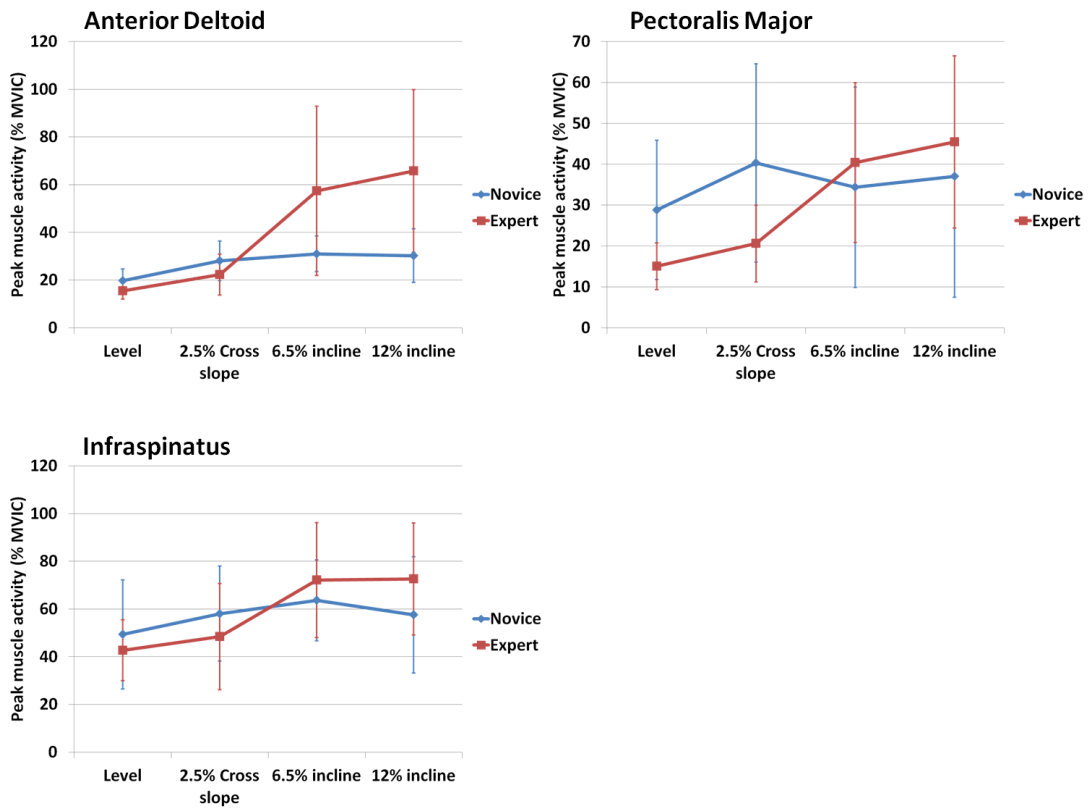
Figure 7-2: Experience level by task interaction for peak muscle activity.

Table 7.5: Difference in peak muscle activity levels between novice and expert users during the different manual wheelchair propulsion tasks. Data are mean (SD), statistically significant results in bold.

| | Task | | | | | Between group comparisons | | | |
	Level	2.5% cross slope	6.5% incline	12% incline	ANOVA	Level	2.5% cross slope	6.5% incline	12% incline
	Peak Anterior Deltoid (% MVIC)								
Novice	19.77 (4.87)	28.05 (8.29)	30.97 (7.46)	30.24 (11.23)	**0.029**	0.099	0.261	0.105	**0.039**
Expert	15.39 (3.30)	22.25 (8.59)	57.34 (35.49)	65.73 (34.17)					
	Peak Pectoralis Major (% MVIC)								
Novice	28.81 (17.04)	40.31 (24.25)	34.37 (24.54)	37.01 (29.52)	**0.012**	0.071	0.075	0.645	0.573
Expert	15.03 (5.74)	20.60 (9.37)	40.39 (19.58)	45.45 (21.06)					
	Peak Infraspinatus (% MVIC)								
Novice	49.34 (22.92)	58.02 (19.91)	63.60 (16.93)	57.57 (24.41)	0.065	0.583	0.468	0.509	0.329
Expert	42.70 (12.77)	48.40 (22.23)	72.11 (24.03)	72.57 (23.51)					

7.4.5 6.5% incline propulsion examined in more detail

The results of the between group comparison during the 6.5% incline task demonstrate that the experts used fewer pushes and were able to maintain a significantly higher mean velocity (t(11) = -3.19, 0.81m.s^{-1} vs. 0.61m.s^{-1}, P = 0.009) despite maintaining a similar push rate as the novices (Table 7.7). The experts achieved this by applying a similar mean moment at a significantly greater mean angular velocity (t(11) = -3.32, 150.48˚ vs. 110.46˚, P = 0.007) to generate a significantly greater mean power output (t(11) = -2.43, 30.45W vs. 21.98W, P = 0.033). The negative impact of this technique was that the experts demonstrated a trend towards higher peak resultant force application and greater peak muscle activity level.

The results in table 7.7 demonstrate that one of the expert group (E6) did not apply the same technique as the rest of the group. Participant E6 was the only participant in the expert group with a mean velocity and mean angular velocity lower than the greatest values demonstrated by the novice group.

Table 7.6: Comparison of propulsion technique between novices (N) and experts (E) during the 6.5% incline task, data are mean per participant, statistically significant difference in P-value row in bold.

	Mean velocity (m.s^{-1})	Push rate (s^{-1})	Mean moment Nm)	Mean angular velocity (˚.s^{-1})	Mean power (W)	Peak resultant force (N)
N1	0.70	0.91	11.66	118.31	25.70	107.37
N2	0.59	1.16	12.89	108.87	24.24	101.59
N3	0.43	0.93	11.76	76.03	17.33	105.61
N4	0.72	1.11	12.39	133.99	29.56	128.15
N5	0.63	0.96	7.88	114.04	16.84	99.93
N6	0.59	0.80	8.66	111.55	18.10	100.17
E1	0.86	0.90	12.48	163.22	36.58	135.41
E2	0.77	1.11	13.43	145.84	35.21	137.97
E3	0.94	1.13	9.96	179.24	33.80	105.99
E4	0.88	1.10	10.12	161.95	27.89	131.63
E5	0.91	0.75	10.88	159.30	31.29	120.61
E6	0.57	0.94	8.63	106.26	16.01	91.02
E7	0.76	0.83	12.81	137.51	32.41	158.06
P-Value	**0.009**	0.872	0.773	**0.007**	**0.033**	0.087

7.5 Discussion

7.5.1 Push rim kinetics

The results demonstrated a significant experience level by task interaction, with the expert users demonstrating a significantly different change in propulsion technique to the novices from the level and cross slope and incline propulsion tasks. During both incline propulsion tasks, the expert group required fewer pushes, and maintained a significantly higher velocity. They achieved this by generating greater power, by applying a similar moment over a greater push arc, at a significantly greater angular velocity, similar to findings during ergometer based testing (Hwang et al., 2013). There were no significant differences in push rate, or percentage push phase. The observed differences in mean velocity, mean power and mean angular velocity were significant despite an outlier in the results. One of the expert group travelled at a mean velocity similar to that of the novices and generated a mean power equivalent to the lower end of the distribution of the novices. This participant was at the top end of the age range of the expert group. Although only conjecture as strength testing was not completed, it is possible that this participant did not have the physical capacity to achieve the technique demonstrated by the rest of the expert group.

During the level and cross slope tasks, the expert group required fewer pushes to maintain a similar velocity to the novices, applying a similar moment to the push rim over a greater push arc at a similar push rate. Although it is important to highlight that these differences were small and not statistically significant, the pattern demonstrated by the experts closely followed the suggested guidelines in terms of push rate and push arc, while minimising push force (Sawatzky et al., 2015). The guidelines advise aiming for a push rate below 1 per second and a push arc between 85˚ and 100˚. The application of these guidelines is discussed in more detail later in the chapter.

7.5.2 Trunk and upper limb kinematics

The expert users demonstrated a significantly greater change in trunk flexion angle during both of the incline propulsion tasks in comparison to the novices. An increase in trunk flexion angle has been previously reported with progressive increases of incline (Gagnon et al., 2015, Chow et al., 2009). Increasing trunk flexion angle enabled the expert users to apply force to the push rim over a greater arc, without a significant increase in thoraco-humeral flexion angle. Increased trunk flexion has also been previously reported as a mechanism of force production for wheelchair propulsion (Rodgers et al., 2000). These results are of interest as the expert group demonstrated greater trunk flexion than the novice group, despite not having full innervation of the trunk and hip flexor muscles.

The only experience level related kinematic difference in thoraco-humeral angle was that the novice group propelled at a greater abduction angle than the expert group, although this difference was not influenced by change in task. Excessive abduction should be avoided, as the combined posture of extreme shoulder joint extension, abduction and internal rotation at the start of the push phase has been identified as a potential cause of injury (Boninger et al., 2005a).

Different propulsion styles have previously been examined (section 2.8.2) (Koontz et al., 2009) and the semi-circular style of propulsion has been advised to minimise the risk of injury (Boninger et al., 2005a). This study only measured trunk and thoraco-humeral kinematics. In the future, it would be beneficial to examine full upper limb kinematics to analyse the association between propulsion styles, push rim kinetics and muscle activity level during over ground propulsion.

7.5.3 Surface EMG

The results demonstrated a significant experience level by task interaction for peak muscle activity level of AD and PM. For each muscle, during the level and cross slope tasks, the expert group demonstrated lower muscle activity

level than the novice group, although there were not significant differences between the groups. The results differ to previous results, which reported significantly greater muscle activity in paraplegic versus able-bodied participants during level ergometer propulsion (Louis and Gorce, 2010). The results may differ, as in this study the two groups travelled at the same velocity during the level and cross slope tasks whereas in the study by Louis and Gorce, (2010) the paraplegic group travelled at a significantly greater velocity.

For each muscle during the 6.5% and 12% incline tasks, the expert group demonstrated higher muscle activity levels than the novice group, significantly so for the AD during the 12% incline task. During the incline tasks, the expert group maintained a higher average velocity by applying a similar push rim moment at a greater angular velocity over a greater push arc. Pushing at faster speed has been shown to require higher levels of muscle activity level in both propulsive and recovery muscles (Qi et al., 2012a).

As was the case in chapter 5, a small number of surface EMG results had to be excluded as values were significantly in excess of 100% MVIC. This indicates the high level of variability in surface EMG readings and reduces confidence in the results of the between group comparisons. For this reason, perhaps the most robust surface EMG finding reported within this chapter is the relative difference between the easier and more challenging tasks demonstrated by the 2 groups.

7.5.4 Application of the propulsion guidelines during level and incline propulsion

During level propulsion, the experts demonstrated a trend towards requiring fewer pushes, applying a similar moment over a greater push arc. However, these results were not conclusive and further research over a greater distance is required to determine whether following the propulsion guidelines is beneficial.

During the 6.5% incline task, the novices and experts propelled with a statistically similar push rate under 1 push per second, with the experts maintaining a significantly greater velocity. The experts applied force over a push arc of 94.32°, whereas the novices applied a push arc over a push arc of 65.15°. In terms of injury risk, the technique demonstrated by the experts resulted in significantly fewer pushes but a greater relative increase in muscle activity level. As discussed further below, further research is required to investigate the optimal balance between reducing repetition at the expense of increasing muscle activity.

7.5.5 Propulsion technique and injury risk

The expert group demonstrated a propulsion technique that enabled completion of each of the propulsion tasks with fewer repetitions than the novices. During the more demanding incline tasks, this technique was associated with significantly higher power output and higher peak muscle activity level than the novices. This highlights the difficulty of informing optimal technique during over ground wheelchair propulsion. Linking back to the section discussing the causes of rotator cuff injury (section 2.5), animal models have suggested that overuse is one of multiple factors involved in rotator cuff degeneration and injury (Soslowsky et al., 2000b), and it is theorised that overload of the tendon can lead to micro trauma (Nho et al., 2008). It is apparent that when modifying propulsion technique, the complex interaction between task repetition and muscle force requirement should be considered. In future research, it would be useful to calculate how altered propulsion technique influences joint contact forces, to further inform the optimal balance between repetition and peak force. Further investigation is also required to determine how expert wheelchair users are able to generate greater power during challenging tasks. A previous study, investigating ergometer propulsion at different speeds reported a correlation between muscle strength and force imparted at the push rim (Ambrosio et al., 2005). Further research to examine correlation between muscle strength and push rim parameters during challenging over ground propulsion could be used to inform physical training for manual wheelchair users.

7.5.6 Real time feedback for wheelchair propulsion training

Previous research has demonstrated the beneficial effect of real time feedback on wheelchair propulsion biomechanics (See chapter 3). During ergometer based studies, both real time visual feedback (Rice et al., 2013, de Groot et al., 2002, DeGroot et al., 2009, Kotajarvi et al., 2006, Richter et al., 2011), and real time haptic feedback (Blouin et al., 2015) have been used to influence wheelchair propulsion biomechanics. A light weight tool such as the Sensewheel has potential to integrate with other systems to provide real time visual, auditory or haptic feedback during daily functional propulsion tasks. Further research is required to determine whether real time feedback during over ground propulsion could be used to train novice wheelchair users to use the technique demonstrated by the experts in this study and what impact this may have on injury risk.

7.5.7 Limitations

The expert user group only included paraplegic participants with SCI below T1 and it is highly likely that tetraplegic subjects would demonstrate significantly different technique, due to reduced muscle strength in the trunk and upper limbs (Newsam et al., 1996). The results presented can therefore only be applied to manual wheelchair users with full use of the upper limbs. The study also compares 'novice' non SCI participants with 'expert' SCI participants. It would be beneficial to examine 'novice' SCI participants, and also examine the natural course of learning of improved technique. The study only measured propulsion biomechanics on the left side. It would be beneficial to measure bilaterally, considering asymmetry in propulsion technique has been previously reported (Hurd et al., 2008). Bilateral analysis would be particularly useful for further analysis of cross slope propulsion as the current findings only report the down slope wheel. The upper limb kinematic analysis did not include elbow and wrist joint motion, and thoraco-humeral rather than GH motion was measured and reported, which excludes the influence of differences in scapula motion (Raina et al., 2012).

7.6 Conclusions

The purpose of this study was to identify experience related biomechanical differences during over ground manual wheelchair propulsion. The results demonstrated that expert users employ a propulsion technique during over ground tasks requiring fewer pushes than novices. During less challenging tasks, this technique was associated with trends towards reduced peak muscle activity levels than the technique used by the novices. During more challenging incline propulsion tasks, this technique was associated with trends towards greater muscle activity levels than the technique used by the novices. Further research is required to determine whether real time feedback during over ground propulsion could be used to improve propulsion technique and what impact this may have on injury risk.

Chapter 8 The Sensewheel and verbal feedback: an adjunct to wheelchair skills training

8.1 Overview

The purpose of this study was to investigate the influence of real time verbal feedback to optimise push arc during over ground manual wheelchair propulsion. 10 healthy non wheelchair users pushed a manual wheelchair for a distance of 25 metres on level paving, initially with no feedback and then with real time verbal feedback aimed at controlling push arc within a range of 85˚-100˚. The real time feedback was provided by a physiotherapist walking behind the wheelchair, viewing real time data on a tablet personal computer received from the Sensewheel. The real time verbal feedback enabled the participants to significantly increase their push arc. This increase in push arc resulted in a non-significant reduction in push rate but a significant increase in peak force application. The intervention enabled participants to complete the task at a higher mean velocity using significantly fewer pushes. This was achieved via a significant increase in the power generated during the push phase. This study identifies that a lightweight instrumented wheelchair wheel such as the Sensewheel is a useful adjunct to wheelchair skills training. Targeting the optimisation of push arc resulted in beneficial changes in propulsion technique.

8.2 Introduction

Wheelchair skills training focuses on minimising task repetition and peak forces to preserve upper limb function (Sawatzky et al., 2015). The specific aims of training are to achieve the required velocity, aiming for a push arc of 85˚-100˚ and a push rate of under 1 push per second (Sawatzky et al., 2015). The availability of instrumented wheelchair wheels enables the provision of real time feedback to optimise manual wheelchair propulsion (Cowan et al., 2008). Previous research has investigated the influence of real time feedback on push rim kinetics (See chapter 3). In summary, real time visual feedback has demonstrated a consistent capacity to reduce push rate and

increase push arc (DeGroot et al., 2009, Rice et al., 2013, Richter et al., 2011). Less consistent results are presented for minimising push force (DeGroot et al., 2009, Richter et al., 2011) and increasing fraction of effective force (de Groot et al., 2002, Kotajarvi et al., 2006). Real time visual feedback can be used in the laboratory or clinic, but it is not practical during outdoor propulsion. During outdoor propulsion, manual wheelchair users are required to focus their visual attention on the terrain that they are negotiating.

Alternative options for providing real time feedback include auditory and haptic feedback. The influence of these types of feedback on motor learning has been reviewed (Sigrist et al., 2013). Auditory feedback has been suggested as a beneficial alternative to visual feedback as auditory feedback does not require a specific orientation or focus of attention (Sigrist et al., 2013). Real time 'concurrent' auditory feedback has been successfully applied in different ways. Real time verbal feedback has been used successfully to alter biomechanics during running (Meardon and Derrick, 2014) and an alarm system to inform optimal knee flexion angle has been used during a kicking task (Helmer et al., 2011). Such alarms or triggers are easy to interpret and useful for detection of which direction the movement should be corrected, however such feedback does not provide precise information on how much a movement needs to be corrected.

8.2.1 Aims and hypothesis

The aim of this study was to investigate whether real time auditory feedback could be used to influence biomechanics during over ground manual wheelchair propulsion. The study focussed on optimising push arc and measured the cross variable effects of any change. It was hypothesised that:

- Providing real time verbal feedback would lead to a significant increase in push arc.
- Increasing push arc would result in a significant reduction in push rate.
- Increasing push arc would result in a significant increase in peak force application.

- Increasing push arc would result in a significant reduction in the number of pushes required to complete the propulsion task.

8.3 Materials and Methods

8.3.1 Participants

The study received ethical approval from the UCL Research Ethics Committee. Healthy participants were recruited if they were aged between 18 and 65 years, were able to propel a manual wheelchair and reported no history of shoulder surgery and no shoulder pain within the previous 3 months. All participants provided written informed consent in advance of data collection.

8.3.2 Experimental protocol

Participants attended for a single visit and were asked to report their gender, age, and had their weight measured. Each participant transferred into the test wheelchair, the Van Os Excel G6 High Active 'Sport Edition'. The right rear wheel of the wheelchair was replaced with the Sensewheel.

The wheelchair propulsion tasks were completed outdoors, over a 25m stretch of straight, level paving slabs. Participants were provided with a practice period. The participants then completed an initial 'baseline' propulsion task, during which propulsion parameters were measured. The task was then repeated with the addition of real time verbal feedback to optimise push arc, whilst propulsion parameters were measured.

8.3.3 Real time feedback

During the propulsion tasks, data was streamed in real time from the Sensewheel to a tablet PC (Samsung XE7001TC-A05UK). A custom LabView GUI provided real time data on chair velocity, peak force and push arc (Figure 8-1).
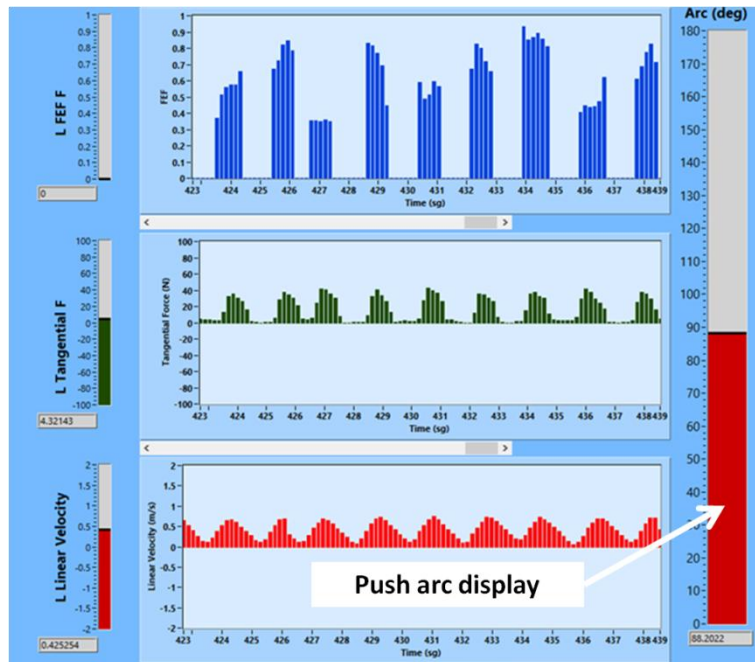
Figure 8-1: The Sensewheel GUI displaying push arc in real time

The tablet was carried by a physiotherapist. The physiotherapist provided real time feedback on push arc, with the aim of maintaining a push arc of 85˚- 100˚ (Sawatzky et al., 2015). The format of the feedback was explained to the participant before the intervention. Immediate feedback was provided during the recovery period of the push cycle. If the previous push was applied over an arc less than 85˚, the participant was instructed to 'push longer'. If the previous push was applied over an arc greater than 100˚, the participant was instructed to 'push shorter'. If the previous push was applied over an arc between 85˚ and 100˚, no instruction was provided.

8.3.4 Push rim kinetics

Push rim parameters were recorded using the Sensewheel Mark 1. Push rim parameters were calculated from each of the pushes required to complete the baseline and real time feedback tasks using Matlab. Each push from each propulsion task was analysed. The start of the task was defined when a positive moment was applied to the wheel and was measured until the braking phase. The number of pushes, push rate and mean chair velocity were calculated from the duration of the task. The individual push phases

143

were identified when a positive moment was applied to the wheel. The mean push arc and percentage push phase were calculated from each push. The mean push phase moment and angular velocity were used to calculate mean push phase power (see section 4.5.2). Peak resultant force was calculated by using measured tangential, radial and axial forces (see section 4.5.2). Mean peak force for the task was calculated from each of the pushes.

8.3.5 Statistical analysis

Using data collected during chapter 7, a sample size calculation confirmed that 4 participants were required to provide sufficient statistical power to detect relevant changes within the group for the outcome of interest, push arc. This data was based on the assumption of a standard deviation of 1.82, a two-sided paired t-test will have 95% power to detect a within group difference from baseline of 22.78˚ using an alpha = 0.05 significance level. Additional participants were recruited to account for the potential of increased variability in novice wheelchair users. Statistical analysis was completed using IBM SPSS Statistics version 22. The Kolmogorov-Smirnov and Shapiro-Wilk tests were used to analyse whether the differences between baseline and intervention results were normally distributed. When data were normally distributed, the influence of the intervention was assessed using the dependent samples t-test. When data were not normally distributed, the Wilcoxon signed rank test was used. The significance level was set at P<0.05.

8.4 Results

Ten non wheelchair users (2 women, 8 men) participated in the study. Each participant reported no previous experience using a manual wheelchair. On average, the participants were 30.1 ± 7.3 years of age and weighed 68.3 ± 7.6 kg.

The push rim parameters measured during the baseline test and with the addition of real time feedback are presented in Table 8.1. The intervention of real time verbal feedback resulted in a 35.27% increase in push arc that was

statistically significant (z = -0.280, 59.85° vs. 80.96°, P = 0.005) (Figure 8-2). This increase resulted in a non significant reduction in push rate (t(9) = 1.91, 0.84sec^{-1} vs. 0.75sec^{-1}, P = 0.088) (Figure 8-3) and a significant increase in peak force of 28.74% (t(9) = -4.65, 43.00N vs. 55.36N, P = 0.003) (Figure 8-4).

The intervention resulted in participants completing the task at a significantly greater mean velocity (t(9) = -5.31, 0.76m·s^{-1} vs. 0.95m·s^{-1}, P = 0.000) (Figure 8-5) with significantly fewer pushes (t(9) = 7.79, 26.40 vs. 18.10, P = 0.000). This was enabled by a significant increase in generation of power during the push phase (t(9) = -4.19, 15.13W vs. 22.26W, P = 0.002), via a significant increase in mean push phase moment (t(9) = -3.31, 6.13N·m vs. 7.37N·m, P = 0.009) and a significant increase in mean push phase angular velocity (t(9) = -4.75, 143.19°·s^{-1} vs. 174.65°·s^{-1}, P = 0.001) with a similar percentage push phase (t(9) = 0.92, 37.87% vs. 35.96%, P = 0.382).

Table 8.1: Push rim parameters measured at baseline and with the addition of real time feedback, data are mean (SD), statistically significant results in bold.

	Baseline	Feedback	P-value
Push rate (s^{-1})	0.84 (0.19)	0.75 (0.19)	0.088
Push arc (˚)	59.85 (11.35)	80.96 (7.44)	**0.005**
Percentage push phase (%)	37.87 (6.83)	35.96 (4.48)	0.382
Mean velocity (m·s^{-1})	0.76 (0.14)	0.95 (0.17)	**0.000**
Number of pushes	26.40 (4.80)	18.10 (3.31)	**0.000**
Mean moment (N·m)	6.13 (1.90)	7.37 (2.71)	**0.009**
Mean angular velocity (˚·s^{-1})	143.19 (27.37)	174.65 (30.25)	**0.001**
Mean power (W)	15.13 (4.87)	22.26 (8.27)	**0.002**
Peak force (N)	43.00 (11.70)	55.36 (17.07)	**0.001**
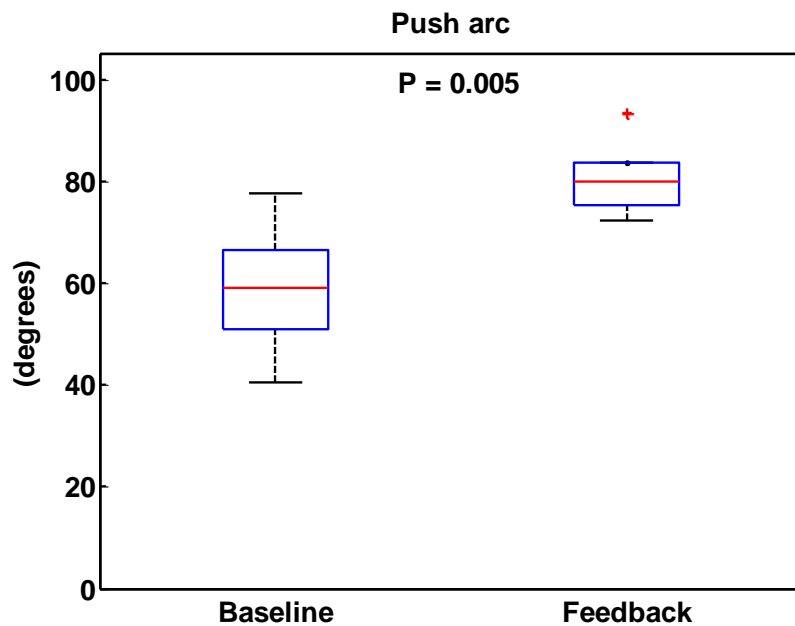
Figure 8-2: Change in push arc with the addition of real time feedback.
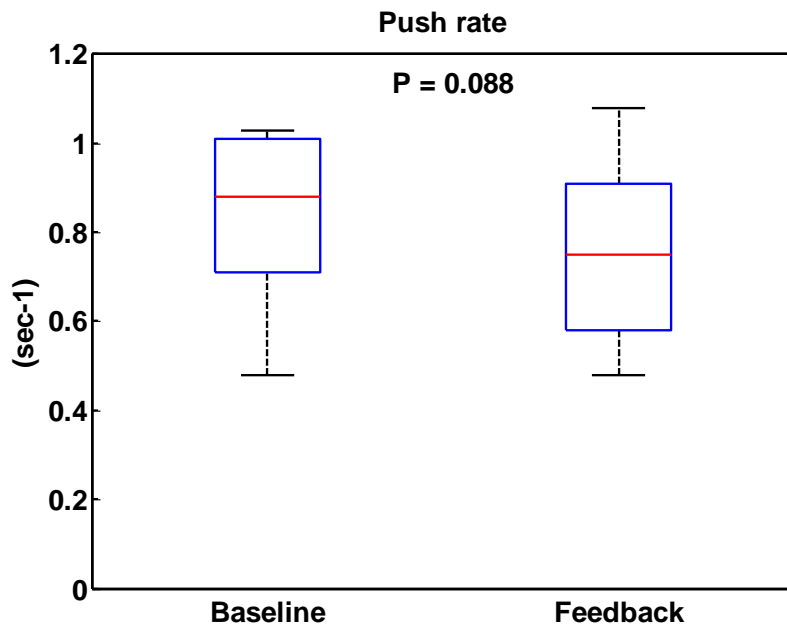
Figure 8-3: Change in push rate with the addition of real time feedback.
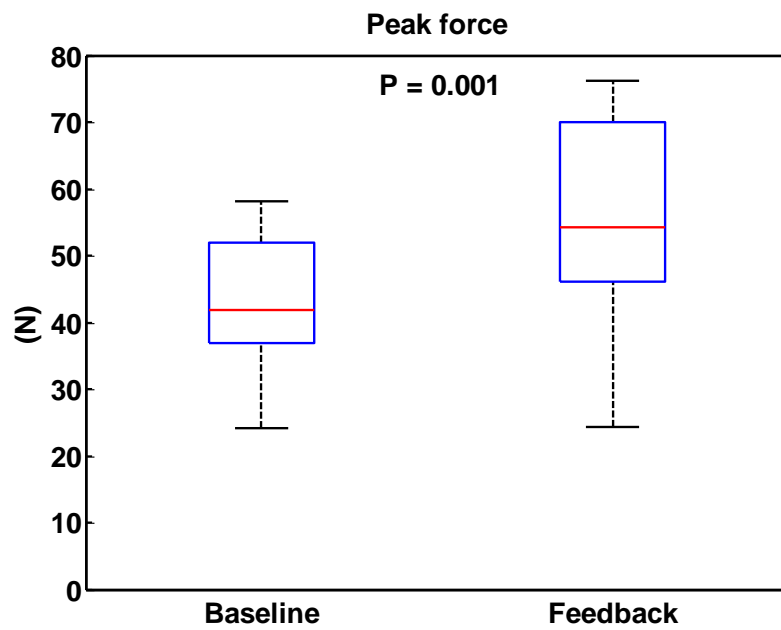
Figure 8-4: Change in peak force with the addition of real time feedback.
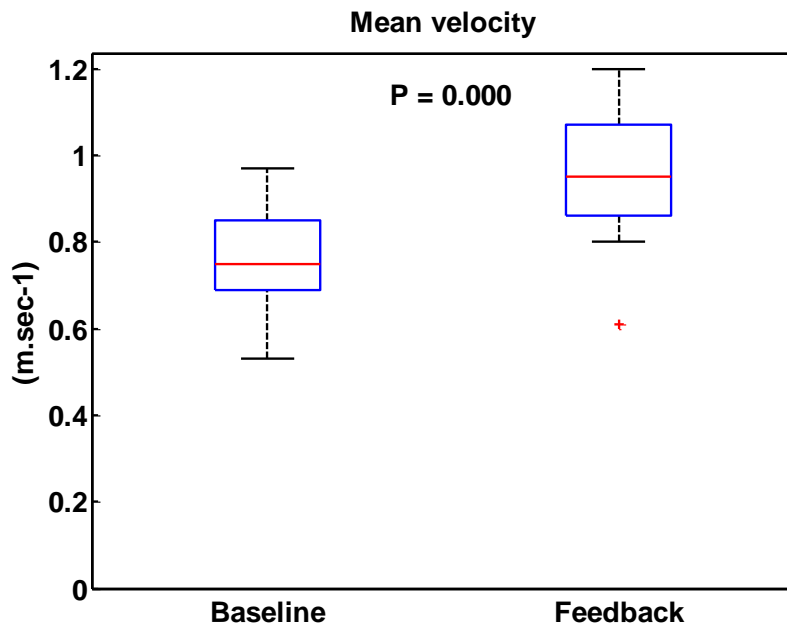
Figure 8-5: Change in mean velocity with the addition of real time feedback.

8.5 Discussion

8.5.1 The result of real time verbal feedback during over ground manual wheelchair propulsion

As hypothesised, the results demonstrated that real time verbal feedback was successful in increasing push arc during over ground manual wheelchair propulsion. Providing real time verbal instruction during the recovery phase of the propulsion cycle resulted in a statistically significant increase in push arc of 35.27%. This result supports previous research suggesting that push arc can be successfully modified with real time feedback. Previous studies have reported similar results using real time visual feedback during ergometer propulsion. Degroot et al., (2009) reported a 28.51% increase in push arc, Rice et al., (2013) a 10.01% increase and Richter et al., (2011) up to a 31% increase.

The aim of the intervention was to achieve a push arc of 85°-100°, suggested as optimal by the propulsion training guidelines (Sawatzky et al., 2015). On average during the real time feedback task, the participants achieved a push

arc of 80.96°. Further training may have enabled the participants to achieve the suggested push arc, but in reality during over ground propulsion, it may be difficult to achieve an average push arc in this range. This is due to the fact that some propulsion strokes are shortened to control the direction of travel of the chair and to manoeuvre the chair.

A previous study has demonstrated significant cross variable effects when maximising push arc using visual feedback (Richter et al., 2011). Richter et al., (2011) reported a 31% increase in push arc, which resulted in a significant 30% reduction in push rate and a significant 34% increase in peak force. The current study intervention, leading to a significant 35.27% increase in push arc resulted in a non significant 10.71% decrease in push rate and a significant 28.74% increase in peak force. In addition, increasing push arc resulted in a significant 31.44% reduction in the number of pushes required to complete the task. A further study by Rice et al., (2013) also reported a significant increase in peak force in the short term when wheelchair users were provided with real time visual feedback to increase push arc. However, when the participants were reviewed three months post intervention, increases in push arc had been maintained and peak force values had reduced to baseline levels. This suggests that with practice, it is possible to push with a greater push arc without an increase in peak force.

8.5.2 The influence of technique changes on injury risk

Increased force application has been linked to an increase in shoulder joint loading (Holloway et al., 2015) and reduced push rate has been associated with a reduction in total muscle power requirement (Rankin et al., 2012). The published clinical guidelines suggest reducing frequency of the task and minimising peak forces to minimise risk of injury (Boninger et al., 2005a, Sawatzky et al., 2015). In this study, the intervention to optimise (increase) push arc resulted in a significant reduction in the number of pushes required with a push rate within the suggested maximum, but a significant increase in push force (55.36N). In a previous study using a musculoskeletal model to estimate shoulder joint contact force, a peak propulsion force of 59.30N

resulted in a GH joint contact force of approximately 1050N (1.25 x body weight) (Veeger et al., 2002). Shoulder joint contact forces have been directly measured by a study assessing functional activities of participants with an instrumented shoulder joint prosthesis (Westerhoff et al., 2009). One of these activities was turning a steering wheel single handed and resulted in a shoulder joint contact force of 1.22 x body weight. This suggests that although increasing push arc did result in a significant increase in peak force, the resultant shoulder load would still be within the limits of standard daily activity.

8.5.3 The influence of technique changes on functional capacity

Increasing the push arc also resulted in a significant increase in mean chair velocity during the task to 0.95m$\cdot$s^{-1}. This has important functional implications for the wheelchair user, as previous research has suggested that an average moving speed of 1.2m$\cdot$s^{-1} is required to safely negotiate a pedestrian crossing (Hoxie and Rubenstein, 1994). The intervention resulted in a greater mean chair velocity with fewer pushes required; due to an increase in push phase power via an increased mean push phase moment and angular velocity. Such technique changes show a similar pattern to the propulsion technique demonstrated by expert wheelchair users in comparison to novices in the previous study of Hwang et al., (2013) and also in the results section of Chapter 7 in this thesis.

8.5.4 The balance between repetition and peak force

Figure 8-6 shows the change in peak resultant force values for each participant from baseline and with the addition of real time feedback. Peak resultant force increased for each participant, but the relative change varied considerably across the group, ranging from 0.6% (participant number 10) to 72.6% (participant number 3). It is interesting to note that the 5 participants with the greatest percentage increases in peak force (participant 1 = 39.97%, participant 3 = 72.60%, participant 4 = 33.22%, participant 6 = 34.62%, participant 9 = 25.10%) also recorded a greater percentage reduction of number of pushes completed compared to the other 5 participants

(participant 1 = 37.04%, participant 3 = 37.04%, participant 4 = 44.83%, participant 6 = 34.29%, participant 9 = 37.93%), see figure 8-7).
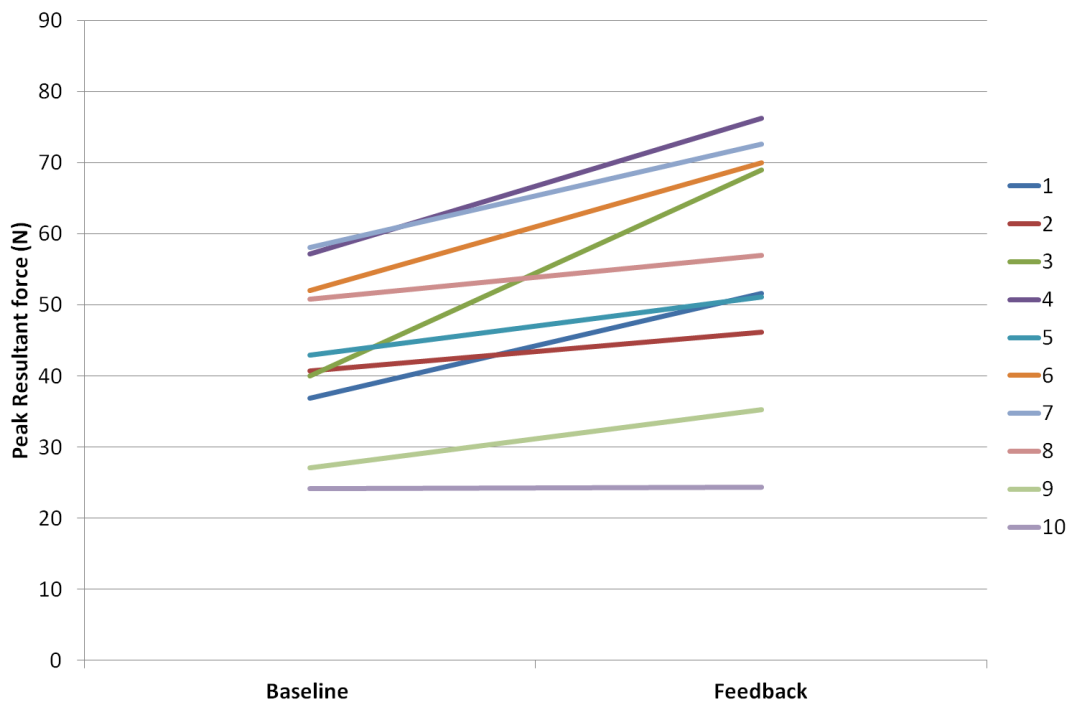
Figure 8-6: Change in peak resultant force between baseline and real time feedback conditions for each participant.
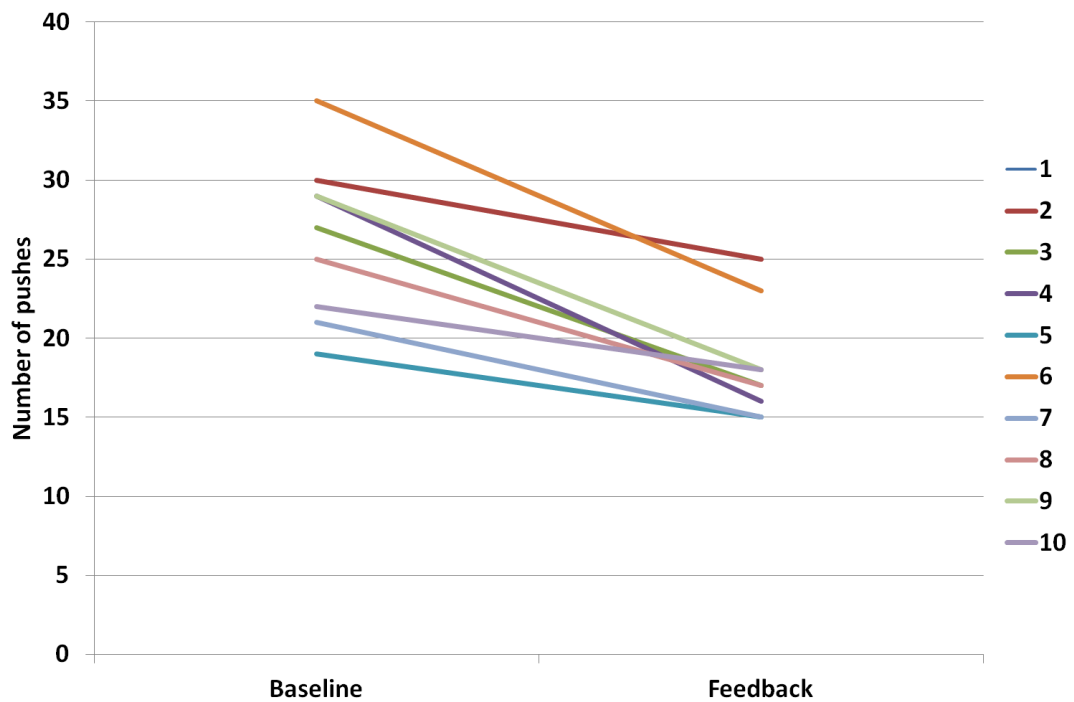
Figure 8-7: Change in number of pushes between baseline and real time feedback conditions for each participant. The data for participant 1 is not visible as the number of pushes completed was the same for participants 1 and 3.

These results highlight the difficulty of measuring the benefit of an intervention when propulsion biomechanics are used as an outcome measure, due to the interaction between peak force and task repetition. Due to the lack of evidence supporting a direct link between push rim force and soft tissue damage (as discussed in section 2.6 of the background chapter), there exists no peak push rim force value that can be used as a threshold, over which pushing is likely to cause shoulder injury. In addition, if it were possible to prove such a link, it is likely that this threshold value would differ between individuals due to the multitude of biological and physiological differences present.

An alternative for quantifying the benefit of an intervention would be to estimate 'cumulative stresses' during a task. Such a principle has been used to predict the risk of developing OA in a group of patients with developmental dysplasia of the hip (Mavcic et al., 2008). To estimate cumulative contact stress, the authors calculated peak stress values at the hip and multiplied this

152

value by age at follow up. A similar idea could be considered in the analysis of wheelchair propulsion. The results in chapter 6 demonstrated a strong positive correlation between peak force at the push rim and peak GH joint contact force, both within the results of this thesis and across other studies. Therefore, peak propulsion force could be used as a measure of GH joint contact force, and this value could be multiplied by the number of pushes to provide an estimate of cumulative stress. Table 8.2 presents such a calculation from the data collected during this study, with 'cumulative stress' calculated by multiplication of the mean peak push force value and number of pushes recorded during the baseline and feedback tasks.

Table 8.2: Change in cumulative stress as a result of real time verbal feedback during manual wheelchair propulsion.

Participant	Baseline	Feedback	% change
1	996.30	878.05	-11.87
2	1221.60	1153.75	-5.55
3	1080.00	1173.68	8.67
4	1659.67	1219.84	-26.50
5	815.1	767.25	-5.87
6	1819.65	1609.77	-11.53
7	1220.31	1090.35	-10.65
8	1271.25	969.34	-23.75
9	786.04	635.54	-19.15
10	532.18	437.94	-17.71

The results presented in table 8.2 were statistically analysed. The differences between baseline and feedback values were found to be normally distributed and the paired samples t-test indicated a significant reduction in cumulative stress during the task with real time verbal feedback ($t(9) = 3.18$, Baseline = 1140.21 (392.55) vs. Feedback = 993.55 (333.40), P = 0.011). Cumulative stress was reduced with the addition of real time feedback in 9 of the participants. Participant 3 demonstrated an 8.67% increase. With reference to figure 8-6, participant 3 demonstrated the greatest increase in peak force of 72.6%, with the metric of 'cumulative stress' used suggesting that the reduction in number of pushes required was not worth such an increase in peak force. If such a metric is to be used to analyse daily propulsion activity, it could only be usefully applied as long as any

intervention did not hinder the ability of the wheelchair user to maintain the required velocity, as discussed in section 8.5.3.

To highlight the interaction between peak force and number of pushes further, 3 dimensional stem plots were created. Figure 8-8 shows that increasing push arc reduced the number of pushes required, but increased peak force. However, when using 'cumulative stress' as the measure of outcome, increasing push arc can be considered as beneficial in reducing overall demand.
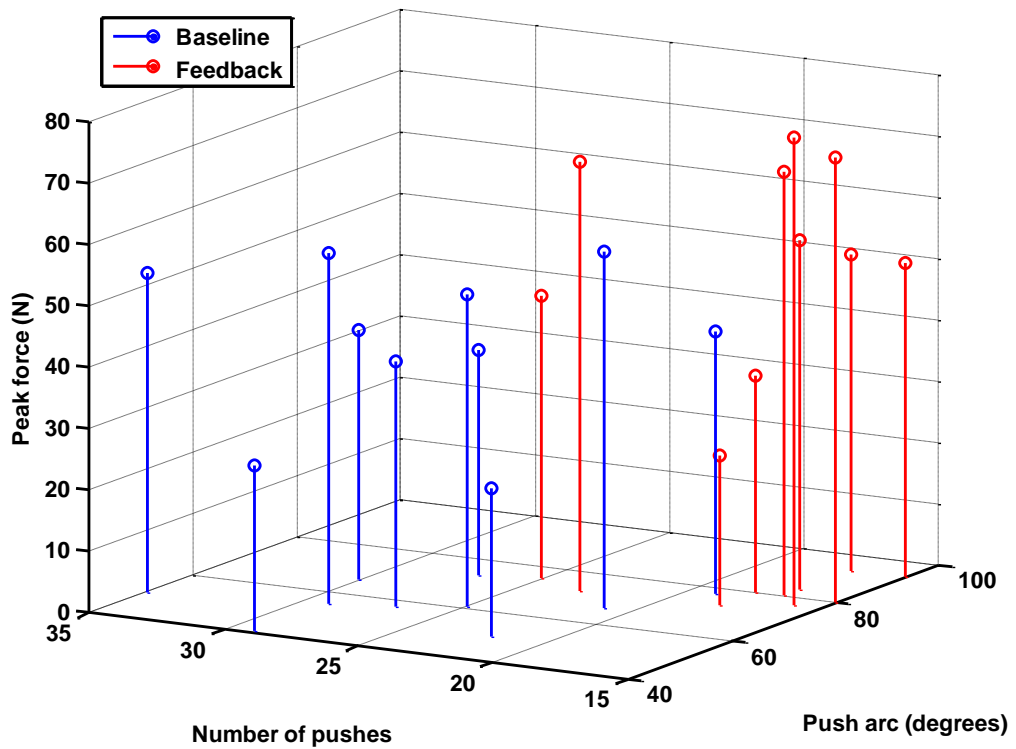
Figure 8-8: Change in push arc, number of pushes and peak force with real time feedback.
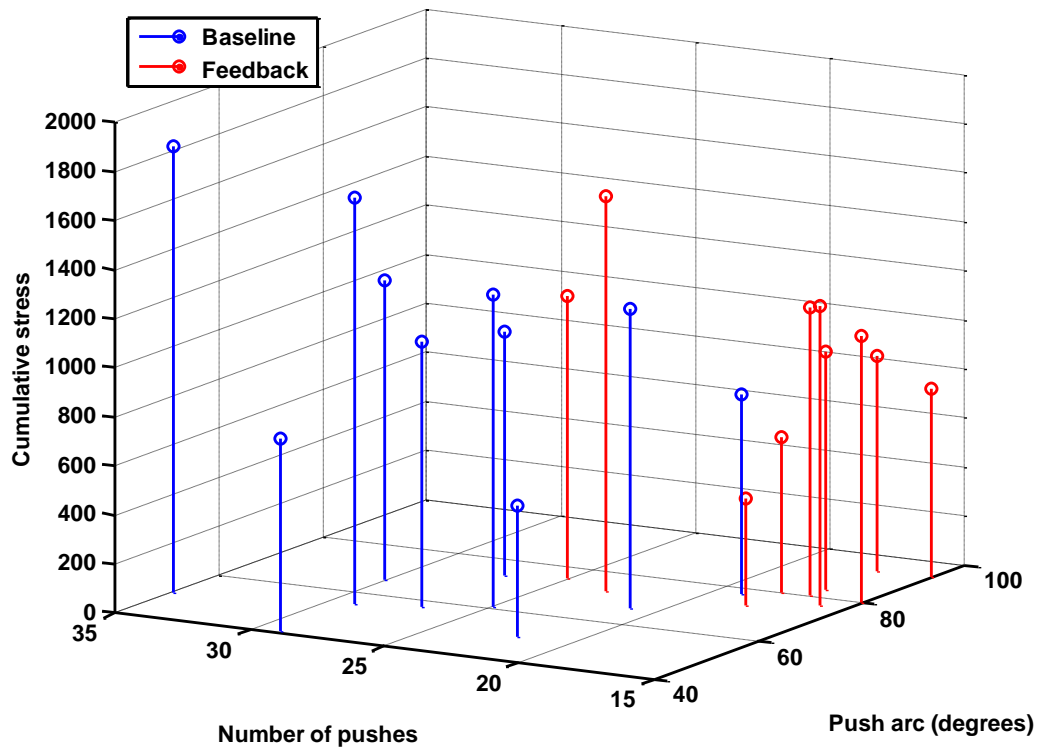
Figure 8-9: Change in push arc, number of pushes and cumulative stress with the addition of real time feedback.

The results of the study suggest that the Sensewheel could be a useful adjunct to the initial phase of wheelchair skills training. The graphical representation of the data to the therapist enables the provision of real time feedback to the patient. The results demonstrate that in a short time period, successful changes in technique can be facilitated. In addition, the outcome of the intervention can be recorded retrospectively to chart progress. The next generation of the Sensewheel is currently under development, to enable transfer of data via Bluetooth to the wheelchair user's smart phone. This development will include the automation of real time feedback to the user, to enable wheelchair propulsion training to continue away from the clinical setting.

8.5.5 Limitations

This study includes only novice non wheelchair users. Further research is needed to determine whether such an intervention could be successful with

different populations of wheelchair users, considering the technique differences that exist (Newsam et al., 1996). In addition, further research should examine the intervention during propulsion over a variety of terrains and journeys. The majority of journeys completed by wheelchair users are completed over short distances, involving starting, stopping and manoeuvring (Sonenblum et al., 2012), so the optimal technique for such tasks should be considered. Negotiating inclines is significantly more demanding than level propulsion (Hurd et al., 2009). Considering that novice wheelchair users may not have the required upper limb strength to achieve the optimal push arc against an increase in propulsion resistance, a graded training program may have to be implemented. This study only investigated the use of single variable auditory feedback for optimising push arc. Haptic feedback has been identified as another form of real time feedback, and has been used to alter biomechanics during walking (Wheeler et al., 2011). It would also be useful to investigate how sonification of movement could be used to guide actual movement towards a reference movement (Sigrist et al., 2013) to combine feedback for more than one variable, for example push rate and push arc during wheelchair propulsion.

8.6 Conclusions

The purpose of this study was to identify whether providing real time verbal feedback to optimise push arc, using data presented in real time by the Sensewheel, could result in improved wheelchair propulsion technique. The results demonstrated that providing simple real time verbal feedback resulted in a consistent and significant increase in push arc during level over ground wheelchair propulsion. Relating to the risk of injury, the intervention demonstrated the beneficial effect of reducing push rate and the number of pushes required to complete the task, however peak force increased. On balance, it seems that reducing the task repetition is worth the increase in peak force, which would not load the shoulder in excess of common activities of daily living. In addition, the intervention resulted in increased mean velocity, achieved by increased generation of power during the push phase. The results suggest that a lightweight instrumented wheelchair wheel such as

the Sensewheel could become a useful adjunct to wheelchair skills training, but should be trialled further during more demanding over ground propulsion tasks.

Chapter 9 General Discussion and Conclusions

9.1 Overview

The aims of this thesis were to introduce a novel lightweight instrumented wheelchair, 'the Sensewheel', and to use this to investigate the potential causes of injury during manual wheelchair propulsion, to examine how people can push more effectively during over ground manual wheelchair propulsion and to investigate the implementation of real time feedback during over ground manual wheelchair propulsion. As introduced in section 1.5, the following objectives were developed:

1) To introduce the design and measurement capability of the Sensewheel, by using it to complete a number of experimental 'proof of concept' studies.
2) To investigate age related differences in propulsion technique and muscle activity levels and relate these factors to risk of shoulder injury.
3) To measure shoulder joint demand during over ground manual wheelchair propulsion and investigate the relationship between forces applied to the wheelchair push rim and shoulder joint demand.
4) To examine key experience related differences in manual wheelchair propulsion biomechanics to inform optimal technique.
5) To investigate the application of real time verbal feedback to optimise propulsion technique during over ground manual wheelchair propulsion.

This chapter will review the outcomes of the experimental chapters, which addressed the objectives listed above, to highlight the advances made in this area. The use of the Sensewheel during the thesis will be summarised. Objectives 2 and 3 will be addressed under the heading 'risk of injury' and objectives 4 and 5 will be addressed under the heading 'optimising over ground manual wheelchair propulsion technique'. Finally, the limitations of the study methods will be summarised and potential areas for ongoing research introduced, before the thesis is concluded.

9.2 The Sensewheel

The extensive analysis of wheelchair propulsion biomechanics has seen the adoption of instrumented wheelchair wheels in the research setting. Both the SmartWheel (Cowan et al., 2008) and OptiPush (Richter et al., 2011) wheels have been widely used within research. The use of such wheels has mainly been limited to the research setting, due to the weight of the wheels. Increasing weight of the wheelchair increases the demand placed on the user and alters propulsion biomechanics, so a valid interpretation of daily propulsion activity cannot be made. The Sensewheel adds no additional weight to the adapted wheel, thereby enabling analysis of 'real life' wheelchair propulsion without additional demand to the user. Throughout the experimental chapters in this thesis, the Sensewheel has been used to measure the four key parameters of wheelchair propulsion identified by Cowan et al., (2008), which include velocity, average peak resultant force, push frequency and push arc. The Sensewheel has also been used to measure the demand of over ground propulsion activities, provide external force data to a musculoskeletal model and also identify propulsion technique differences. In addition, the Sensewheel has been used to provide real time feedback to modify propulsion technique.

The current limitations of and future development plans for the Sensewheel are introduced in chapter 4. The ongoing developments for the Sensewheel Mark 2 include updating the method of data transmission to Bluetooth, strengthening the load cell and updating the GUI. The results of the experimental chapters within this thesis demonstrate how, with these technical improvements, the Sensewheel could be used in a clinical setting.

9.3 Risk of injury

In the background chapter, it was identified that there is a high incidence of shoulder injury due to sustained manual wheelchair use (Fullerton et al., 2003), and such injury can lead to a lack of functional independence and reduced quality of life (Gutierrez et al., 2007). More specifically, there exists a significantly greater rate of rotator cuff injury in manual wheelchair users

than age matched controls (Akbar et al., 2010). Rotator cuff injury is associated with increasing age (Tempelhof et al., 1999) and also repetitive loading (Nho et al., 2008), which links with the finding that such injuries are associated with increasing age and time as a wheelchair user (Akbar et al., 2011). Accordingly, the objectives were designed to investigate how increasing age may increase risk of injury and also to quantify shoulder demand during daily propulsion. To investigate these objectives, the appropriate methods to quantify upper limb demand and 'injury risk' were considered.

9.3.1 Rationale for choice of measures of upper limb demand

There is limited evidence demonstrating an association between peak forces applied to the push rim and shoulder injury measured using MRI (Mercer et al., 2006). It is therefore an assumption that the increased rate of rotator cuff injury is due to repetitive high level of muscle activity and joint loading. The basis for this assumption is general evidence demonstrating that repeated tendon loading leads to damage that if not given sufficient time to heal results in degenerative change (Nho et al., 2008, Soslowsky et al., 2000a). Increased shoulder joint loading requires greater rotator cuff muscle activity to stabilise the humeral head in the glenoid (Terry and Chopp, 2000, Bunker, 2002). Unless manual wheelchair users have an implanted instrumented shoulder prosthesis, researchers rely on the estimation of joint contact forces using musculoskeletal models, as used for the study described in chapter 6. Muscle activity level can be measured using EMG. It is not feasible to use fine wire EMG during over ground manual wheelchair propulsion, therefore surface EMG was used to measure muscle activity during the studies reported in chapters 5, 6 and 7. Muscle activity level is not directly associated with muscle force during anisometric contraction, such as need to be measured during manual wheelchair propulsion. During this thesis, muscle activity levels were normalised to activity levels collected during MVIC to enable comparison between participants (Burden, 2010). The IS muscle is active during the push phase of manual wheelchair propulsion, so can be validly measured using surface EMG (Johnson et al., 2011). During

this thesis, muscle activity level of the IS muscle is used as a measure of rotator cuff demand.

9.3.2 The impact of ageing on injury risk

As discussed, the frequency of rotator cuff injuries increase naturally with age (Ozaki et al., 1988) and specific to wheelchair users increasing age is directly associated with an increase in rate of rotator cuff injury (Akbar et al., 2011). Older wheelchair users have demonstrated different pushing styles to younger users (Mercer et al., 2006, Hers et al., 2015), but there has been little investigation into the shoulder demand experienced by older people. Chapter 5 investigated the propulsion biomechanics of younger and older healthy participants during ergometer propulsion, using muscle activity as a measure of shoulder joint demand. The younger and older groups adopted a similar technique in terms of the key propulsion parameters. The older group demonstrated greater muscle activity in each of the muscles than the younger group, but these differences were not statistically significant. The results were not conclusive in supporting the theory that due to age related weakness, relative muscle activity would be greater and the risk of injury increased. As the results were not conclusive, further research would be useful to determine age related differences during more demanding tasks, including analysis of links between muscle strength and measures of injury risk to inform muscle strengthening programmes for older wheelchair users.

9.3.3 The impact of repeated joint loading during over ground manual wheelchair propulsion on injury risk

In addition to increasing age, rotator cuff injury is caused by repeated joint loading. Previous research examining incline propulsion has revealed that wheelchair users experience high levels of muscle activity (Gagnon et al., 2015) and GH joint contact forces (Morrow et al., 2010c). There existed little if any evidence investigating shoulder joint demand during daily functional activities such as negotiating a cross slope, or climbing a bus access ramp. Chapter 6 reports the use of the Sensewheel and wireless body worn surface EMG sensors and MIMU's to quantify shoulder joint demand during these

functional tasks, and assesses whether push rim kinetics can be used to predict this demand. The results demonstrated significantly greater shoulder joint demand during the incline propulsion tasks. During the 12% incline, shoulder joint contact forces were 2031.55N and peak muscle activity levels as high as 92% maximum. These findings suggest studies examining tendon U/S changes following manual wheelchair propulsion to identify a direct link with tendon injury may need to include more demanding tasks to quantify injury risk, rather than focusing on sustained periods of level propulsion (Collinger et al., 2010).

9.3.4 Using the Sensewheel to track upper limb demand

The results presented in Chapter 6 also demonstrated a strong positive correlation between resultant propulsion forces and resultant joint contact forces, indicating that the Sensewheel could be a useful tool for tracking demand and minimising risk of injury. An example of such an application could be during the early stages of rehabilitation, when wheelchair users have their wheelchair adjusted. Clinicians could use data from repeated propulsion tasks to determine whether their intervention has had a beneficial effect on reducing upper limb demand. The Sensewheel could be used similarly to assess the benefit of wheelchair skills training.

9.3.5 Injury risk: a summary

The results of chapter 6 demonstrated the high demand at the shoulder joint experienced by manual wheelchair users during over ground propulsion that may cause injury. This risk of injury may increase with age, as muscle strength deteriorates and tasks become relatively harder. In summary, the results demonstrated that the greater the force application required at the wheelchair push rim across the different tasks, the greater the shoulder joint demand (contact force and muscle activity level). It is therefore evident that to minimise injury risk, wheelchair users need to minimise peak force application and the number of pushes required (Boninger et al., 2005a, Sawatzky et al., 2015). This leads on to objectives 4 and 5, to analyse how

wheelchair propulsion technique can alter efficiency during over ground manual wheelchair propulsion and how technique can be improved.

9.4 Optimising over ground manual wheelchair propulsion technique

9.4.1 Analysing effective over ground propulsion technique

Section 2.8 of the background chapter introduces the strategies identified for optimising manual wheelchair propulsion, including wheelchair skills training (Rice et al., 2014). Previous research has identified technique differences between novice and expert manual wheelchair users during ergometer propulsion (Rodgers et al., 2003, Hwang et al., 2013, Louis and Gorce, 2010). The aim of chapter 7 was to assess whether expert users were able to apply these different techniques during over ground wheelchair propulsion. The results demonstrated that the expert users were able to complete propulsion tasks with fewer pushes. During the level and cross slope propulsion tasks, the expert users applied a similar force over a greater push arc with a trend towards reduced muscle activity level. During the incline tasks, the experts generated greater power by applying a similar moment over a greater push arc at greater angular velocity with a trend towards increased muscle activity. The study supported the finding that aiming to apply force to the push rim over a greater push arc is more effective during level propulsion, supporting the guidelines to aim for a push arc between 85˚ and 100˚ (Sawatzky et al., 2015). Following the guidelines during incline propulsion resulted in reduced repetition but greater peak forces, with further research required to determine whether this reduces injury risk. This chapter discussed that further research is required to determine whether novice wheelchair users can be trained to adopt the technique demonstrated by the experts. This links with the final thesis objective, to investigate the influence of real time feedback on manual wheelchair propulsion biomechanics.

9.4.2 Optimising manual wheelchair propulsion technique with real time verbal feedback

Wheelchair skills training can improve the functional ability of manual wheelchair users (MacPhee et al., 2004, Ozturk and Ucsular, 2011) and instrumented wheelchair wheels enable the provision of real time feedback. A systematic review of the literature (Chapter 3) identified that push arc and push rate can be consistently optimised using real time visual feedback (Rice et al., 2013, Richter et al., 2011, DeGroot et al., 2009). Such findings have limited applicability, as each study was completed during ergometer propulsion and visual feedback is not a feasible option during over ground manual wheelchair propulsion. Other options for providing real time feedback include auditory and haptic (Sigrist et al., 2013). Chapter 8 investigated the influence of real time verbal feedback on over ground manual wheelchair propulsion biomechanics. A physiotherapist walking behind the moving wheelchair used real time data from the Sensewheel streamed to a tablet PC, to provide instruction on optimisation of push arc. The intervention, inducing a significant increase in push arc, resulted in the beneficial effects of reducing task repetition and increasing mean chair velocity, whilst also resulting in the undesirable impact of increasing peak force. The balance between reducing task repetition at the cost of an increased peak force is discussed in detail in Chapters 3 and 8. In summary, it is concluded that the intervention was successful as it resulted in a significant reduction in task repetition, without increasing joint loading in excess of that experienced during daily life.

9.5 Summary of key limitations

Study specific limitations have been listed within each of the experimental chapters. This section expands on the key limitations that have been introduced.

9.5.1 Measures of injury risk

Using muscle activity levels recorded using surface EMG as a measure of muscle demand is limited in that activity is not directly proportional to muscle force during anisometric contractions. In addition, the calculation of joint contact force has limitations. As discussed in chapter 6, the model used was simplified by constraining motion to trunk lean, three degrees of freedom at the shoulder joint and elbow joint flexion and extension. Calculation of muscle activity levels to enable joint contact analysis was achieved via static optimisation, utilising an objective function to minimise muscle activation. Although the model was scaled to participant mass, the model actuators (muscles) were not customised to the participant, so the contribution of potentially important variations, such as 'muscle balance' around the shoulder girdle were not accounted for. Options for patient specific customisation of upper limb musculoskeletal models have been presented. In hemiplegic patients, the force generating capacity of individual muscles has been estimated following scanning of hemiparetic muscles (Knarr et al., 2013) and other models have been 'validated' against surface EMG measurements (Morrow et al., 2010b). These methods have limitations, the data collected from assessing volume and quality of muscle tissue does not accurately predict force generating capacity and measurement of timing and activity level of muscle using surface EMG is not valid for all muscles around the shoulder. So whilst the measures used to quantify demand are useful for analysis of relative change in demand of different tasks between participants, it is clear that further developments are required to measure absolute loading values with confidence.

9.5.2 Lack of diversity of participants

The biomechanical data analysed during chapters 6 and 7 was gathered from a small sample of experienced manual wheelchair users with a SCI, with the level of injury ranging from T5-L1. Each 'expert' participant had full upper limb function. Wheelchair users with tetraplegia (Newsam et al., 1996) and other neurological conditions such as Multiple Sclerosis, Muscular Dystrophy, or older wheelchair users may not be able to achieve the suggested

propulsion techniques due to an inability to apply the required forced smoothly over the suggested push arc. Future research should focus on a more inclusive group of wheelchair users, so results can be extrapolated more widely.

9.5.3 Method of delivery of real time feedback

The majority of studies that have previously implemented real time feedback during manual wheelchair propulsion have done so during steady state ergometer propulsion (Blouin et al., 2015, Rice et al., 2013, Richter et al., 2011, DeGroot et al., 2009, Kotajarvi et al., 2006, de Groot et al., 2002). The study presented in Chapter 8 was novel in that real time feedback was provided during over ground propulsion, but the tasks were still limited to a straight line. In reality, daily propulsion requires as much starting, stopping and manoeuvring as steady state pushing (Sonenblum et al., 2012). Further research is required to identify optimal technique for starting, stopping and manoeuvring in order to inform real time feedback in training for such activities.

9.6 Future research

The developments made in this thesis have highlighted a number of areas of focus for future research.

1) **Analysis of more 'functional journeys' and how feedback can be applied**

Further research could be conducted, initially during propulsion around a controlled route, and then during daily propulsion activities. These future studies could be used to examine whether real time feedback is applied most effectively during an initial training session or during the journey itself, as presented in chapter 8.

2) **Investigation of the physical capacity of the user in executing technique changes**

166

As discussed in chapter 7, reduced upper limb strength may limit the ability of wheelchair users to execute the optimal technique in response to real time feedback. Further research is required to associate baseline upper limb muscle strength with the ability to make technique changes in response to real time feedback during demanding manual wheelchair propulsion tasks.

3) Investigation into how propulsion pattern relates to push rim biomechanics during demanding over ground wheelchair propulsion tasks

As introduced in the background chapter (section 2.8.2), wheelchair users are advised to adopt a semi-circular kinematic propulsion pattern to improve propulsion efficiency, reduce push rate and increase push arc, but do not often apply such a technique during over ground propulsion. Further research is required to analyse the association between propulsion patterns and push rim parameters during over ground propulsion. It is possible that different propulsion patterns may be associated with optimal push rim parameters depending on the terrain being negotiated by the wheelchair user.

4) Investigation into how real time feedback is delivered

In the study presented in chapter 8, real time feedback was delivered verbally, using simple trigger phrases. Further research is required to assess the effectiveness and acceptability of other forms of real time feedback, including haptic vibration and sonification of movement. Identifying the optimal mode of feedback is vital in conjunction with the development of the Mark II Sensewheel, with the goal of providing feedback directly from the wheel to the smart phone of the wheelchair user.

5) Alternatives to the Sensewheel

The Sensewheel provides a lightweight alternative to other instrumented wheels previously used for research. Although cheaper than these alternatives, the Sensewheel currently costs approximately £1500 per wheel to manufacture and is not commercially available. Research into cheaper

and universally applicable alternatives should be considered. Such an alternative for providing real time feedback on the temporal parameters of propulsion would be a gyroscope attached to the wheel, activated by a pressure sensor on the palmar surface of the wheelchair user's glove, or alternatively push cycles could be identified directly from the gyroscope output. This would be sufficient to guide the user on push rate, push arc, push distance and chair velocity, but kinetic data would not be recorded. Such a method could be applied in the field of wheelchair sports, during which wheelchair users often apply force to the drive wheel in addition to the push rim. For clarity of data collection, the Sensewheel requires all force to be applied to the push rim, whereas this alternative method would not have such a requirement.

6) Combining data gathered using the Sensewheel and a wheelchair tracking sensor to map accessible routes

By combining the propulsion data from the Sensewheel with data gathered using a GPS tracking device, it would be possible to generate an 'interactive map'. This would enable wheelchair users to view how demanding a particular journey will be.

9.7 Conclusions

It was shown in Chapter 2 that shoulder injury, particularly rotator cuff injury is common among manual wheelchair users and is associated with increasing age and time as a manual wheelchair user. Such injuries are associated with repetitive loading, giving rise to the guidelines to reduce task repetition and peak force to minimise risk of injury. There exists little evidence explaining the direct link between push rim biomechanics and shoulder injury, so biomechanical measures including measurement of muscle activity levels and joint kinetics via musculoskeletal modelling are used to quantify shoulder joint demand.

This thesis introduced the design and function of the Sensewheel, a novel lightweight instrumented wheelchair wheel. The Sensewheel is the first

instrumented wheelchair wheel capable of measuring the key parameters of manual wheelchair propulsion that does not add significant weight to the existing wheelchair wheel. The Sensewheel is used in this thesis in a number of experimental studies, to quantify demand during different propulsion tasks, analyse technique differences and inform real time feedback to optimise technique during over ground manual wheelchair propulsion.

It was identified in Chapter 2 that little is known about how ageing may increase the risk of injury and also how extensive the demand is that is placed on the shoulder joint during over ground manual wheelchair propulsion. Although the results of chapter 5 are not conclusive, likely due to the methodological limitations identified, it is theorised that as the rotator cuff muscles age and strength decreases, an increase in relative demand during wheelchair propulsion will increase the risk of injury. The results of chapter 6 demonstrated the high demand placed on the GH joint, particularly during the more challenging incline propulsion tasks. With reference to the models of tendon degeneration presented in chapter 2, it is evident that injury may occur due to repeated loading experienced during daily manual wheelchair propulsion. The results also identified that the Sensewheel could be used to estimate GH joint demand during over ground propulsion.

Chapter 2 introduced the suggested propulsion technique for minimising risk of injury and identified that these guidelines required testing during over ground wheelchair propulsion. The results of chapter 7 identified that expert users were able to apply the principles of these guidelines to push more effectively to reduce task repetition, but during incline propulsion this increased upper limb demand. Chapters 2 and 3 discussed the use of real time feedback for improving propulsion technique, identifying that although potentially successful, further research was required to investigate the method of application and success of such an intervention during over ground propulsion. The results of chapter 8 demonstrated that real time verbal feedback was successful in improving propulsion technique during level over ground propulsion.

The results presented in this thesis suggest that the Sensewheel could be applied as a useful research and clinical tool, to quantify the demand of a task, identify propulsion technique differences and provide propulsion technique training.

References

AKBAR, M., BALEAN, G., BRUNNER, M., SEYLER, T. M., BRUCKNER, T., MUNZINGER, J., GRIESER, T., GERNER, H. J. & LOEW, M. 2010. Prevalence of rotator cuff tear in paraplegic patients compared with controls. *Journal of Bone and Joint Surgery-American Volume,* 92A**,** 23-30.

AKBAR, M., BRUNNER, M., BALEAN, G., GRIESER, T., BRUCKNER, T., LOEW, M. & RAISS, P. 2011. A cross-sectional study of demographic and morphologic features of rotator cuff disease in paraplegic patients. *Journal of Shoulder and Elbow Surgery,* 20**,** 1108-1113.

AMBROSIO, F., BONINGER, M. L., SOUZA, A. L., FITZGERALD, S. G., KOONTZ, A. M. & COOPER, R. A. 2005. Biomechanics and strength of manual wheelchair users. *Journal of Spinal Cord Medicine,* 28**,** 407-414.

ANDERSON, F. C. & PANDY, M. G. 2001. Static and dynamic optimization solutions for gait are practically equivalent. *Journal of Biomechanics,* 34**,** 153-161.

ARNET, U., VAN DRONGELEN, S., VEEGER, D. H. E. J. & VAN DER WOUDE, L. H. V. 2012. Are the force characteristics of synchronous handcycling affected by speed and the method to impose power? *Medical Engineering & Physics,* 34**,** 78-84.

BERNASCONI, S. M., TORDI, N., RUIZ, J. & PARRATTE, B. 2007. Changes in oxygen uptake, shoulder muscles activity, and propulsion cycle timing during strenuous wheelchair exercise. *Spinal Cord,* 45**,** 468-474.

BLOUIN, M., LALUMIERE, M., GAGNON, D. H., CHENIER, F. & AISSAOUI, R. 2015. Characterization of the Immediate Effect of a Training Session on a Manual Wheelchair Simulator With Haptic Biofeedback: Towards More Effective Propulsion. *IEEE Transactions on Neural Systems and Rehabilitation Engineering,* 23**,** 104-115.

BOETTCHER, C. E., GINN, K. A. & CATHERS, I. 2008. Standard maximum isometric voluntary contraction tests for normalizing shoulder muscle EMG. *Journal of Orthopaedic Research,* 26**,** 1591-1597.

BOHANNON, R. W. & SAUNDERS, N. 1990. Hand-held dynamometry: a single trial may be adequate for measuring muscle strength in healthy individuals. *Physiotherapy Canada,* 42**,** 6-9.

BOLSTERLEE, B., VEEGER, D. & CHADWICK, E. K. 2013. Clinical applications of musculoskeletal modelling for the shoulder and upper limb. *Medical & Biological Engineering & Computing,* 51**,** 953-963.

BONINGER, M., WATERS, R., CHASE, T., DIJKERS, M., GELLMAN, H., GIRONDA, R., GOLDSTEIN, B., JOHNSON-TAYLOR, S., KOONTZ, A. & MCDOWELL, S. 2005a. Preservation of upper limb function following spinal cord injury: A clinical practice guideline for health-care professionals (Reprinted). *Journal of Spinal Cord Medicine,* 28**,** 433-470.

BONINGER, M. L., BALDWIN, M., COOPER, R. A., KOONTZ, A. & CHAN, L. 2000. Manual wheelchair pushrim biomechanics and axle position. *Archives of Physical Medicine and Rehabilitation,* 81**,** 608-613.

BONINGER, M. L., COOPER, R. A., BALDWIN, M. A., SHIMADA, S. D. & KOONTZ, A. 1999. Wheelchair Pushrim kinetics: Body weight and median nerve function. *Archives of Physical Medicine and Rehabilitation,* 80**,** 910-915.

BONINGER, M. L., COOPER, R. A., SHIMADA, S. D. & RUDY, T. E. 1998. Shoulder and elbow motion during two speeds of wheelchair propulsion: a description using a local coordinate system. *Spinal Cord,* 36**,** 418-426.

BONINGER, M. L., DICIANNO, B. E., COOPER, R. A., TOWERS, J. D., KOONTZ, A. M. & SOUZA, A. L. 2003. Shoulder magnetic resonance imaging abnormalities, wheelchair propulsion, and gender. *Archives of Physical Medicine and Rehabilitation,* 84**,** 1615-1620.

BONINGER, M. L., IMPINK, B. G., COOPER, R. A. & KOONTZ, A. M. 2004. Relation between median and ulnar nerve function and wrist kinematics during wheelchair propulsion. *Archives of Physical Medicine and Rehabilitation,* 85**,** 1141-1145.

BONINGER, M. L., KOONTZ, A. M., SISTO, S. A., DYSON-HUDSON, T. A., CHANG, M., PRICE, R. & COOPER, R. A. 2005b. Pushrim biomechanics and injury prevention in spinal cord injury: Recommendations based on CULP-SCI investigations. *Journal of Rehabilitation Research and Development,* 42**,** 9-19.

BONINGER, M. L., SOUZA, A. L., COOPER, R. A., FITZGERALD, S. G., KOONTZ, A. M. & FAY, B. T. 2002. Propulsion patterns and pushrim biomechanics in manual wheelchair propulsion. *Archives of Physical Medicine and Rehabilitation,* 83**,** 718-723.

BREGMAN, D. J. J., VAN DRONGELEN, S. & VEEGER, H. E. J. 2009. Is effective force application in handrim wheelchair propulsion also efficient? *Clinical Biomechanics,* 24**,** 13-19.

BUNKER, T. 2002. Rotator cuff disease. *Current Orthopaedics,* 16**,** 223-233.

BURDEN, A. 2010. How should we normalize electromyograms obtained from healthy participants? What we have learned from over 25 years of research. *Journal of Electromyography and Kinesiology,* 20**,** 1023-1035.

CHOW, J. W., MILLIKAN, T. A., CARLTON, L. G., CHAE, W.-S., LIM, Y.-T. & MORSE, M. I. 2009. Kinematic and electromyographic analysis of wheelchair propulsion on ramps of different slopes for young men with paraplegia. *Archives of Physical Medicine and Rehabilitation,* 90**,** 271-278.

CHOW, J. W., MILLIKAN, T. A., CARLTON, L. G., CHAE, W. S. & MORSE, M. I. 2000. Effect of resistance load on biomechanical characteristics of racing wheelchair propulsion over a roller system. *Journal of Biomechanics,* 33**,** 601-608.

CHOW, J. W., MILLIKAN, T. A., CARLTON, L. G., MORSE, M. I. & CHAE, W. S. 2001. Biomechanical comparison of two racing wheelchair propulsion techniques. *Medicine and Science in Sports and Exercise,* 33**,** 476-484.

COLLINGER, J. L., BONINGER, M. L., KOONTZ, A. M., PRICE, R., SISTO, S. A., TOLERICO, M. L. & COOPER, R. A. 2008. Shoulder biomechanics during the push phase of wheelchair propulsion: A multisite study of persons with paraplegia. *Archives of Physical Medicine and Rehabilitation,* 89**,** 667-676.

COLLINGER, J. L., IMPINK, B. G., OZAWA, H. & BONINGER, M. L. 2010. Effect of an intense wheelchair propulsion task on quantitative ultrasound of shoulder tendons. *PM&R,* 2**,** 920-925.

COWAN, R. E., BONINGER, M. L., SAWATZKY, B. J., MAZOYER, B. D. & COOPER, R. A. 2008. Preliminary outcomes of the SmartWheel Users' Group database: a proposed framework for clinicians to objectively evaluate manual wheelchair propulsion. *Archives of Physical Medicine and Rehabilitation,* 89**,** 260-268.

COWAN, R. E., NASH, M. S., COLLINGER, J. L., KOONTZ, A. M. & BONINGER, M. L. 2009. Impact of surface type, wheelchair weight, and axle position on wheelchair propulsion by novice older adults. *Archives of Physical Medicine and Rehabilitation,* 90**,** 1076-1083.

CURTIS, K. A., TYNER, T. M., ZACHARY, L., LENTELL, G., BRINK, D., DIDYK, T., GEAN, K., HALL, J., HOOPER, M., KLOS, J., LESINA, S. & PACILLAS, B. 1999. Effect of a standard exercise protocol on shoulder pain in long-term wheelchair users. *Spinal Cord,* 37**,** 421-429.

CUTTI, A. G., GIOVANARDI, A., ROCCHI, L., DAVALLI, A. & SACCHETTI, R. 2008. Ambulatory measurement of shoulder and elbow kinematics through inertial and magnetic sensors. *Medical & Biological Engineering & Computing,* 46**,** 169-178.

DALYAN, M., CARDENAS, D. D. & GERARD, B. 1999. Upper extremity pain after spinal cord injury. *Spinal Cord,* 37**,** 191-195.

DE GROOT, S., VEEGER, H. E. J., HOLLANDER, A. P. & VAN DER WOUDE, L. H. V. 2002. Consequence of feedback-based learning of an effective hand rim wheelchair force production on mechanical efficiency. *Clinical Biomechanics,* 17**,** 219-226.

DE GROOT, S., VEEGER, H. E. J., HOLLANDER, A. P. & VAN DER WOUDE, L. H. V. 2003. Short-term adaptations in co-ordination during the initial phase of learning manual wheelchair propulsion. *Journal of Electromyography and Kinesiology,* 13**,** 217-228.

DE LUCA, C. J. 1997. The use of surface electromyography in biomechanics. *Journal of Applied Biomechanics,* 13**,** 135-163.

DE WILDE, L. F., AUDENAERT, E. A. & BERGHS, B. M. 2004. Shoulder prostheses treating cuff tear arthropathy: a comparative biomechanical study. *Journal of Orthopaedic Research,* 22**,** 1222-1230.

DEGROOT, K. K., HOLLINGSWORTH, H. H., MORGAN, K. A., MORRIS, C. L. & GRAY, D. B. 2009. The influence of verbal training and visual feedback on manual wheelchair propulsion. *Disability and rehabilitation. Assistive technology,* 4**,** 86-94.

DELP, S. L., ANDERSON, F. C., ARNOLD, A. S., LOAN, P., HABIB, A., JOHN, C. T., GUENDELMAN, E. & THELEN, D. G. 2007. OpenSim: open-source software to create and analyze dynamic Simulations of movement. *IEEE Transactions on Biomedical Engineering,* 54**,** 1940-1950.

DESROCHES, G., AISSAOUI, R. & BOURBONNAIS, D. 2008a. Relationship between resultant force at the pushrim and the net shoulder joint moments during manual wheelchair propulsion in elderly persons. *Archives of Physical Medicine and Rehabilitation,* 89**,** 1155-1161.

DESROCHES, G., AISSAOUI, R. & BOURBONNAIS, D. 2008b. The effect of resultant force, at the pushrim on shoulder kinetics during manual wheelchair propulsion: A simulation study. *Ieee Transactions on Biomedical Engineering,* 55**,** 1423-1431.

DOWNS, S. H. & BLACK, N. 1998. The feasibility of creating a checklist for the assessment of the methodological quality both of randomised and non-randomised studies of health care interventions. *Journal of Epidemiology and Community Health,* 52**,** 377-384.

DUBOWSKY, S. R., RASMUSSEN, J., SISTO, S. A. & LANGRANA, N. A. 2008. Validation of a musculoskeletal model of wheelchair propulsion and its application to minimizing shoulder joint forces. *Journal of Biomechanics,* 41**,** 2981-2988.

DUBOWSKY, S. R., SISTO, S. A. & LANGRANA, N. A. 2009. Comparison of kinematics, kinetics, and EMG throughout wheelchair propulsion in able-bodied and persons with paraplegia: an integrative approach. *Journal of biomechanical engineering,* 131**,** 021015-021015.

FERRARI, A., CUTTI, A. G., GAROFALO, P., RAGGI, M., HEIJBOER, M., CAPPELLO, A. & DAVALLI, A. 2010. First in vivo assessment of "Outwalk": a novel protocol for clinical gait analysis based on inertial and magnetic sensors. *Medical & Biological Engineering & Computing,* 48**,** 1-15.

FULLERTON, H. D., BORCKARDT, J. J. & ALFANO, A. P. 2003. Shoulder pain: A comparison of wheelchair athletes and nonathletic wheelchair users. *Medicine and Science in Sports and Exercise,* 35**,** 1958-1961.

GAGNON, D., BABINEAU, A.-C., CHAMPAGNE, A., DESROCHES, G. & AISSAOUI, R. 2015. Trunk and shoulder kinematic and kinetic and electromyographic adaptations to slope increase during motorized treadmill propulsion among manual wheelchair users with a spinal cord injury. *Biomed Research International.* DOI: 10/1155/2015/636319.

GAGNON, D., NADEAU, S., NOREAU, L., ENG, J. J. & GRAVEL, D. 2008. Trunk and upper extremity kinematics during sitting pivot transfers performed by individuals with spinal cord injury. *Clinical Biomechanics,* 23**,** 279-290.

GAGNON, D. H., BABINEAU, A.-C., CHAMPAGNE, A., DESROCHES, G. & AISSAOUI, R. 2014. Pushrim biomechanical changes with progressive increases in slope during motorized treadmill manual wheelchair propulsion in individuals with spinal cord injury. *Journal of Rehabilitation Research and Development,* 51**,** 789-802.

GAUR, D. K., SHENOY, S. & SANDHU, J. S. 2007. Effect of aging on activation of shoulder muscles during dynamic activities: An electromyographic analysis. *International Journal of Shoulder Surgery,* 1**,** 51-57.

GIL-AGUDO, A., SOLIS-MOZOS, M., CRESPO-RUIZ, B., DEL-AMA ENG, A. J., PEREZ-RIZO, E., SEGURA-FRAGOSO, A. & JIMENEZ-DIAZ, F. 2014. Echographic and kinetic changes in the shoulder joint after manual wheelchair propulsion under two different workload settings. *Frontiers in bioengineering and biotechnology,* 2**,** 77-77.

GRAY, H. 1918. *Gray's Anatomy of the Human Body* [Online]. Available: http://www.bartleby.com/107/ [Accessed 07/06/2016].

GUTIERREZ, D. D., MULROY, S. J., NEWSAM, C. J., GRONLEY, J. K. & PERRY, J. 2005. Effect of fore-aft seat position on shoulder demands during wheelchair propulsion: Part 2. An electromyographic analysis. *Journal of Spinal Cord Medicine,* 28**,** 222-229.

GUTIERREZ, D. D., THOMPSON, L., KEMP, B., MULROY, S. J. & PTCLINRESNET 2007. The relationship of shoulder pain intensity to quality of life, physical activity, and community participation in persons with paraplegia. *Journal of Spinal Cord Medicine,* 30**,** 251-255.

HASHIMOTO, T., NOBUHARA, K. & HAMADA, T. 2003. Pathologic evidence of degeneration as a primary cause of rotator cuff tear. *Clinical Orthopaedics and Related Research,* 415 111-120.

HELMER, R. J. N., FARROW, D., BALL, K., PHILLIPS, E., FAROUIL, A. & BLANCHONETTE, I. 2011. A pilot evaluation of an electronic textile for lower limb monitoring and interactive biofeedback. *5th Asia-Pacific Congress on Sports Technology (Apcst),* 13**,** 513-518.

HERMENS, H. J., FRERIKS, B., DISSELHORST-KLUG, C. & RAU, G. 2000. Development of recommendations for SEMG sensors and sensor placement procedures. *Journal of Electromyography and Kinesiology,* 10**,** 361-374.

HERS, N., SAWATZKY, B. & SHEEL, W. 2015. Age-related changes to wheelchair efficiency and sprint power output in novice able-bodied males. *Ergonomics,* July**,** 1-7.

HODGES, P. W. & BUI, B. H. 1996. A comparison of computer-based methods for the determination of onset of muscle contraction using electromyography. *Electromyography and Motor Control-Electroencephalography and Clinical Neurophysiology,* 101**,** 511-519.

HOENIG, H., TAYLOR, D. H. & SLOAN, F. A. 2003. Does assistive technology substitute for personal assistance among the disabled elderly? *American Journal of Public Health,* 93**,** 330-337.

HOLLOWAY, C. & TYLER, N. 2013. A micro-level approach to measuring the accessibility of footways for wheelchair users using the Capability Model. *Transportation Planning and Technology,* 36**,** 636-649.

HOLLOWAY, C. S., SYMONDS, A., SUZUKI, T., GALL, A., SMITHAM, P. & TAYLOR, S. 2015. Linking wheelchair kinetics to glenohumeral joint demand during everyday accessibility activities. *Conference proceedings : ... Annual International Conference of the IEEE Engineering in Medicine and Biology Society. IEEE Engineering in Medicine and Biology Society. Annual Conference,* 2015**,** 2478-81.

HOLZBAUR, K. R. S., MURRAY, W. M. & DELP, S. L. 2005. A model of the upper extremity for simulating musculoskeletal surgery and analyzing neuromuscular control. *Annals of Biomedical Engineering,* 33**,** 829-840.

HOOKE, A., MORROW, M., AN, K.-N. & KAUFMAN, K. 2009. Capturing wheelchair propulsion kinematics using inertial sensors. *American Society of Biomechanics.* PA.

HOWARTH, S. J., PRONOVOST, L. M., POLGAR, J. M., DICKERSON, C. R. & CALLAGHAN, J. P. 2010. Use of a geared wheelchair wheel to reduce propulsive muscular demand during ramp ascent: Analysis of muscle activation and kinematics. *Clinical Biomechanics,* 25**,** 21-28.

HOWELL, S. M. & GALINAT, B. J. 1989. THE GLENOID-LABRAL SOCKET - A CONSTRAINED ARTICULAR SURFACE. *Clinical Orthopaedics and Related Research,* 243 122-125.

HOXIE, R. E. & RUBENSTEIN, L. Z. 1994. Are older pedestrians allowed enough time to cross intersections safely. *Journal of the American Geriatrics Society,* 42**,** 241-244.

HUGHES, R. E., JOHNSON, M. E., O'DRISCOLL, S. W. & AN, K. N. 1999. Age-related changes in normal isometric shoulder strength. *American Journal of Sports Medicine,* 27**,** 651-657.

HURD, W. J., MORROW, M. M., KAUFMAN, K. R. & AN, K.-N. 2008. Biomechanic evaluation of upper-extremity symmetry during manual wheelchair propulsion over varied terrain. *Archives of Physical Medicine and Rehabilitation,* 89**,** 1996-2002.

HURD, W. J., MORROW, M. M. B., KAUFMAN, K. R. & AN, K.-N. 2009. Wheelchair propulsion demands during outdoor community ambulation. *Journal of Electromyography and Kinesiology,* 19**,** 942-947.

HWANG, S., KIM, S., SON, J., KIM, Y. & LEE, J. 2013. Upper limb joint motion of two different user groups during manual wheelchair propulsion. *Journal of the Korean Physical Society,* 62**,** 648-656.

JOHNSON, V. L., HALAKI, M. & GINN, K. A. 2011. The use of surface electrodes to record infraspinatus activity is not valid at low infraspinatus activation levels. *Journal of Electromyography and Kinesiology,* 21**,** 112-118.

KANNUS, P. & JOZSA, L. 1991. Histopathological changes preceding spontaneous rupture of a tendon - a controlled study of 891 patients. *Journal of Bone and Joint Surgery-American Volume,* 73A**,** 1507-1525.

KARAS, V., WANG, V. M., DHAWAN, A. & COLE, B. J. 2011. Biomechanical factors in rotator cuff pathology. *Sports Medicine and Arthroscopy Review,* 19**,** 202-206.

KEMP, B. J., BATEHAM, A. L., MULROY, S. J., THOMPSON, L., ADKINS, R. H. & KAHAN, J. S. 2011. Effects of reduction in shoulder pain on quality of life and community activities among people living long-term with SCI paraplegia: a randomized control trial. *Journal of Spinal Cord Medicine,* 34**,** 278-284.

KILKENS, O. J. E., POST, M. W. M., DALLMEIJER, A. J., VAN ASBECK, F. W. A. & VAN DER WOUDE, L. H. V. 2005. Relationship between manual wheelchair skill performance and participation of persons with spinal cord injuries 1 year after discharge from inpatient rehabilitation. *Journal of Rehabilitation Research and Development,* 42**,** 65-73.

KIM, C. S., LEE, D., KWON, S. & CHUNG, M. K. 2014. Effects of ramp slope, ramp height and users' pushing force on performance, muscular activity and subjective ratings during wheelchair driving on a ramp. *International Journal of Industrial Ergonomics,* 44**,** 636-646.

KLOOSTERMAN, M. G. M., SNOEK, G. J., VAN DER WOUDE, L. H. V., BUURKE, J. H. & RIETMAN, J. S. 2013. A systematic review on the pros and cons of using a pushrim-activated power-assisted wheelchair. *Clinical Rehabilitation,* 27**,** 299-313.

KNARR, B. A., RAMSAY, J. W., BUCHANAN, T. S., HIGGINSON, J. S. & BINDER-MACLEOD, S. A. 2013. Muscle volume as a predictor of maximum force generating ability in the plantar flexors post stroke. *Muscle & Nerve,* 48**,** 971-976.

KOBRICK, R., CARR, C., MEYEN, F., DOMINGUES, A., NEWMAN, D. & JACOBS, S. 2012. Using inertial measurement units for measuring spacesuit mobility and work envelope capability for intravehicular and extravehicular activities. *63rd International Astronautical Conference.* Naples, Italy.

KOONTZ, A. M., COOPER, R. A., BONINGER, M. L., YANG, Y. S., IMPINK, B. G. & VAN DER WOUDE, L. H. V. 2005. A kinetic analysis of manual wheelchair propulsion during start-up on select indoor and outdoor surfaces. *Journal of Rehabilitation Research and Development,* 42**,** 447-458.

KOONTZ, A. M., ROCHE, B. M., COLLINGER, J. L., COOPER, R. A. & BONINGER, M. L. 2009. Manual wheelchair propulsion patterns on natural surfaces during start-up propulsion. *Archives of Physical Medicine and Rehabilitation,* 90**,** 1916-1923.

KOTAJARVI, B. R., BASFORD, J. R., AN, K. N., MORROW, D. A. & KAUFMAN, K. R. 2006. The effect of visual biofeedback on the propulsion effectiveness of experienced wheelchair users. *Archives of Physical Medicine and Rehabilitation,* 87**,** 510-515.

KWARCIAK, A. M., SISTO, S. A., YAROSSI, M., PRICE, R., KOMAROFF, E. & BONINGER, M. L. 2009. Redefining the manual wheelchair stroke cycle: Identification and impact of nonpropulsive pushrim contact. *Archives of Physical Medicine and Rehabilitation,* 90**,** 20-26.

KWARCIAK, A. M., TURNER, J. T., GUO, L. & RICHTER, W. M. 2012. The effects of four different stroke patterns on manual wheelchair propulsion and upper limb muscle strain. *Disability and rehabilitation. Assistive technology,* 7**,** 459-63.

LEVY, C. E., CHOW, J. W., TILLMAN, M. D., HANSON, C., DONOHUE, T. & MANN, W. C. 2004. Variable-ratio pushrim-activated power-assist wheelchair eases wheeling over a variety of terrains for elders. *Archives of Physical Medicine and Rehabilitation,* 85**,** 104-112.

LIGHTHALL-HAUBERT, L., REQUEJO, P. S., MULROY, S. J., NEWSAM, C. J., BONTRAGER, E., GRONLEY, J. K. & PERRY, J. 2009. Comparison of shoulder muscle electromyographic activity during standard manual wheelchair and push-rim activated power assisted wheelchair propulsion in persons with complete tetraplegia. *Archives of Physical Medicine and Rehabilitation,* 90**,** 1904-1915.

LOUIS, N. & GORCE, P. 2010. Surface electromyography activity of upper limb muscle during wheelchair propulsion: Influence of wheelchair configuration. *Clinical Biomechanics,* 25**,** 879-885.

MACPHEE, A. H., KIRBY, R. L., COOLEN, A. L., SMITH, C., MACLEOD, D. A. & DUPUIS, D. J. 2004. Wheelchair skills training program: A randomized clinical trial of wheelchair users undergoing initial rehabilitation. *Archives of Physical Medicine and Rehabilitation,* 85**,** 41-50.

MASON, B., VAN DER WOUDE, L., LENTON, J. P. & GOOSEY-TOLFREY, V. 2012a. The effect of wheel size on mobility performance in wheelchair athletes. *International Journal of Sports Medicine,* 33**,** 807-812.

MASON, B., VAN DER WOUDE, L., TOLFREY, K. & GOOSEY-TOLFREY, V. 2012b. The effects of rear-wheel camber on maximal effort mobility performance in wheelchair athletes. *International Journal of Sports Medicine,* 33**,** 199-204.

MASON, B. S., VAN DER WOUDE, L. H. V., TOLFREY, K., LENTON, J. P. & GOOSEY-TOLFREY, V. L. 2012c. Effects of wheel and hand-rim size on submaximal propulsion in wheelchair athletes. *Medicine and Science in Sports and Exercise,* 44**,** 126-134.

MAVCIC, B., IGLIC, A., KRALJ-IGLIC, V., BRAND, R. A. & VENGUST, R. 2008. Cumulative hip contact stress predicts osteoarthritis in DDH. *Clinical Orthopaedics and Related Research,* 466**,** 884-891.

MEARDON, S. A. & DERRICK, T. R. 2014. Effect of step width manipulation on tibial stress during running. *Journal of Biomechanics,* 47**,** 2738-2744.

MERCER, J. L., BONINGER, M., KOONTZ, A., REN, D. X., DYSON-HUDSON, T. & COOPER, R. 2006. Shoulder joint kinetics and pathology in manual wheelchair users. *Clinical Biomechanics,* 21**,** 781-789.

MORGAN, K., ENGSBERG, J. & GRAY, D. 2015. Important wheelchair skills for new manual wheelchair users: health care professional and wheelchair user perspectives. *Disability and Rehabilitation: Assistive Technology.* DOI: 10.3109/17483107.2015.1063015.

MORROW, M. M., RANKIN, J. W., NEPTUNE, R. R. & KAUFMAN, K. R. 2014. A comparison of static and dynamic optimization muscle force

predictions during wheelchair propulsion. *Journal of Biomechanics, 47*, 3459-3465.

MORROW, M. M. B., HURD, W. J., KAUFMAN, K. R. & AN, K. N. 2010a. Shoulder demands in manual wheelchair users across a spectrum of activities. *Journal of Electromyography and Kinesiology, 20*, 61-67.

MORROW, M. M. B., KAUFMAN, K. R. & AN, K.-N. 2010b. Shoulder model validation and joint contact forces during wheelchair activities. *Journal of Biomechanics, 43*, 2487-2492.

MORROW, M. M. B., KAUFMAN, K. R. & AN, K. N. 2010c. Shoulder model validation and joint contact forces during wheelchair activities. *Journal of Biomechanics, 43*, 2487-2492.

MORROW, M. M. B., KAUFMAN, K. R. & AN, K. N. 2011. Scapula kinematics and associated impingement risk in manual wheelchair users during propulsion and a weight relief lift. *Clinical Biomechanics, 26*, 352-357.

MULROY, S. J., FARROKHI, S., NEWSAM, C. J. & PERRY, J. 2004. Effects of spinal cord injury level on the activity of shoulder muscles during wheelchair propulsion: An electromyographic study. *Archives of Physical Medicine and Rehabilitation, 85*, 925-934.

MULROY, S. J., GRONLEY, J. K., NEWSAM, C. J. & PERRY, J. 1996. Electromyographic activity of shoulder muscles during wheelchair propulsion by paraplegic persons. *Archives of Physical Medicine and Rehabilitation, 77*, 187-193.

MULROY, S. J., NEWSAM, C. J., GUTIERREZ, D. D., REQUEJO, P., GRONLEY, J. K., HAUBERT, L. L. & PERRY, J. 2005. Effect of fore-aft seat position on shoulder demands during wheelchair propulsion: Part 1. A kinetic analysis. *Journal of Spinal Cord Medicine, 28*, 214-221.

MULROY, S. J., THOMPSON, L., KEMP, B., HATCHETT, P. P., NEWSAM, C. J., LUPOLD, D. G., HAUBERT, L. L., EBERLY, V., GE, T.-T., AZEN, S. P., WINSTEIN, C. J. & GORDON, J. 2011. Strengthening and Optimal Movements for Painful Shoulders (STOMPS) in Chronic Spinal Cord Injury: A Randomized Controlled Trial. *Physical Therapy, 91*, 305-324.

NEWSAM, C. J., MULROY, S. J., GRONLEY, J. K., BONTRAGER, E. L. & PERRY, J. 1996. Temporal-spatial characteristics of wheelchair propulsion - Effects of level of spinal cord injury, terrain, and propulsion rate. *American Journal of Physical Medicine & Rehabilitation, 75*, 292-299.

NHO, S. J., YADAV, H., SHINDLE, M. K. & MACGILLIVRAY, J. D. 2008. Rotator cuff degeneration - Etiology and pathogenesis. *American Journal of Sports Medicine, 36*, 987-993.

OFFICE FOR NATIONAL STATISTICS 2012. *Population ageing in the United Kingdom, its constituent countries and the European Union* [Online]. Available: http://www.ons.gov.uk/ons [Accessed 07/05/2016].

OPENSIM. 2012. *Getting started with Inverse dynamics* [Online]. Available: http://simtk-confluence.stanford.edu:8080/display/OpenSim/Getting+Started+with+Inverse+Dynamics [Accessed 07/05/2016].

OPENSIM. 2013a. *Joint Reaction Analysis* [Online]. Available: http://simtk-confluence.stanford.edu:8080/display/OpenSim/Joint+Reactions+Analysis [Accessed 01/02/2017].

OPENSIM. 2013b. *Static optimisation setup file* [Online]. Available: http://simtk-confluence.stanford.edu:8080/display/OpenSim/Static+Optimization+Settings+Files+and+XML+Tags [Accessed 01/02/2017].

OPENSIM. 2014. *Point kinematics example* [Online]. Available: http://simtk-confluence.stanford.edu:8080/display/OpenSim/Point+Kinematics+Example [Accessed 01/02/2017].

OPENSIM. 2015a. *Getting started with static optimisation* [Online]. Available: http://simtk-confluence.stanford.edu:8080/display/OpenSim/Getting+Started+with+Static+Optimization [Accessed 07/05/2016].

OPENSIM. 2015b. *How to use the Inverse Dynamics Tool* [Online]. Available: http://simtk-confluence.stanford.edu:8080/display/OpenSim/How+to+Use+the+Inverse+Dynamics+Tool [Accessed 01/02/2017].

OPENSIM. 2015c. *Thelen 2003 muscle model* [Online]. Available: http://simtk-confluence.stanford.edu:8080/display/OpenSim/Thelen+2003+Muscle+Model [Accessed 08/07/2016].

OPENSIM. 2016. *Reserve Actuator setup file* [Online]. Available: http://simtk-confluence.stanford.edu:8080/display/OpenSim/Settings+Files+and+XML+Tag+Definitions [Accessed 01/02/2017].

OZAKI, J., FUJIMOTO, S., NAKAGAWA, Y., MASUHARA, K. & TAMAI, S. 1988. Tears of the rotator cuff of the shoulder assoicated with pathological changes in the acromion - a study in cadavers. *Journal of Bone and Joint Surgery-American Volume,* 70A**,** 1224-1230.

OZTURK, A. & UCSULAR, F. D. 2011. Effectiveness of a wheelchair skills training programme for community-living users of manual wheelchairs in Turkey: a randomized controlled trial. *Clinical Rehabilitation,* 25**,** 416-424.

PAPWORTH TRUST 2013. *Disability in the United Kingdom 2013: Facts and figures* [Online]. Available: http://www.papworthtrust.org.uk/sites/default/files/Facts%20and%20Figures%202013%20web_0.pdf [Accessed 07/05/2016].

PARSONS, I. M., APRELEVA, M., FU, F. H. & WOO, S. L. Y. 2002. The effect of rotator cuff tears on reaction forces at the glenohumeral joint. *Journal of Orthopaedic Research,* 20**,** 439-446.

QI, L., WAKELING, J., GRANGE, S. & FERGUSON-PELL, M. 2012a. Changes in surface electromyography signals and kinetics associated with progression of fatigue at two speeds during wheelchair propulsion. *Journal of rehabilitation research and development,* 49**,** 23-34.

QI, L., WAKELING, J., GRANGE, S. & FERGUSON-PELL, M. 2012b. Effect of velocity on shoulder muscle recruitment patterns during wheelchair propulsion in nondisabled individuals: Pilot study. *Journal of Rehabilitation Research and Development,* 49**,** 1527-1535.

RAINA, S., MCNITT-GRAY, J. L., MULROY, S. & REQUEJO, P. S. 2012. Effect of increased load on scapular kinematics during manual wheelchair propulsion in individuals with paraplegia and tetraplegia. *Human Movement Science,* 31**,** 397-407.

RANKIN, J. W., KWARCIAK, A. M., RICHTER, W. M. & NEPTUNE, R. R. 2010. The influence of altering push force effectiveness on upper extremity demand during wheelchair propulsion. *Journal of Biomechanics,* 43, 2771-2779.

RANKIN, J. W., KWARCIAK, A. M., RICHTER, W. M. & NEPTUNE, R. R. 2012. The influence of wheelchair propulsion technique on upper extremity muscle demand: A simulation study. *Clinical Biomechanics,* 27**,** 879-886.

REININGA, I. H. F., STEVENS, M., WAGENMAKERS, R., BOERBOOM, A. L., GROOTHOFF, J. W., BULSTRA, S. K. & ZIJLSTRA, W. 2011. Compensatory Trunk Movements in Patients with Hip Osteoarthritis Accuracy and Reproducibility of a Body-Fixed Sensor-Based Assessment. *American Journal of Physical Medicine & Rehabilitation,* 90**,** 681-687.

REQUEJO, P. S., FURUMASU, J. & MULROY, S. J. 2015. Evidence-based strategies for preserving mobility for elderly and aging manual wheelchair users. *Topics in Geriatric Rehabilitation,* 31**,** 26-41.

REQUEJO, P. S., LEE, S. E., MULROY, S. J., HAUBERT, L. L., BONTRAGER, E. L., GRONLEY, J. K. & PERRY, J. 2008. Shoulder muscular demand during lever-activated vs pushrim wheelchair propulsion in persons with spinal cord injury. *Journal of Spinal Cord Medicine,* 31**,** 568-577.

RICE, I. M., POHLIG, R. T., GALLAGHER, J. D. & BONINGER, M. L. 2013. Handrim wheelchair propulsion training effect on overground propulsion using biomechanical real-time visual feedback. *Archives of Physical Medicine and Rehabilitation,* 94**,** 256-263.

RICE, L., SMITH, I., KELLEHER, A., GREENWALD, K. & BONINGER, M. 2014. Impact of a wheelchair education protocol based on practice guidelines for preservation of upper-limb function: A randomised trial. *Archives of Physical Medicine and Rehabilitation,* 95**,** 10-19.

RICHTER, W. M., KWARCIAK, A. M., GUO, L. & TURNER, J. T. 2011. Effects of single-variable biofeedback on wheelchair handrim biomechanics. *Archives of Physical Medicine and Rehabilitation,* 92**,** 572-577.

RICHTER, W. M., RODRIGUEZ, R., WOODS, K. R. & AXELSON, P. W. 2007a. Consequences of a cross slope on wheelchair handrim biomechanics. *Archives of Physical Medicine and Rehabilitation,* 88**,** 76-80.

RICHTER, W. M., RODRIGUEZ, R., WOODS, K. R. & AXELSON, P. W. 2007b. Stroke pattern and handrim biomechanics for level and uphill wheelchair propulsion at self-selected speeds. *Archives of Physical Medicine and Rehabilitation,* 88**,** 81-87.

RIEMANN, B. L., DAVIES, G. J., LUDWIG, L. & GARDENHOUR, H. 2010. Hand-held dynamometer testing of the internal and external rotator musculature based on selected positions to establish normative data and unilateral ratios. *Journal of Shoulder and Elbow Surgery,* 19**,** 1175-1183.

RODGERS, M. M., KEYSER, R. E., GARDNER, E. R., RUSSELL, P. J. & GORMAN, P. H. 2000. Influence of trunk flexion on biomechanics of wheelchair propulsion. *Journal of Rehabilitation Research and Development,* 37**,** 283-295.

RODGERS, M. M., MCQUADE, K. J., RASCH, E. K., KEYSER, R. E. & FINLEY, M. A. 2003. Upper-limb fatigue-related joint power shifts in experienced wheelchair users and nonwheelchair users. *Journal of Rehabilitation Research and Development,* 40**,** 27-37.

SABICK, M. B., KOTAJARVI, B. R. & AN, K. N. 2004. A new method to quantify demand on the upper extremity during manual wheelchair propulsion. *Archives of Physical Medicine and Rehabilitation,* 85**,** 1151-1159.

SASAKI, M., STEFANOV, D., OTA, Y., MIURA, H. & NAKAYAMA, A. 2015. Shoulder joint contact force during lever-propelled wheelchair propulsion. *ROBOMECH Journal,* 2.13.

SAWATZKY, B., DIGIOVINE, C., BERNER, T., ROESLER, T. & KATTE, L. 2015. The need for updated clinical practice guidelines for

preservation of upper extremities in manual wheelchair users a position paper. *American Journal of Physical Medicine & Rehabilitation,* 94**,** 313-324.

SIGRIST, R., RAUTER, G., RIENER, R. & WOLF, P. 2013. Augmented visual, auditory, haptic, and multimodal feedback in motor learning: A review. *Psychonomic Bulletin & Review,* 20**,** 21-53.

SONENBLUM, S. E., SPRIGLE, S. & LOPEZ, R. A. 2012. Manual wheelchair use: bouts of mobility in everyday life. *Rehabilitation research and practice,* 2012, DOI: 10.1155/2012/753165.

SOSLOWSKY, L. J., THOMOPOULOS, S., TUN, S., FLANAGAN, C. L., KEEFER, C. C., MASTAW, J. & CARPENTER, J. E. 2000a. Neer Award 1999 - Overuse activity injures the supraspinatus tendon in an animal model: A histologic and biomechanical study. *Journal of Shoulder and Elbow Surgery,* 9**,** 79-84.

SOSLOWSKY, L. J., THOMOPOULOS, S., TUN, S., FLANAGAN, C. L., KEEFER, C. C., MASTAW, J. & CARPENTER, J. E. 2000b. Neer Award 1999. Overuse activity injures the supraspinatus tendon in an animal model: a histologic and biomechanical study. *Journal of shoulder and elbow surgery,* 9**,** 79-84.

SPAIN, R. I., GEORGE, R. J. S., SALARIAN, A., MANCINI, M., WAGNER, J. M., HORAK, F. B. & BOURDETTE, D. 2012. Body-worn motion sensors detect balance and gait deficits in people with multiple sclerosis who have normal walking speed. *Gait & Posture,* 35**,** 573-578.

STARRS, P., CHOHAN, A., FEWTRELL, D., RICHARDS, J. & SELFE, J. 2012. Biomechanical differences between experienced and inexperienced wheelchair users during sport. *Prosthetics and Orthotics International,* 36**,** 324-331.

STEELE, K. M., DEMERS, M. S., SCHWARTZ, M. H. & DELP, S. L. 2012. Compressive tibiofemoral force during crouch gait. *Gait & Posture,* 35**,** 556-560.

TAYLOR, S., GASSAWAY, J., HEISLER-VARRIALE, L. A., KOZLOWSKI, A., TEETER, L., LABARBERA, J., VARGAS, C., NATALE, A. & SWIRSKY, A. 2015. Patterns in wheeled mobility skills training, equipment evaluation, and utilization: findings from the SCIRehab project. *Assistive technology : the official journal of RESNA,* 27**,** 59-68.

TEMPELHOF, S., RUPP, S. & SEIL, R. 1999. Age-related prevalence of rotator cuff tears in asymptomatic shoulders. *Journal of Shoulder and Elbow Surgery,* 8**,** 296-299.

TERRY, G. C. & CHOPP, T. M. 2000. Functional anatomy of the shoulder. *Journal of Athletic Training,* 35**,** 248-255.

THOMPSON, W. O., DEBSKI, R. E., BOARDMAN, D., TASKIRAN, E., WARNER, J. J. P., FU, F. H. & WOO, S. L. Y. 1996. A biomechanical analysis of rotator cuff deficiency in a cadaveric model. *American Journal of Sports Medicine,* 24**,** 286-292.

TURNER, N., FERGUSON, K., MOBLEY, B. W., RIEMANN, B. & DAVIES, G. 2009. Establishing Normative Data on Scapulothoracic Musculature Using Handheld Dynamometry. *Journal of Sport Rehabilitation,* 18**,** 502-520.

VAN DER WOUDE, L. H. V., BOUW, A., VAN WEGEN, J., VAN AS, H., VEEGER, D. & DE GROOT, S. 2009. Seat height: effects on submaximal hand rim wheelchair performance during spinal cord injury rehabilitation. *Journal of Rehabilitation Medicine,* 41**,** 143-149.

VAN DRONGELEN, S., VAN DER WOUDE, L. H., JANSSEN, T. W., ANGENOT, E. L., CHADWICK, E. K. & VEEGER, D. J. H. 2005. Glenohumeral contact forces and muscle forces evaluated in wheelchair-related activities of daily living in able-bodied subjects versus subjects with paraplegia and tetraplegia. *Archives of Physical Medicine and Rehabilitation,* 86**,** 1434-1440.

VEEGER, H. E. J., ROZENDAAL, L. A. & VAN DER HELM, F. C. T. 2002. Load on the shoulder in low intensity wheelchair propulsion. *Clinical Biomechanics,* 17**,** 211-218.

VELHO, R., HOLLOWAY, C., SYMONDS, A. & BALMER, B. 2016. The effect of transport accessibility on the social inclusion of wheelchair users: A mixed method analysis. *Social Inclusion,* 4, ISSN:2183-2803.

WAITE, D. L., BROOKHAM, R. L. & DICKERSON, C. R. 2010. On the suitability of using surface electrode placements to estimate muscle activity of the rotator cuff as recorded by intramuscular electrodes. *Journal of Electromyography and Kinesiology,* 20**,** 903-911.

WESTERHOFF, P., GRAICHEN, F., BENDER, A., HALDER, A., BEIER, A., ROHLMANN, A. & BERGMANN, G. 2009. In vivo measurement of shoulder joint loads during activities of daily living. *Journal of Biomechanics,* 42**,** 1840-1849.

WESTERHOFF, P., GRAICHEN, F., BENDER, A., HALDER, A., BEIER, A., ROHLMANN, A. & BERGMANN, G. 2011. Measurement of shoulder joint loads during wheelchair propulsion measured in vivo. *Clinical Biomechanics,* 26**,** 982-989.

WHEELER, J. W., SHULL, P. B. & BESIER, T. F. 2011. Real-time knee adduction moment feedback for gait retraining through visual and tactile displays. *Journal of Biomechanical Engineering-Transactions of the Asme,* 133.

WILEN, J., SISTO, S. A. & KIRSHBLUM, S. 2002. Algorithm for the detection of muscle activation in surface electromyograms during periodic activity. *Annals of Biomedical Engineering,* 30**,** 97-106.

XSENS. 2016. *MTw Development kit* [Online]. Available: https://www.xsens.com/products/mtw-development-kit/ [Accessed 08/07/2016].

Appendix 1: Sensewheel limitations and future developments

1) Method of data transmission: The data from each load cell was wired to the master. The master was not water proof, so the Sensewheel Mark one could not be used outside during wet weather. The data was transmitted from the master to the receiver attached to the PC via UHF radio. This method of data transmission resulted in small sections of data loss, which had to be accounted for retrospectively via linear interpolation, to ensure consistency of results. To account for these limitations, the Mark 2 Sensewheel is designed with wireless Bluetooth connections between each load cell and a master mounted on the wheelchair (ultimately a Smart Phone), and each individual load cell will be sealed and thus water resistant.

2) Mechanical strength of the load cell: The load cells developed for the Sensewheel Mark 1 were made of aluminium alloy and so did not have sufficient mechanical strength for sustained use. Figure 9-1 (A) shows a damaged load cell, highlighting the weak point where the connecting pillar sheared from the load cell diaphragm during use. Resistance to cyclic loading of the load cells is vital if the Sensewheel is to become a useful clinical tool, as wheelchair users apply repeated high forces during negotiation of daily journeys. The Sensewheel also has potential for use as a training tool for wheelchair sports athletes. If it is to be used to track performance during wheelchair court sports, it will need to be able to resist the direct impact imparted by other wheelchairs to the push rim in addition to the load applied in tangent to the wheel by the user. Steps have been taken to address this mechanical weakness in the designs for the Mark 2 Sensewheel. The Mark 2 load cell (Figure 9-1 (B)) will be manufactured from Titanium rather than aluminium and the connecting pillar has a greater diameter and a tapered connection to the load cell diaphragm.
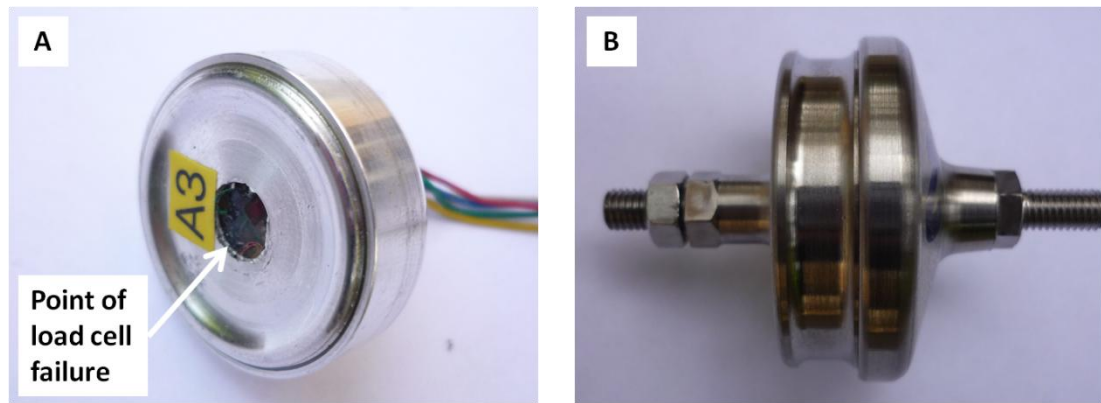
Figure 9-1: The failed Sensewheel Mark 1 load cell (A) and an example of the Sensewheel Mark 2 load cell (B).

3) Transmission frequency: The Sensewheel Mark 1 operated a sampling frequency of 50Hz, lower than both the SmartWheel (240Hz) and the OptiPush (200Hz). 50Hz is high enough to capture the power spectra associated with the main pushing functions. Increasing the sampling frequency to 100Hz will improve the measurement accuracy of faster transients.

4) Adaptability: The Mark 1 Sensewheel load cells were only tested on one wheel type, with a 60 cm diameter and screw fixings between the push rim and wheel. For the Sensewheel to be clinically applicable, the system requires the flexibility to adapt wheels of different diameter and design.

5) Additional chair width: The load cell on the Mark 1 Sensewheel adds an additional 12 mm between the push rim and drive wheel. This has the potential to make manoeuvring through thin doorways challenging. In addition, even if a small difference, increasing the required angle of GH joint abduction required due to an increased width between the push rims may increase risk of injury. The design for the Mark 2 Sensewheel will reduce the distance between the push rim and drive wheel.

6) User interface: The interface for the Sensewheel Mark 1 was programmed using LabView. The process for resetting the wheel, capturing and processing data and exporting results is appropriate for the research environment, but too laborious for the clinical setting. An

upgraded GUI is required, to run on an android tablet, with simple visual data for real time feedback, and a simple process for capturing and exporting data for clinical review.

Appendix 2: OpenSim model muscle properties

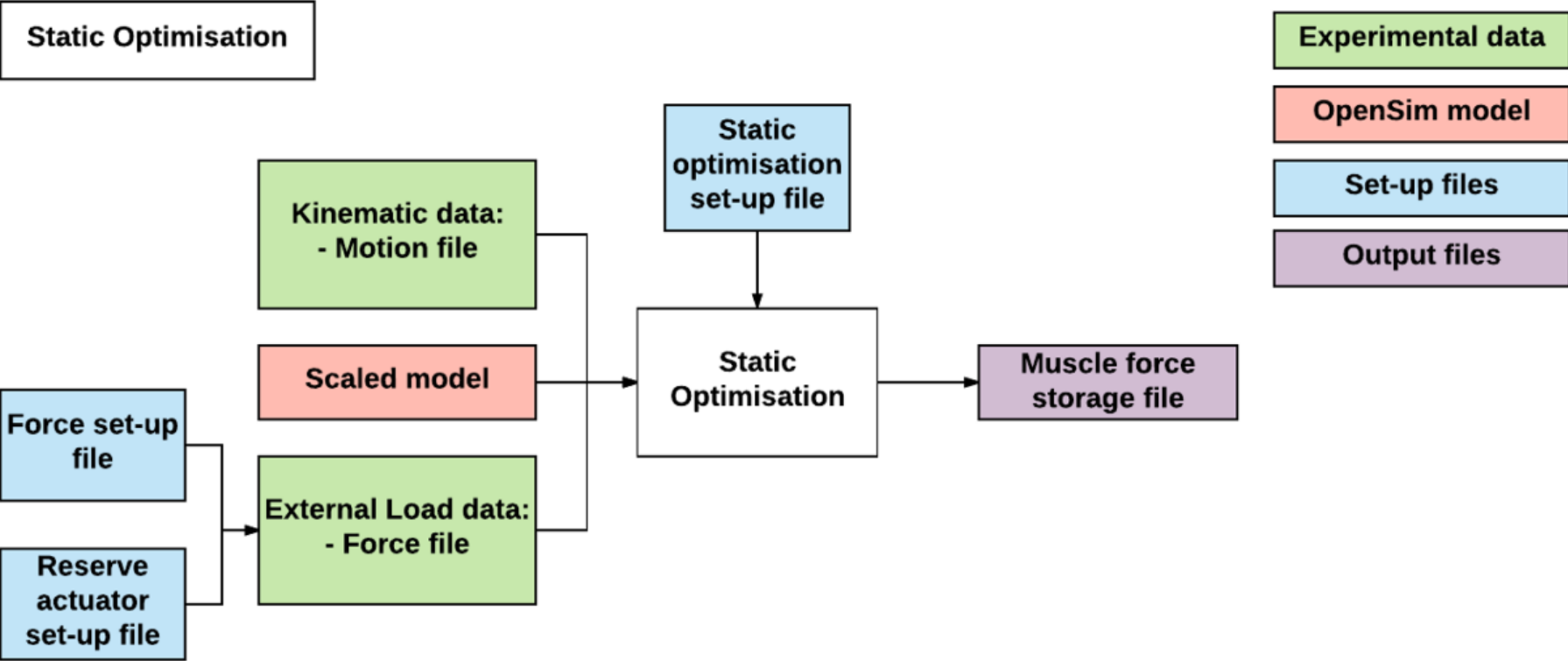**Table 9.1: Muscle properties of the OpenSim model 'Dynamic Arms 2013.'**

Muscle	Peak Isometric force (N)	Optimal fibre length (m)	Tendon slack length (m)	Pennation angle at optimal (radians)
Anterior Deltoid	1142.60	0.10	0.09	0.38
Middle Deltoid	1142.60	0.11	0.11	0.26
Posterior Deltoid	259.88	0.14	0.04	0.31
Supraspinatus	487.82	0.07	0.04	0.12
Infraspinatus	1210.84	0.08	0.03	0.32
Subscapularis	1377.81	0.09	0.03	0.35
Teres Minor	354.25	0.07	0.07	0.42
Teres Major	425.39	0.16	0.02	0.28
Pectoralis Major (Clavicular)	364.41	0.14	0.003	0.30
Pectoralis Major (Sternal 1)	515.41	0.14	0.09	0.44
Pectoralis Major (Sternal 2)	390.55	0.14	0.13	0.44
Latissimus Dorsi 1	389.10	0.25	0.12	0.44
Latissimus Dorsi 2	389.10	0.23	0.18	0.33
Latissimus Dorsi 3	281.66	0.28	0.14	0.37
Coracobrachialis	242.46	0.09	0.10	0.00
Triceps Longus	798.52	0.13	0.14	0.21
Triceps Lateralis	624.30	0.11	0.01	0.16
Triceps Medialis	624.30	0.11	0.01	0.16
Anconeus	350.00	0.03	0.02	0.00
Bicep (long head)	624.30	0.12	0.27	0.00
Bicep (short head)	435.56	0.13	0.19	0.00
Brachialis	987.26	0.09	0.05	0.00
Brachioradialis	261.33	0.17	0.13	0.00

Muscle	Peak Isometric force (N)	Optimal fibre length (m)	Tendon slack length (m)	Pennation angle at optimal (radians)
Extensor Carpi Radialis Longus	304.89	0.08	0.22	0.00
Extensor Carpi Radialis Brevis	100.52	0.06	0.22	0.16
Extensor Carpi Ulnaris	93.17	0.06	0.23	0.06
Flexor Carpi Radialis	73.96	0.06	0.24	0.05
Flexor Carpi Ulnaris	128.93	0.05	0.27	0.21
Pronator Teres	566.22	0.05	0.10	0.17

Appendix 3: Flow diagram: OpenSim Point kinematic function
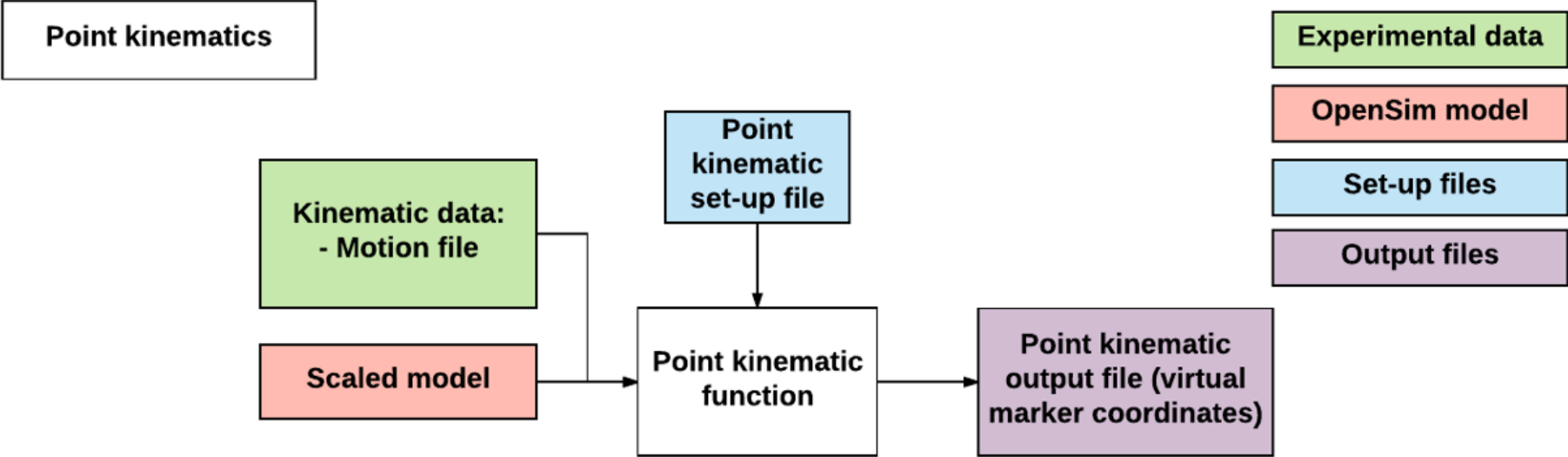
Appendix 4: Flow diagram: OpenSim Static Optimisation function

Appendix 5: Flow diagram: OpenSim Joint Reaction Analysis

Joint Reaction Analysis

Experimental data

OpenSim model

Set-up files

Output files

Kinematic data:
- Motion file

Joint reaction analysis set-up file

Scaled model

Force set-up file

External Load data:
- Force file
- Muscle force storage file

Reserve actuator set-up file

Joint reaction analysis

Joint reaction analysis output file